

Rochester Institute of Technology

RIT Scholar Works

Theses

5-1-1996

Visual determination of hue suprathreshold tolerances

Yue Qiao

Follow this and additional works at: <https://scholarworks.rit.edu/theses>

Recommended Citation

Qiao, Yue, "Visual determination of hue suprathreshold tolerances" (1996). Thesis. Rochester Institute of Technology. Accessed from

This Thesis is brought to you for free and open access by RIT Scholar Works. It has been accepted for inclusion in Theses by an authorized administrator of RIT Scholar Works. For more information, please contact ritscholarworks@rit.edu.

Visual Determination of Hue Suprathreshold Tolerances

by

Yue Qiao

B.Eng. Beijing University of Science and Technology

(1988)

A thesis submitted in partial fulfillment of the
requirements for the degree of Master of Science
in the Chester F. Carlson Center for Imaging Science
College of Science
Rochester Institute of Technology

May 1996

Signature of the Author:_____

Accepted by Dana G. Marsh May 30, 1996
Coordinator, M.S. Degree Program Date

**CHESTER F. CARLSON
CENTER FOR IMAGING SCIENCE
COLLEGE OF SCIENCE
ROCHESTER INSTITUTE OF TECHNOLOGY
ROCHESTER, NEW YORK**

CERTIFICATE OF APPROVAL

M.S. DEGREE THESIS

The M.S. Degree Thesis of Yue Qiao
Has been examined and approved by the
thesis committee as satisfactory for the
thesis requirement for the
Master of Science degree

Dr. Roy S. Berns, Thesis Advisor

Ms. Lisa A. Reniff, Thesis Advisor

Dr. Mark D. Fairchild

5/30/96
Date

**THESIS RELEASE PERMISSION
ROCHESTER INSTITUTE OF TECHNOLOGY
COLLEGE OF SCIENCE
CHESTER F. CARLSON
CENTER FOR IMAGING SCIENCE**

Title of Thesis: Visual Determination of Hue Suprathreshold Tolerances

I, Yue Qiao, hereby grant permission to the Wallace Memorial Library of Rochester Institute of Technology to reproduce my thesis in whole or in part. Any reproduction will not be for commercial use or profit.

Signature: _____

Date: 5 / 30 / 196

Visual Determination of Hue Suprathreshold Tolerances

By
Yue Qiao

Submitted to the
Center for Imaging Science
in partial fulfillment of the requirements
for the Master of Science Degree
at the Rochester Institute of Technology

ABSTRACT

A visual experiment was performed to generate suprathreshold tolerances sampling the direction of CIELAB hue, thereby extending the RIT-Dupont dataset. Thirty nine color centers including three complete hue circles at different lightness or chroma levels and three CIE recommended colors (red, green, blue) were evaluated for hue discrimination. Forty five observers participated in the pass/fail experiments. A total of 32,226 visual observations were made. The statistical method, logit analysis with 3-dimensional normit function, was used to determine the hue discrimination suprathreshold for each color center. The results indicated that the hue discrimination suprathresholds of observers varied with hue angle. The suprathreshold also increased with the chroma position of a given color center. The results were compared with current color-difference formulae, CMC, BFD and CIE94. A mathematical equation was derived from the present dataset.

ACKNOWLEDGMENTS

This research was supported by the Industrial Color Difference Consortium. The members are 3M Company, Datacolor International, Detroit Color Council, Dupont Automotive, Dystar & Bayer Corporation, ISCC, Macbeth, Society of Plastics Engineers, and Xerox Corporation.

I would like to thank:

All my forty five observers who graciously volunteered their time.

My thesis advisors, Dr. R. S. Berns, Ms. L. A. Reniff, and my committee member, Dr. M. D. Fairchild, for bringing this project and creating a research environment in which there were plenty of freedom, and the proper amount of guidance.

Mr. Kazuhiko Takemura for providing the look-up table of the Fuji printer and enlightening discussions.

My family and my friends for their loving support and encouragement.

My husband, Jeffrey Wang. It would be impossible for me to achieve anything without his love, understanding, support, and many things far too numerous to name.

To my late father Jinshan Qiao

TABLE OF CONTENTS

INTRODUCTION	1
Overview of the Development of Color-difference	
Experimental Datasets.....	2
1. Overview of the McDonald Dataset.....	2
2. Overview of the Witt Dataset.....	5
3. Overview of the Luo and Rigg Dataset.....	8
4. Overview of the RIT-Dupont Dataset.....	13
Overview of the Development of Color-Difference Equations.....	21
1. FMC-1 and FMC-2	21
2. CIELAB and CIELUV	23
3. JPC 79 and CMC(<i>l:c</i>).....	25
4. BFD(<i>l:c</i>)	30
5. CIE94.....	34
Purpose of the Current Thesis	41
EXPERIMENTS ON BACKGROUND AND SURROUND	
EFFECT	43
Experiments	43
Results and Discussion of Background and Surround Experiments	48
MAIN EXPERIMENTS.....	55
Printer Testing and Calibration	55
Determination of Statistical Analysis.....	60
1. The Logit Program with 3-D normit Function.....	60
2. Criteria for Assessing Model Fit.....	63
3. Determination of T50 value and Fiducial Limits	64
4. Testing of the Logit Program with 3-D Normit Function.....	66
Sample Design.....	71
Preparation of Samples.....	73
Viewing Conditions.....	74
Sample Measurements.....	75
Psychophysical Experiments.....	76

RESULTS AND DISCUSSION	79
Sample Measurements	76
Observer Variability	83
1. Observer Variance	83
2. Mean Variance of Each Color Center.....	87
3. Inter-observer Variance.....	90
Results of Logit Analysis	92
Model Fit	103
1. Testing the CMC Model Fit.....	103
2. Testing the BFD Model Fit	104
3. Model Derived from Current Dataset.....	108
CONCLUSIONS	117
REFERENCES	120
APPENDIX A.....	124
The measurements of the 393 color pairs.....	124
APPENDIX B.....	148
The measurements of the color-difference of the 393 color pairs	148
APPENDIX C	160
The Programs used in Data Analysis.....	160

LIST OF FIGURES

Fig. 1. ANLAB50 distribution of color centers lightness groups.....	3
Fig. 2 ANLAB50 tolerance ellipsoids (full size).....	4
Fig. 3 Five color centers suggested by CIE TC -1.3.....	6
Fig. 4. Threshold ellipses in three planes in $\Delta(x_{10}, y_{10}, Y_{10})$ space for observer groups of yellow samples.....	7
Fig. 5. Arrangement of samples for gray-scale assessments	10
Fig. 6. Final ellipses after adjustment using individual color center factors and $Y=30$	12
Fig. 7. An a^*b^* pot of the equal color difference vector results from Phase I (magnified 5 times).....	16
Fig. 8. Color centers studied in both Phase I and Phase II	17
Fig. 9. Vectors directions F, G, H, and I, which simultaneously sample lightness and chromaticness	18
Fig. 10. Ellipses of RIT-Dupont dataset in chromaticness plane.....	19
Fig. 11. Ellipses of RIT-Dupont dataset in L^*b^* plane.....	20
Fig. 12. The relationship between L^* and S_L factors.....	29
Fig. 13. The relationship between C^* and S_C factors.....	29
Fig. 14. The relation between the ratio T and angle θ	30
Fig. 15. Comparison of experimental ($\Delta v=1.5$) and CMC ($\Delta E=1.68$) ellipses in a^*b^* diagram.....	33
Fig. 16. Experimental ellipses ($\Delta V=1.5$) and BFD ellipses ($\Delta E=2.20$).....	33

Fig. 17. Equal visual lightness differences	35
Fig. 18. Equal visual chroma differences.....	36
Fig. 19. Equal visual hue differences.....	36
Fig. 20. Equal visual hue differences corrected for C^* position.....	37
Fig. 21. Spectral radiance of the Macbeth lightbooth.....	46
Fig. 22. Results of background/surround experiments	49
Fig. 23. Background adjusted Munsell value V_a plotted against nominal Munsell value V_s for backgrounds of nominal Munsell value.....	53
Fig. 24. The lightness L^* change with the position in width.....	56
Fig. 25. Color coordinate a^* change with the position in width.....	56
Fig. 26. Color coordinate b^* change with the position in width.....	57
Fig. 27. An example of color sampling in hue direction.....	58
Fig. 28. The gamut of the Fuji printer located in Munsell Color Science Laboratory.....	59
Fig. 29. The thirty nine centers studied.....	72
Fig. 30. The arrangement of the sample pair	74
Fig. 31. Typical desirable sampling about a given color center	80
Fig. 32. Typical undesirable sampling about a given color center	80
Fig. 33. Influence of matching leniency on disagreements of each observer comparing with majority decision.....	85
Fig. 34. Mean variance comparing majority decision with the change of hue angles.....	87

Fig. 35. Influence of matching leniency on inter observer variance	91
Fig. 36. T50 values vs. CIELAB hue angle for the hue circle at chroma close to 20, lightness close to 40	95
Fig. 37. T50 values vs. CIELAB hue angle for the hue circle at chroma close to 35, lightness close to 40	96
Fig. 38. T50 values vs. CIELAB hue angle for the hue circle at chroma close to 20, lightness close to 60	96
Fig. 39. T50 values as function of CIELAB hue angle for all color centers	97
Fig. 40. Comparing L40C20 data with CMC, CIE94 and BFD	100
Fig. 41. Comparing L40C35 data with CMC, CIE94 and BFD	100
Fig. 42. Comparing L60C20 data with CMC, CIE94 and BFD	101
Fig. 43. CMC model fit with its original data	103
Fig. 44. Comparing the optimized BFD equation with the data L40C20	105
Fig. 45. Comparing the optimized BFD equation with the data L40C35	106
Fig. 46. Comparing the optimized BFD equation with the data L60C20	106
Fig. 47. The BFD model fit with its original data	107
Fig. 48. Derivation of the model	109
Fig. 49. Equal visual hue differences corrected for chroma position	112
Fig. 50. The average hue discrimination corrected for chroma position	113
Fig. 51. Testing the model fit for L60C20 hue circle	114
Fig. 52. Testing the model fit for L40C35 hue circle	114
Fig. 53. Testing the model fit for L40C20 hue circle	115

LIST OF TABLES

Table I. Thesis outline.....	42
Table II. The comparison of probit analysis results for each vector on different backgrounds.....	48
Table III. Comparison of the data of cyan D vector on the two different backgrounds.....	50
Table IV. Coordinates of all color centers in CIELAB space and variation in lightness and chroma directions	81
Table V. Variance of each observer comparing with majority decision.....	85
Table VI. The mean and standard deviation of observers' disagreements comparing with majority decision for each color center.....	88
Table VII. Results of logit analysis and T50 values with 95% fiducial limits.....	93
Table VIII. The RMS values by comparing experimental data with CMC, BFD, and CIE94 equations.....	101
Table IX. The RMS values by comparing each data point with the present model, CMC,BFD, and CIE94 equations.....	116

INTRODUCTION

Improvement of industrial color-difference evaluation is a critical need in international industries as diverse as construction materials (carpet, paint, glass, building materials), automotive (paint, fabric, interior and exterior trim), consumer goods (apparel, home furnishings), and image reproduction (printing, photography, computer). In general these industries have effective process technologies for measurement, understanding, and control of the coloration process but lack efficient means to evaluate the color fidelity of their product in agreement with the visual decisions of the product's consumers. Lack of an effective color-difference evaluation technology forces industry to adopt inefficient, labor-intensive solutions and is a major barrier to statistical process control, product design and specification, and automated process control in these industries.¹ The way to solve this problem is to develop an accurate relationship between visual color-difference perception and color measurement values. Progress toward this objective has been made by the development of large experimental datasets describing perceptual response to color difference and the development of theoretical or empirical models that approximate the experimental data in terms of color-difference metrics.²

Overview of the Development of Color-Difference Experimental Datasets

Recent developments in color-difference research have been focused on small color-differences which most closely correspond to the commercially-important task of color-product acceptance. There has been added interest in defining, not just the average color-difference perception, but also accounting for the variability of color-discrimination decisions.

1. Overview of the McDonald Dataset

McDonald's publications describing the development of empirical-theoretical models during the 1980's were a major breakthrough in color-difference evaluation. In the first part of his work, McDonald³ generated a large pass/fail dataset. He produced samples of spun-polyester sewing thread by using a recipe-prediction program. The color centers were different in four lightness levels. Eight equally-spaced hue sectors were radially covered on chromaticity planes of the ANLAB50 color space (equivalent to CIELAB). Three color centers were chosen on each radial line. One lay near neutral gray; one lay near the edge of the gamut of the disperse dyes available; one lay at roughly half way between the edge of the gamut and neutral gray. Fifty five color centers were produced, which are shown in Fig. 1. 640 samples grouped around the 55 standards were uniformly distributed along the axes of

lightness, chroma and hue. Each of the eight observers performed pass/fail experiments five times for acceptability matching. A total of 25,590 pass/fail decisions were analyzed to provide acceptability ratings for each of the sample pairs.

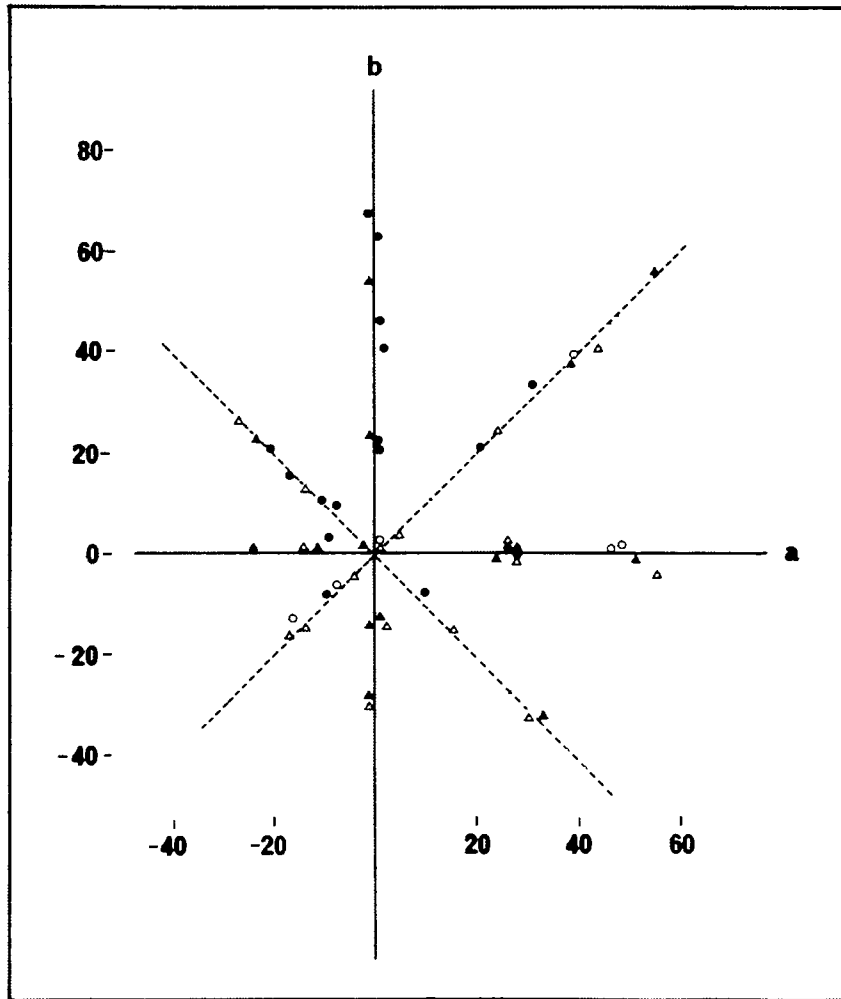


Fig. 1. ANLAB50 distribution of color centers lightness groups: Δ L42-L52; Δ L58-L63; o L74-L76; o L87-L91.³

McDonald then tried several different methods of fitting tolerance ellipsoids around each of these 55 color standards. The best method he found was the 'normal ogive curve fit' which converted the color difference values from the ellipsoids to percent acceptability values of the normal ogive from the calculation of the observers' standard deviation of color matching using least squares goodness criterion for curve fitting. The ANLAB50 major and minor axes of tolerance ellipsoids are shown in Fig. 2.

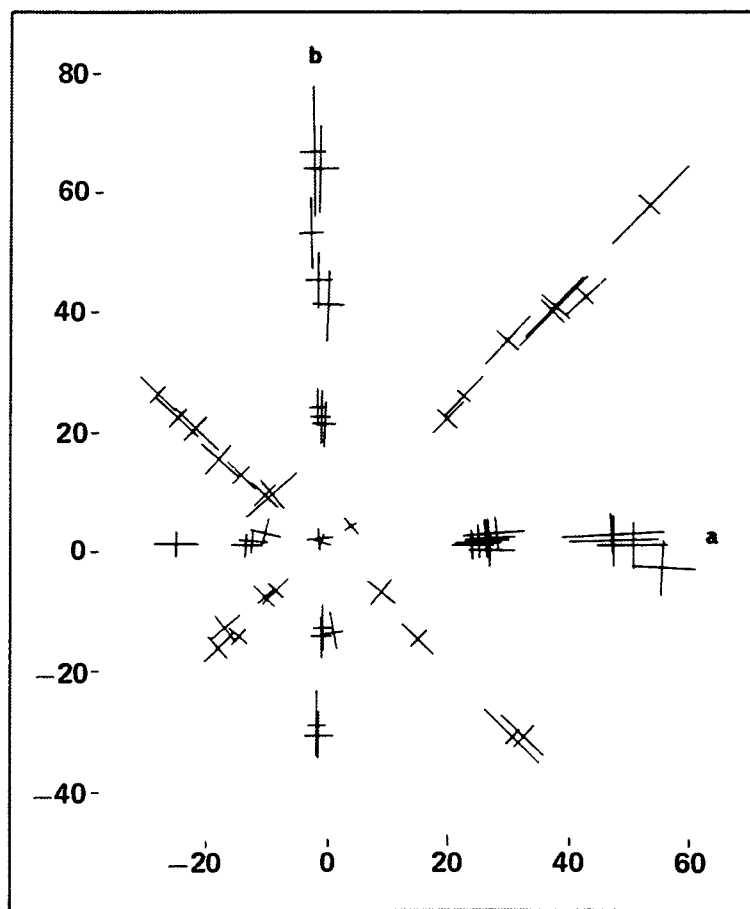


Fig. 2. ANLAB50 tolerance ellipsoids (full size).⁴

The results showed that the hue and chroma dimensions of the tolerance ellipsoids increased in size with the chroma of the color standards, and the lightness dimension increased with the lightness of the standards. The tolerance ellipsoids also varied in the hue dimension as the hue angle of the standards changed. The hue dimension of the tolerance ellipsoids seems smallest in the brown and violet regions and largest in the red and turquoise regions.

Based on these results, in the second part of his work, McDonald generated a much larger dataset of pass/fail decisions carried out by a single observer in a commercial dyehouse. 599 color standards were chosen, and 8454 pass/fail decisions were made. The visual color assessment was carried out under conditions similar to that of his first work described above. The JPC79 and the CMC color-difference equations were based on this single-observer dataset.⁵

2. Overview of the Witt Dataset

The CIE guidelines⁶ for coordinated research on color-difference evaluation (TC-1.3) encouraged further research on the perceptibility of color differences using samples in the neighborhood of five color centers and exploring systematic effects of the various parametric factors. The five centers are plotted in Fig. 3.

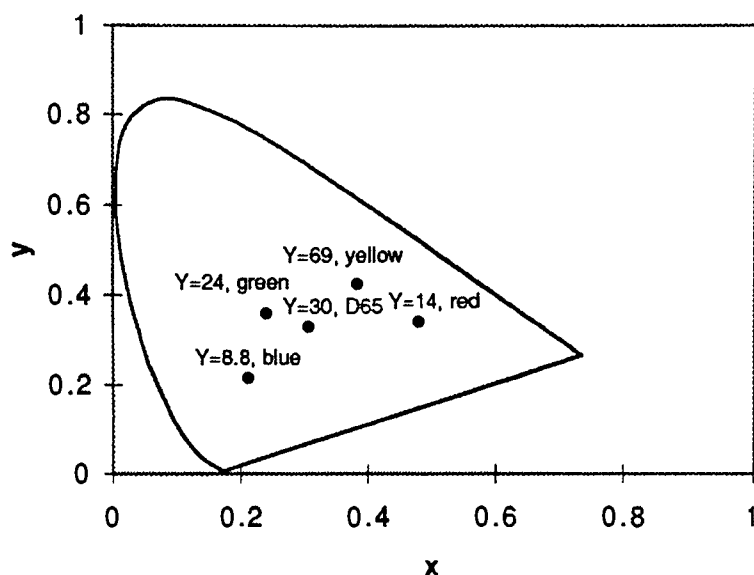


Fig. 3. Five color centers suggested by CIE TC -1.3.

As a pilot experiment, Witt, et al.⁷⁻⁸ tested the parametric variations in a threshold color-difference ellipsoid for green painted samples. They produced 54 more-or-less randomly distributed color samples near the green reference color by application of color-recipe formulation without changing pigmentation, but only concentration, in order to reduce metamerism. More than twenty observers performed two visual experiments. One was carried out by an absolute-threshold method. The other was carried out by a paired-comparison method. The paired comparison method was used to reduce the scattering of the absolute-threshold data, and yielded more certain judgments. Perceptibility ellipsoids at and near threshold were determined from different

mathematical models. The logistic function with the maximum-likelihood estimation was chosen following the proposal of the CIE guidelines.⁹

Based on this pilot work, the remaining color centers (red, yellow, white, and blue) were investigated. Sets of painted samples near these four color centers were produced. They clustered irregularly in tristimulus space. The color-difference pairs varied in color from zero to just perceptible. 50 to 64 sample pairs were selected about each color center. More than twenty observers performed the absolute-threshold visual experiments. The Monte-Carlo method of producing random deviates of variables were applied to produce deviation ellipsoids that described shells of uncertainty inherent in the data.

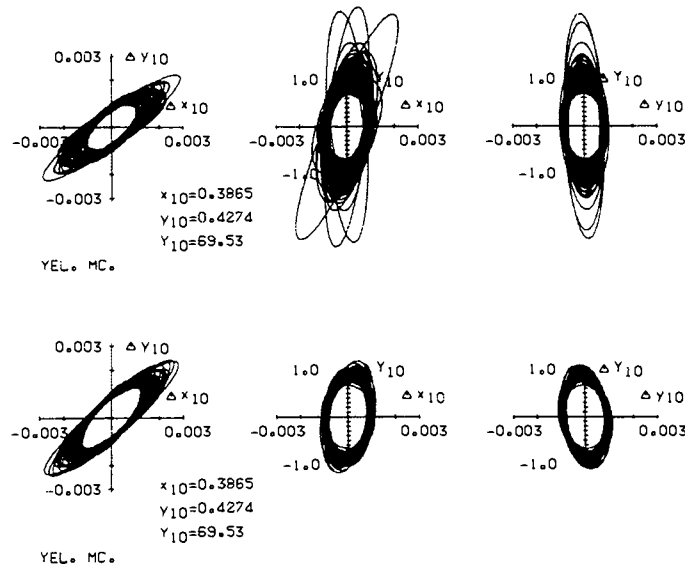


Fig. 4. Threshold ellipses in three planes in $\Delta(x_{10}, y_{10}, Y_{10})$ space for observer groups of yellow samples.⁷

It is clear that the amount of noise is quite evident, but it did not significantly distort the shape of the ellipsoids. These results indicate that color-difference formulas should be able to predict color differences within the shells of uncertainty.

3. Overview of the Luo and Rigg Dataset

The differences between the individual studies in color-difference tolerances are very difficult to quantify because the influence of factors such as the use of different visual scales, the use of different substrates, and the use of different levels of luminance are not well understood. This significant variability in the results of the individual experiments becomes a major barrier in the development of a universal color-difference metric. There is an urgent need to develop a reliable database representing a population's small color-difference decisions under conditions representative of industrial practice.² Luo and Rigg⁹ have addressed this problem by developing a self-consistent dataset of chromaticity-discrimination ellipses for surface colors based on thirteen published datasets deemed suitable for a limited visual experiment which was carried out to overcome the problems of the relative size of the ellipses.

The first step of this task was to generate their own experimental data. The samples were produced by dyeing plain wool serge with acid dyes. Ninety

color centers were studied in which seventy color centers were chosen similar to the centers previously studied, and twenty color centers close in chromaticity to five of the centers previously studied, but of different luminance factor. 413 sample pairs were generated close to these centers, with systematic differences in chromaticity and minor differences in luminance factor to enable the estimation of chromaticity-discrimination ellipses. All of the pairs were nonmetameric. Twenty observers participated in the visual experiments over a period of months. Observers judged each sample pair against a gray scale by using a ratio method. The experimental setup is shown in Fig. 5. Samples 1 to 5 were gray-scale samples. Observers were asked to pick a sample from the gray scale, put it along the standard, and compare the difference with that for the sample pair. Different gray-scale samples were tried until the one giving a difference from the standard closest in magnitude to that for the sample pair was found. The observers were also asked to give a grade to the sample pair. The grade indicated that how much larger that the color difference of the sample pair was than that between the standard and the chosen gray-scale sample. The advantage of using the ratio method is that it anchors the results to a fixed visual scale.

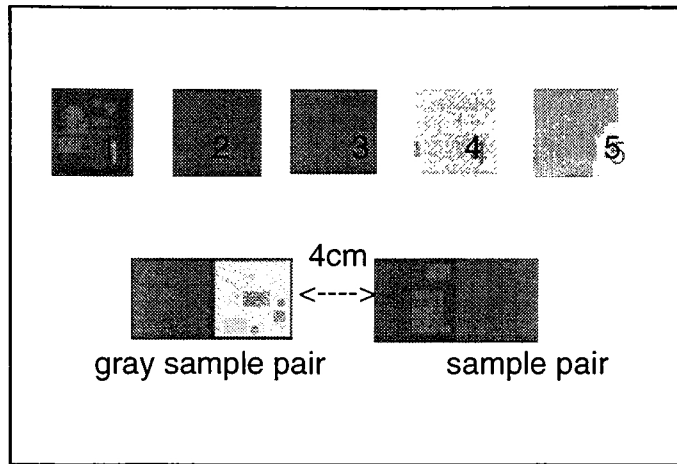


Fig. 5. Arrangement of samples for gray-scale assessments.⁶

They then calculated chromaticity-discrimination ellipses for each published dataset and tested the reliability of each-published ellipse. For each color center, the ellipses were calculated by altering the experimental data in small increments thereby simulating the estimated experimental errors. If an ellipse calculated from the simulated data did not differ greatly from that calculated from the original experimental data and if the plots of the ellipse fit the general pattern of the tilt angle θ and the axial ratios a/b values, the ellipse was considered to be reliable. A total of 132 reliable ellipses (94 chromaticity ellipses and 38 x , y , Y ellipsoids) were obtained.

The next step of their task was to produce a self-consistent set of ellipses. Seventy color centers were chosen from the thirteen published data sets. At least one color center from each data set was included. The centers chosen

were reasonably distributed over the chromaticity plane. It also included all of the color centers for which the ellipses appeared particularly odd. Samples of five centers were prepared at different luminance factors, so that it was possible to check the variation of chromaticity discrimination with luminance factor level.

The individual color centers were adjusted by applying assumptions about the influence of various parametric factors, using individual set factor (\bar{R}).

The set factor (\bar{R}) was defined as the mean of the ratio of a pair of samples $\Delta E/\Delta V$ where ΔE was calculated from the appropriate ellipse equation and ΔV was obtained from the gray scale assessment. If the individual value was not available for a particular color center, the appropriate set factor (SF) which was defined as the

mean of the \bar{R} values for each group was used. The size was adjusted on the basis of the gray-scale results. It was found that a luminance factor of 30 was an appropriate common value. These adjustments brought data from different sources onto a common scale. The results are shown in Fig. 6.

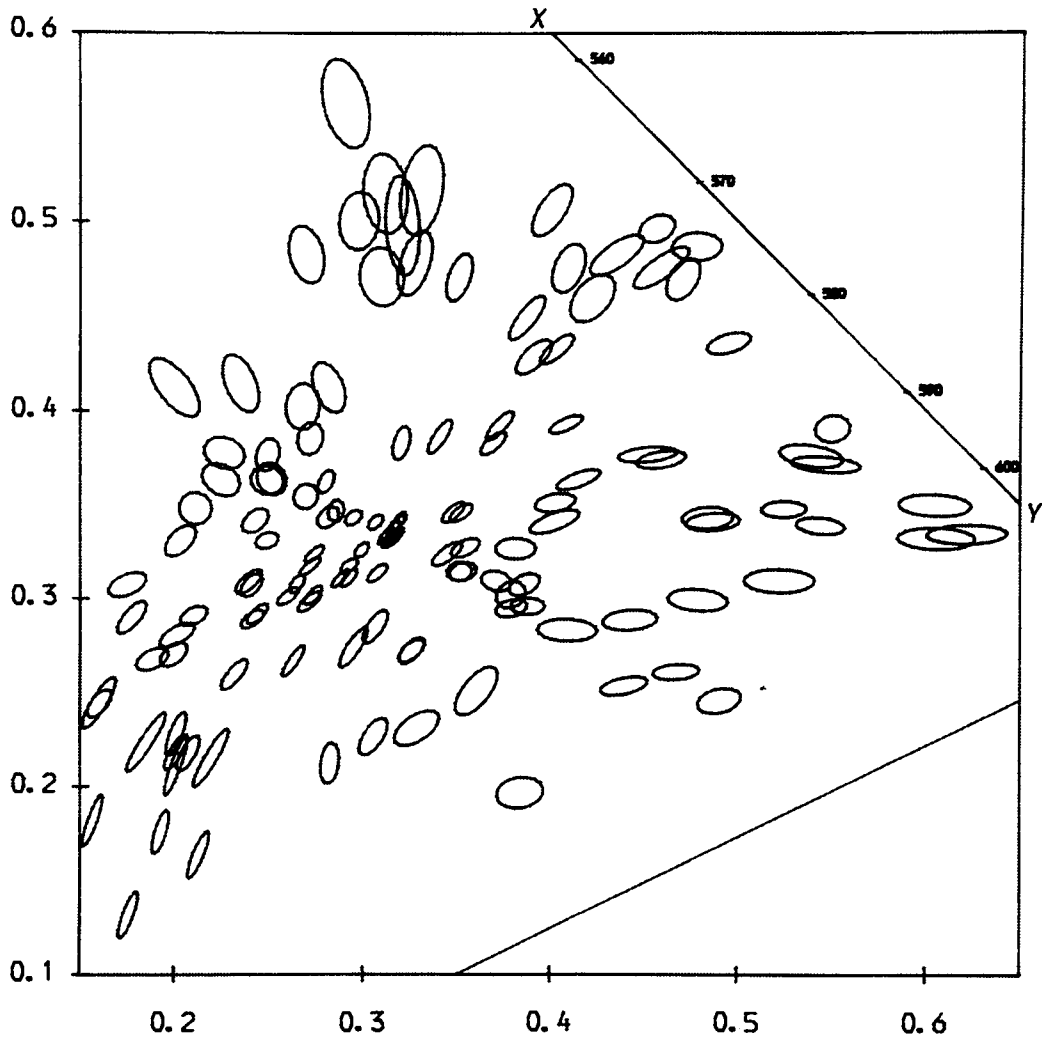


Fig. 6. Final ellipses after adjustment using individual color-center factors and $Y=30$.⁸

Fig. 6 shows that for any direction from the neutral point, the size tends to increase as this distance increases. The ellipses' tilt angle θ and axial ratios a/b varied systematically over the chromaticity diagram, the patterns from

acceptability, perceptibility, textile, and non-textile ellipses being very similar. These results indicate that the reliability of the ellipses are reasonable.

4. Overview of the RIT-Dupont Dataset

Berns and co-workers have chosen a different approach. They intended to develop a high-precision experimental-tolerance database representing small color-difference perceptions under conditions consistent with industrial practice. The research was performed in two phases. Phase I developed a precise performance-testing tolerance dataset of known uncertainty that was used to test the accuracy of existing color-difference metrics. The approach was unusual in that it explicitly treated population tolerances as distributions rather than as critical values represented by a boundary (e.g., ellipses) between acceptable and unacceptable differences. Phase II extended the Phase I experiments in order to develop a tolerance dataset with adequate sampling for the development of an improved tolerance metric.²

(1) Phase I: Performance testing of color-difference metrics ^{2,6}

Nine color positions were defined covering the range of chromatic variables in CIELAB space. They corresponded to a gray, four medium chroma hues (orange, yellow-green, blue-green, purple), and four high

chroma hues (red, yellow, green, blue). The color positions varied in lightness (L^*) so that the positions recommended for study by CIE TC 1.3 were included (gray, red, yellow, green, blue). CIELAB lightness varied from 79 (yellow) to 35 (blue) in such a way that a tilted plane near $L^*=50$ through the CIELAB space was sampled. Five vectors were sampled at each color position; $-L^*$ to L^* , $-a^*$ to a^* , $-b^*$ to b^* , $-a^*-b^*$ to $+a^*+b^*$ and $-a^*+b^*$ to $+a^*-b^*$. Samples were prepared at nominal color-difference positions of -2, -1, -0.5, -0.25, 0, 0.25, 0.5, 1, 2 units from the nominal color center along each vector. The samples were glossy acrylic-lacquer paints. Color-difference pairs varying from 0 to 4 units of difference were selected from these samples. Pairs were selected so that positive and negative sampling along each vector was balanced.

Ten observers participated in a pilot experiment which located the approximate tolerance value. Several color-difference stimuli were selected with color-difference magnitudes concentrated near the estimated tolerance and additional stimuli with distinctly smaller and larger color differences were provided to bracket the expected tolerance. Six to nine stimuli were presented for each color vector. The anchor color-difference stimulus was prepared using near-neutral gray samples yield a CIELAB total color difference of about unity. The color-difference stimulus subtended a 10° by 5°

field of view. The stimuli were illuminated by a filtered tungsten source approximating illuminant D65 (Macbeth spectralight). The illumination and viewing geometry was 0/45.

The 317 color-difference stimuli were arranged in a random order. There were four observer sessions with four sample sequences. The order of these sequences and direction through the random order were randomized for each observer. Fifty color-normal observers participated in the visual assessments. The observers made forced choice pass/fail judgments of the magnitude of the test stimulus visual color difference in comparison to the anchor stimulus. The experimental responses were the population frequency of rejection decisions. Probit analysis was applied to the response frequencies for each vector to estimate the parameters of the distribution and the median-tolerance values, T50. The tolerance determinations for 36 color-difference vectors (omitting the $-L^*$ to $+L^*$ vectors) at nine color centers are shown in Fig. 7. by filled circles connected by lines representing positive and negative T50 vectors from the center point for each vector.

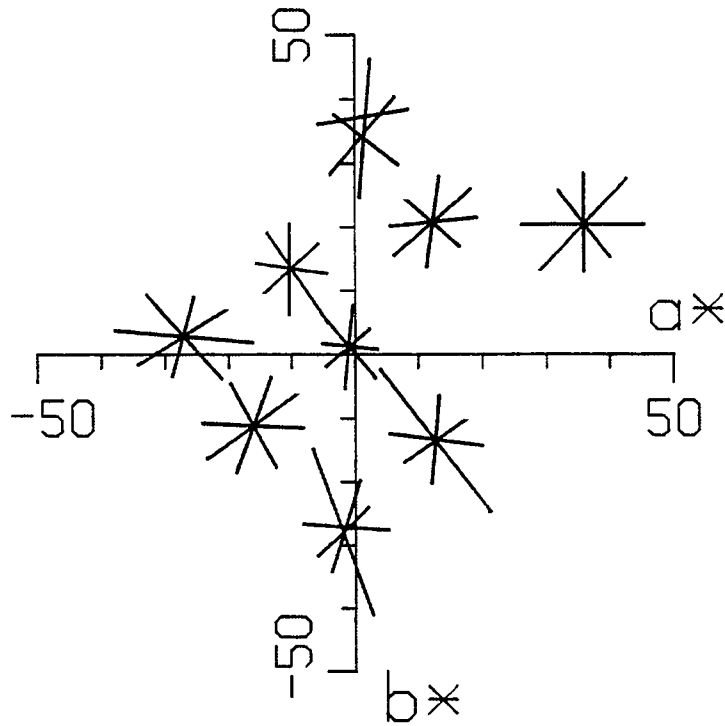


Fig. 7. An $a^* b^*$ plot of the equal color difference vector resulting from Phase I (magnified 5 times).¹⁰

The response-frequency results indicated that the underlying cumulative normal distribution adequately modeled the response distributions of the observer population and the weighted CIELAB color-difference metrics provided significant incremental improvement in color-difference uniformity compared to the current CIE recommended formulae. This approach provided an opportunity to improve color-difference metric performance while retaining the familiar CIELAB color space.⁶

(2) Phase II: Visual Determination of Suprathreshold Color-Difference Tolerance^{10,11}

The nine phase I color centers were positioned on a tilted plane in CIELAB space which included the five color centers recommended by CIE TC 1.3 for study. Five color centers were added above this plane (higher L^* values) and five color center were added below (lower L^* values). An effort was made to include near-white and black positions. The 19 color centers tested in Phase I and Phase II are plotted in Fig. 8.

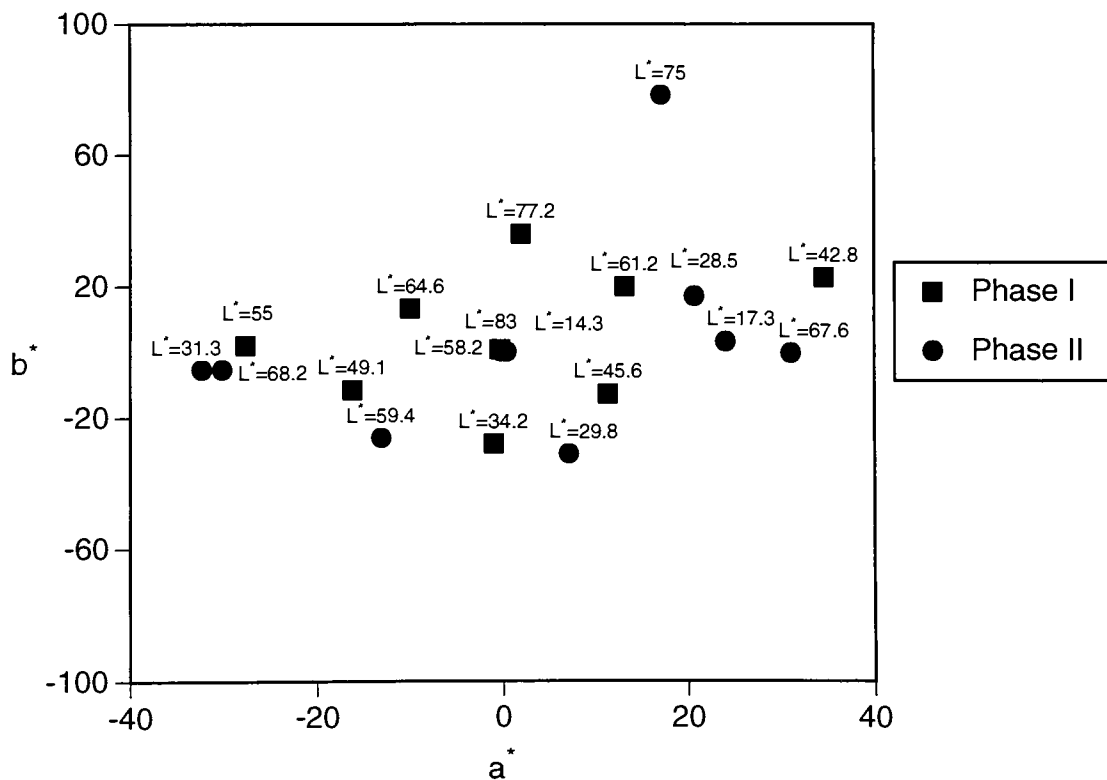


Fig. 8. Color centers studied in both Phase I and Phase II.

The five vector directions about each color center from phase I that varied independently in lightness and chromaticness were retained in Phase II. Since four out of these five vector directions varied within a^*b^* plane, and only one varied in the lightness (L^*) direction with constant hue and chroma, apparently, the color space was not adequately sampled for model development. The lack of sampling along the vector orientation which represented the interaction between the lightness and chromaticness would decrease the accuracy of any derived color-discrimination threshold ellipsoid. Four new vectors (F, G, H, I) were added shown in Fig. 9, to improve the three-dimensional sampling.

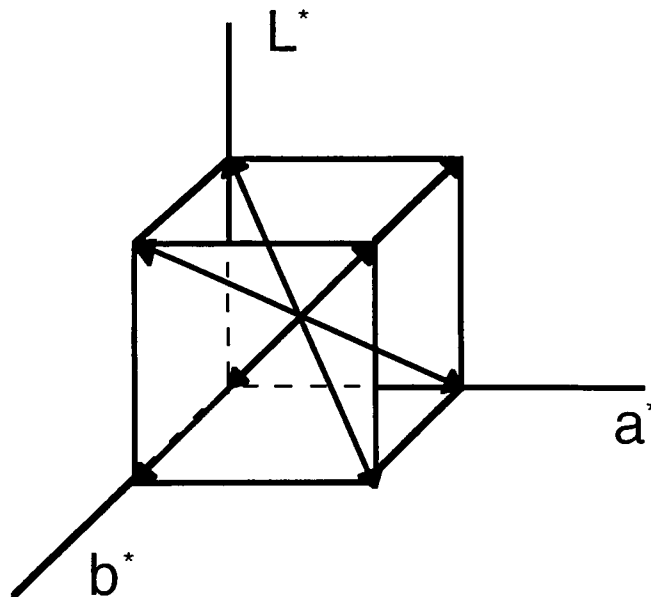


Fig. 9. Vectors directions F, G, H, and I, which simultaneously sample lightness and chromaticness.¹⁰

Samples were prepared, additionally, to sample the four new vectors for the phase I color centers. A total of 119 vectors, corresponding to 642 color-difference pairs, were scaled in a manner similar to the phase I experiment. Fifty color-normal observers judged the magnitudes of each difference pair relative to the same near-neutral anchor pair as was used in phase I. The same visual experimental method and statistical method were employed. The complete results of RIT-Dupont dataset are shown in Fig. 10 and Fig. 11.

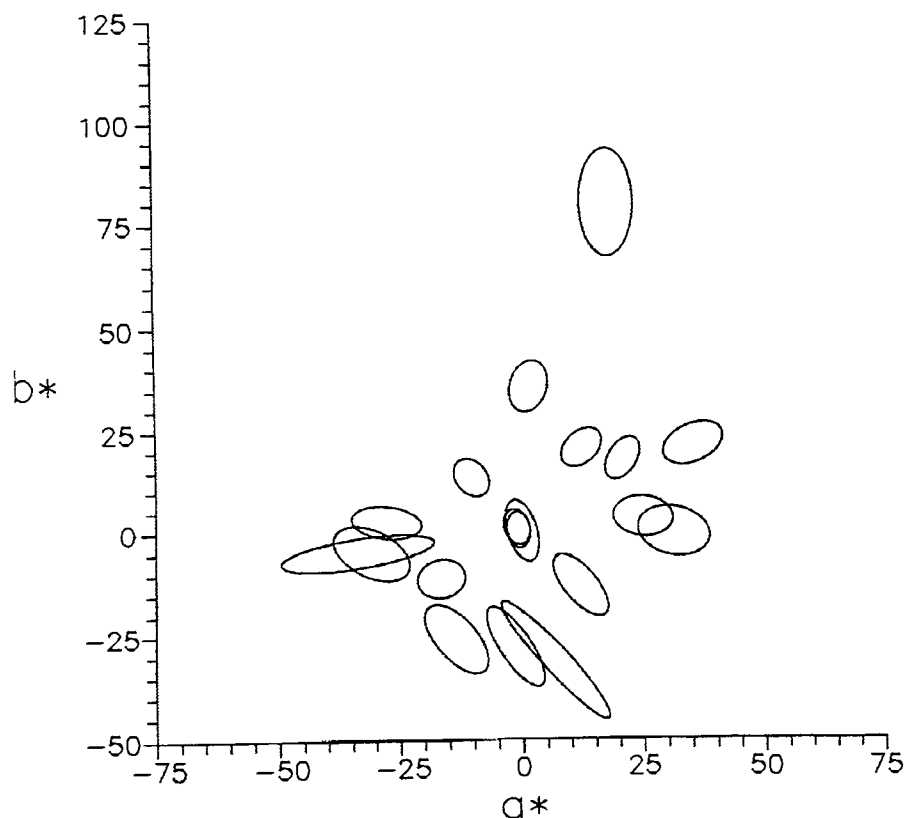


Fig. 10 Ellipses of RIT-Dupont dataset in chromaticness plane.

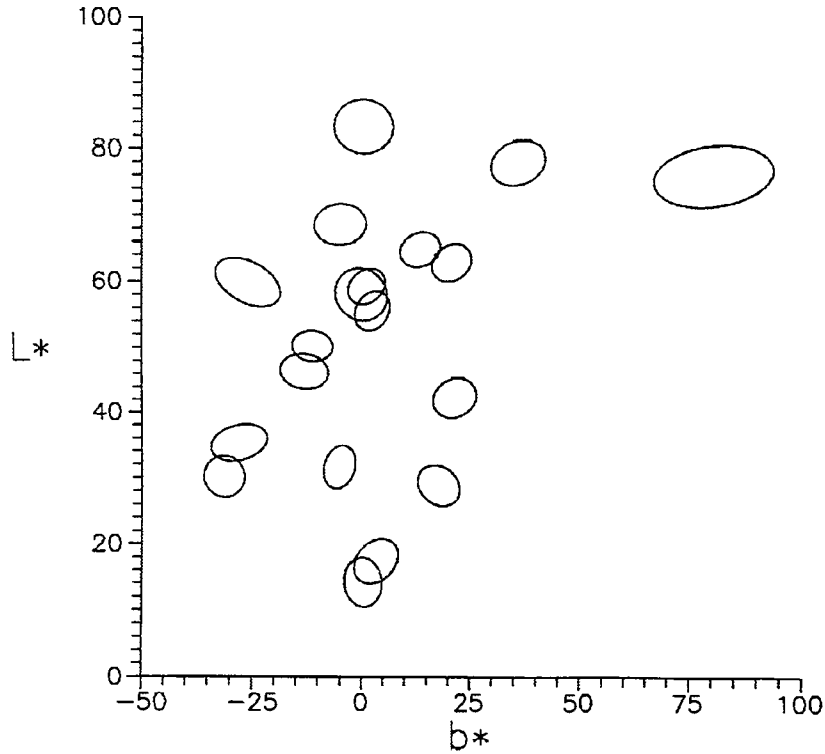


Fig. 11 Ellipses of RIT-Dupont dataset in L^*b^* plane.

The overwhelming trend in the plots was that the tolerance vectors were largest when orientated toward the origin. Differences of CIELAB chroma produced smaller visual responses than equivalent differences in CIELAB hue. The magnitudes also increased as the CIELAB chroma of the color center increased. Furthermore, the vectors that corresponded to CIELAB hue changes increased with increasing CIELAB chroma. The results indicated that CIELAB color differences in the range from 0.78 to 5.11 are perceptually equal to the unit color difference of the anchor pair.¹⁰

Overview of the Development of Color-Difference Equations

1. FMC-1 and FMC-2

Color difference can be assessed by two approaches, line elements and the color-difference formulae. Suppose there are two points P1 and P2 in three dimensional color space (U1, U2, U3). In Euclidean space, the color difference of these two points is the distance between P1 and P2 represented by ds.

$$ds^2 = (dU_1)^2 + (dU_2)^2 + (dU_3)^2 \quad (1)$$

In the use of line elements, Riemannian space is assumed:

$$\begin{aligned} ds^2 = & g_{11}(dU_1)^2 + g_{12}(dU_1 dU_2) + g_{22}(dU_2)^2 + g_{23}(dU_2 dU_3) \\ & + g_{33}(dU_3)^2 + g_{31}(dU_3 dU_1) \end{aligned} \quad (2)$$

These equations show that Euclidean space is a special case of Riemannian space. A color difference is a straight line in Euclidean space, and is a curve in Riemannian space. According to McDonald:¹³

“Line elements are normally based on threshold measurements and on standard deviations of color matching. All line elements proposed to date have been assumed to have the Riemannian form which defined the color difference by a positive quadratic equation for the just noticeable color difference ds. This means that for two samples in Riemannian color space, the color difference between them mathematically corresponds to integrating

the equation along the geodesic distance between the two points and dividing the result by the constant value, ds , representing the least perceptible difference."

In the 1960's, Friele¹³ transformed the experimentally-determined color matching ellipsoids of Brown and Brown-MacAdam into line elements using estimates of the fundamental primaries of the visual mechanism. Chickering then optimize Friele's line elements by using the ellipses of one of MacAdam's observers data. This optimization resulted in the FMC-1 equation.

$$\Delta E = (\Delta C^2 + \Delta L^2)^{1/2} \quad (3)$$

where

$$\Delta C = [(\Delta C_1)^2 + (\Delta C_3)^2]^{1/2} \quad (4)$$

ΔC_1 and ΔC_3 represented the yellow-blue red-green components of chromaticness differences respectively. The ΔL consisted of the "Friele-type" lightness difference.

Chickering then extended it into three dimensions resulting in the FMC-2 equation.

$$\Delta E = (K_1(\Delta C)^2 + K_2(\Delta L)^2)^{1/2} \quad (5)$$

where ΔC and ΔL were the same definitions as those in the FMC-1. K_1 and K_2 are functions of luminance factor. The FMC-2 equation was recommended by the CIE in 1967 for further study and was used widely in industry before 1976.

2. CIELAB and CIELUV

In 1976, CIE recommended the use of two alternative color spaces. One is CIELAB, which was based on the Munsell color order system and derived from ANLAB. The only difference between CIELAB and ANLAB is that the complex 5th degree Judd polynomial was replaced by the much simpler cube root equation.

$$\begin{aligned}
L^* &= 116(Y/Y_n)^{1/3} - 16 && \text{for } Y/Y_n > 0.008856 \\
L^* &= 903.3(Y/Y_n) && \text{for } Y/Y_n \leq 0.008856 \\
a^* &= 500[(X/X_n)^{1/3} - (Y/Y_n)^{1/3}] && X/X_n > 0.008856 \\
&&& \text{for } Y/Y_n > 0.008856 \\
b^* &= 200[(Y/Y_n)^{1/3} - (Z/Z_n)^{1/3}] && Z/Z_n > 0.008856
\end{aligned} \tag{6}$$

The rectangular color co-ordinates, L^* , a^* , b^* are calculated for each color sample from the X , Y , Z tristimulus values of the sample and X_n , Y_n , Z_n , the tristimulus values of a perfect reflecting diffuser with respect a specified illuminant and observer. Because these ratios of the tristimulus values are incorporated as cube-root, there is no chromaticity diagram associated with the CIELAB space, and therefore no correlated of saturation.

The other recommended space is CIELUV, which was based on MacAdam's rectangular uniform chromaticity diagram derived from the Judd uniform chromaticity diagram. It is a modification to the 1964 CIE $U^*V^*W^*$ formula.

$$\begin{aligned}
L^* &= 116(Y/Y_n)^{1/3} - 16 && \text{for } Y/Y_n > 0.008856 \\
L^* &= 903.3(Y/Y_n) && \text{for } Y/Y_n \leq 0.008856 \\
u^* &= 13L^*(u' - u'_n) \\
v^* &= 13L^*(v' - v'_n)
\end{aligned} \tag{7}$$

The CIELUV space has been widely used in television industry because of the very simple way in which additive color mixtures are presented on the $u'v'$ chromaticity diagram.

These formulae provided the basis for color tolerances by quantifying the differences between colors. But the main deficiency is that both CIELAB and CIELUV are not uniform enough for critical color-difference work and provided only simplistic chromatic adaptation models.

3. JPC 79 and CMC(l:c)

In the late 70's, McDonald developed an empirical-theoretical model, JPC79. He analyzed his own pass/fail small color-difference datasets and established weighting functions to correct the variation sensitivity to lightness difference, chroma difference and hue difference based on the older ANLAB50 color-difference formula, the predecessor of CIELAB. He found that the chroma

limits for acceptability dyeing were large and increased significantly as the chroma of the target increased. The hue limits also increased significantly with chroma but were much smaller limits than the chroma limits. The lightness limits were not found to increase with chroma but did increase significantly with increase in lightness of the target. JPC79 was derived based on these facts.

$$\Delta E = \left[\left(\frac{\Delta L^*}{L_t} \right)^2 + \left(\frac{\Delta C^*}{C_t} \right)^2 + \left(\frac{\Delta H^*}{H_t} \right)^2 \right]^{1/2} \quad (8)$$

where

$$L_t = 0.149L_1^* / (1 + 0.0155L_1^*),$$

$$C_t = 0.105C_1^* (1 + 0.115C_1^*) + 1.2$$

$$H_t = T * C_t$$

$$\text{if } \theta < 164^\circ \text{ or } \theta > 345^\circ$$

$$\text{then, } T = 0.36 + |0.4 \cos(\theta + 35)|$$

$$\text{otherwise, } T = 0.56 + |0.2 \cos(\theta + 168)|$$

This formula represented a substantial improvement over earlier efforts such as the 1976 CIELAB formula. The agreement with published data was much better and the formula was applied successfully in industrial shade passing. However, there were several problems when using the formula. First, it was found that the JPC79 formula was too tight for very dark samples with lightness less than 16. Second, in the JPC79 formula, there was a unsatisfactory discontinuity where the elliptical chromaticity cross section of the tolerance ellipsoid was made to change abruptly to a circle for samples with chroma less than 0.638.¹⁴ The third problem was that since the JPC79 formula was derived based on acceptability dataset, it was found to give poor performance when applied to perceptibility data.

In 1984, CMC (l:c) was derived to overcome the JPC79 deficiencies. The formula was based on a large dataset of a single observer's observations. The final CMC(l:c) formula is

$$\Delta E = \left[\left(\frac{\Delta L^*}{1 S_L} \right)^2 + \left(\frac{\Delta C_{ab}^*}{c S_C} \right)^2 + \left(\frac{\Delta H_{ab}^*}{S_H} \right)^2 \right]^{1/2} \quad (9)$$

where

$$S_L = 0.040975 L_1^* / (1 + 0.01765 L_1^*),$$

unless $L_1^* < 16$ $S_L = 0.511$

$$S_C = 0.0638 C_{ab,1}^* / (1 + 0.0131 C_{ab,1}^*) + 0.638$$

$$S_H = S_C (Tf + 1 - f)$$

$$f = \{ (C_{ab,1}^*)^4 / [(C_{ab,1}^*)^4 + 1900] \}^{1/2}$$

if $h_{ab,1} < 164^\circ$ or $h_{ab,1} > 345^\circ$

$$\text{then, } T = 0.36 + |0.4 \cos(h_{ab,1} + 35)|$$

$$\text{otherwise, } T = 0.56 + |0.2 \cos(h_{ab,1} + 168)|$$

and where L_1^* , $C_{ab,1}^*$, $h_{ab,1}$ refer to the standard of a pair of samples, these values and ΔL^* , ΔC_{ab}^* , and ΔH_{ab}^* being calculated from CIELAB. S_L , S_C , S_H indicate the lengths of the half-axis of the ellipsoid defining unit ΔE .

The “l” and “c” attributes were chosen to give the most appropriate weighting of differences in lightness and chroma, respectively, relative to differences in hue. For predicting the perceptibility of color differences, l and c are both set equal to unity, and this is referred to as CMC(1:1) formula. For predicting the acceptability of color differences, it is sometimes preferable to set l and c at values greater than unity, normally, it is referred as CMC(2:1).

The lightness, chroma, and hue weighting functions are shown in Figs. 12-14.

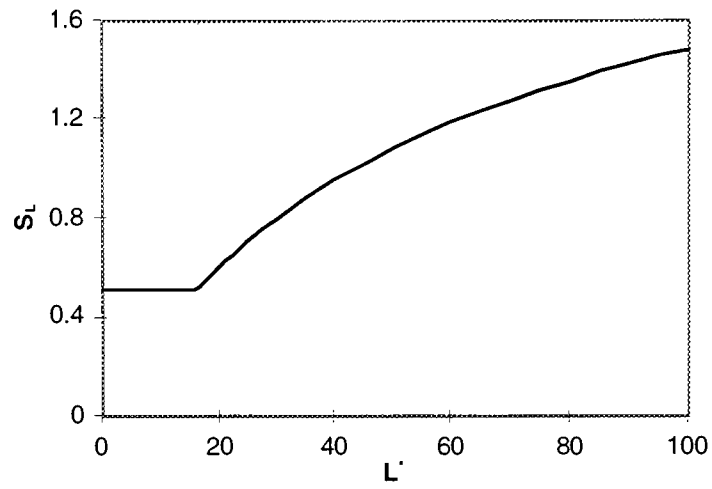


Fig. 12. The relationship between L^* and S_L factors.

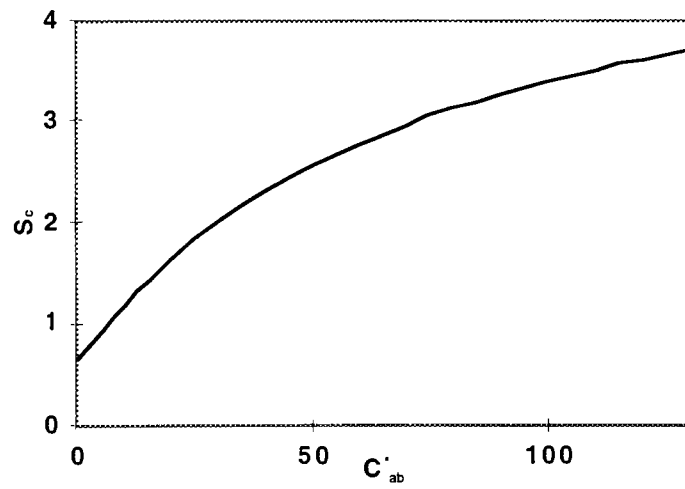


Fig. 13. The relationship between C_{ab}^* and S_c factors.

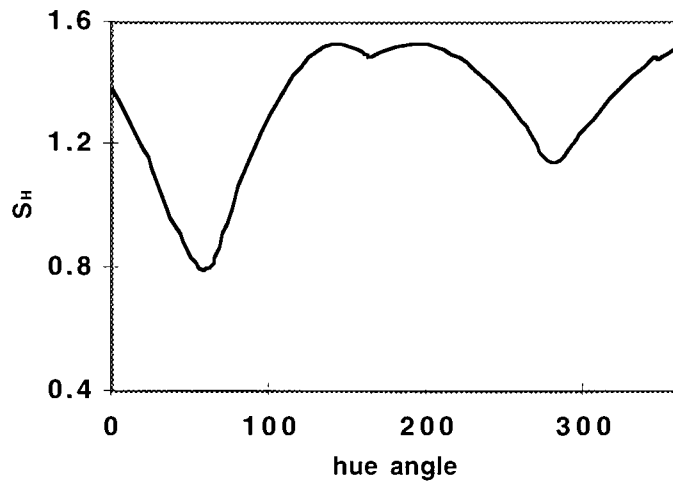


Fig. 14. The relation between the ratio T and angle θ .

The CMC color-difference formula was found to give better correlation for quantifying the perceptibility of color differences than CIELAB. It was recommended by the Society of Dyers and Colourist's Color Measurement Committee during the 1980's. Now it is widely used in industry, especially the textile industry where it will soon be recommended internationally. One of the disadvantages of the CMC(l:c) formula is that there is no associated uniform Euclidean color space.¹⁵

4. BFD(l:c)

Kuehni¹⁶ has claimed that one disadvantage of the JPC79 formula was that constant CIELAB ellipses based on the formula all point along lines of constant hue in an a^*b^* plot. The CMC formula suffers from the same defect.

As mentioned above, in 1986, Luo and Rigg⁹ developed a data set which pooled the results of earlier experiments together with new results forming a new large dataset. Rigg and Luo¹⁸ then evaluated ellipse dataset in CIELAB space and found that ellipses did not all point along lines of constant hue, supporting Kuehni's claim. This phenomenon is particularly severe in the saturated blue region, where all the experimental ellipses have higher θ and a/b values than the JPC79 or CMC formulae ellipses. This is shown in Fig. 15.

One way to overcome this problem is to introduce a $\Delta C_{ab}^* \Delta H_{ab}^*$ component into the color-difference formula, resulting in the BFD(l:c) color difference formula.

$$\Delta E(\text{BFD}) = \left[\left(\frac{\Delta L^*}{1} \right)^2 + \left(\frac{\Delta C_{ab}^*}{c D_C} \right)^2 + \left(\frac{\Delta H_{ab}^*}{D_H} \right)^2 + R_T \left(\frac{\Delta C_{ab}^*}{D_C} \right) \left(\frac{\Delta H_{ab}^*}{D_H} \right) \right]^{1/2} \quad (10)$$

Where

$$D_C = 0.035 \bar{C}^* / (1 + 0.00365 \bar{C}^*) + 0.521$$

$$D_H = D_C (G_T + 1 - G)$$

$$G = \left\{ \left(\overline{C_{ab}^*} \right)^4 / \left[\left(\overline{C_{ab}^*} \right)^4 + 14000 \right] \right\}^{1/2}$$

$$T = 0.627 + 0.055 \cos(\overline{h_{ab}} - 254^0) - 0.040 \cos(2\overline{h_{ab}} - 136^0) + \\ 0.070 \cos(3\overline{h_{ab}} - 32^0) + 0.049 \cos(4\overline{h_{ab}} + 114^0) - 0.015 \cos(5\overline{h_{ab}} - 103^0)$$

The value of R_T value determines the extent of rotation of the ellipses.

$$R_T = R_H R_C$$

$$R_C = \left\{ \left(\overline{C^*} \right)^6 / \left[\left(\overline{C^*} \right)^6 + 7 * 10^7 \right] \right\}^{1/2}$$

$$R_H = -0.260 \cos(\overline{h_{ab}} - 308^0) - 0.379 \cos(2\overline{h_{ab}} - 160^0) - \\ 0.636 \cos(3\overline{h_{ab}} + 254^0) + 0.226 \cos(4\overline{h_{ab}} + 140^0) - 0.194 \cos(5\overline{h_{ab}} + 280^0)$$

The terms, $\overline{C_{ab}^*}$ and $\overline{h_{ab}}$, refer to the mean of the C_{ab}^* and h values for the standard and sample, these values ΔC^* and ΔC_{ab}^* being calculated from the CIELAB formula. The visual ellipses in comparison with the BFD(l:c) ellipses are shown in Fig. 16.

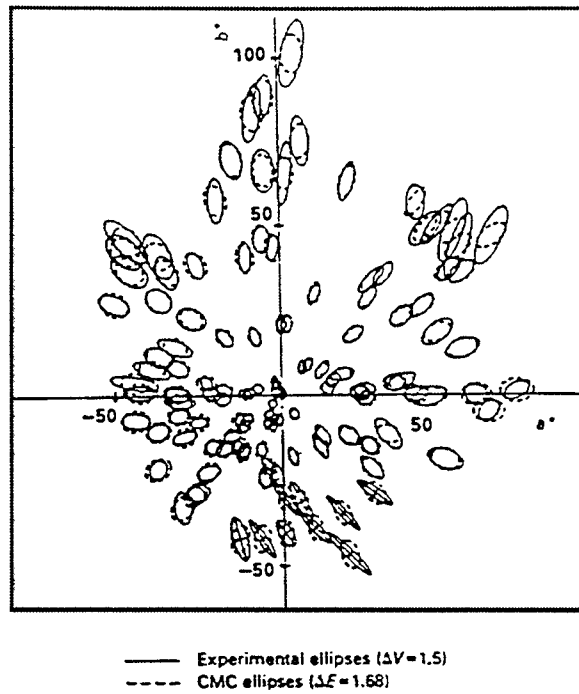


Fig. 15. Comparison of experimental ($\Delta V=1.5$) and CMC ($\Delta E=1.68$) ellipses.¹⁸

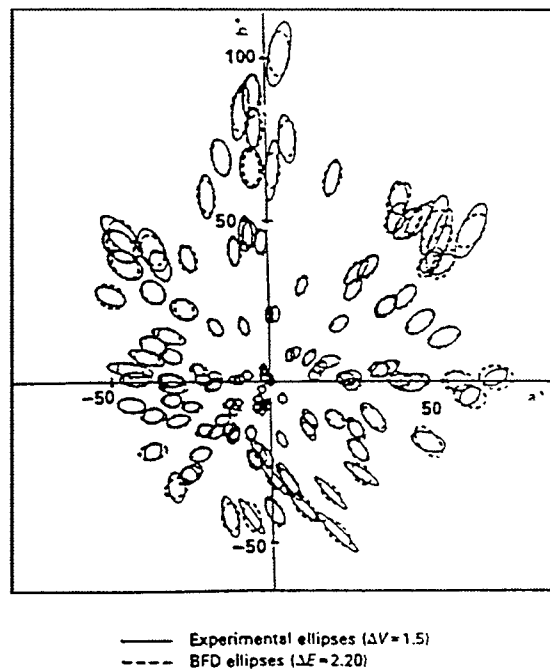


Fig. 16. Experimental ellipses ($\Delta V=1.5$) and BFD ellipses ($\Delta E=2.20$).¹⁸

It is clear that the agreement between the experimental ellipses and those from the BFD formula is better in the saturated blue and red regions than that in Fig. 15 showing the CMC predictions.

Overall, the BFD(l:c) formula is a modification of the CMC(l:c) with a new lightness function, newly derived coefficients, and an added feature which accounts for color-difference ellipsoids which do not have their major axis aligned with a CIELAB constant hue locus.

5. CIE94

The newest formula, CIE94, was disclosed in 1994.¹⁷ Three datasets were selected for study, Witt,⁷⁻⁸ Luo and Rigg,⁹ and Berns, et al.¹⁰⁻¹¹ These three datasets were discussed above. Each dataset consists of equal visual tolerances with different magnitude. These datasets were selected because of their use of surface colors, the number of observers used, and their inclusion of visual uncertainty estimates. Maier⁶ transformed the Witt and Luo and Rigg x , y ellipses and x , y , Y ellipsoids to L^* , a^* , b^* coordinates and from them, derived CIELAB lightness, chroma, and hue tolerances. Maier also derived tolerances from the RIT-Dupont vector dataset. Berns adjusted each dataset to a common visual scale to facilitate quantitative comparisons.

The development of the CIE94 equation began with an analysis of the normalized tolerances. The data were used to plot ΔL^* vs. L^* , ΔC_{ab}^* vs. C_{ab}^* , ΔH_{ab}^* vs. C_{ab}^* , and $\Delta H_{ab}^* / (1 + 0.015 C_{std}^*)$ vs. h_{ab} .¹⁹ They are shown in Figs. 17, 20, respectively.

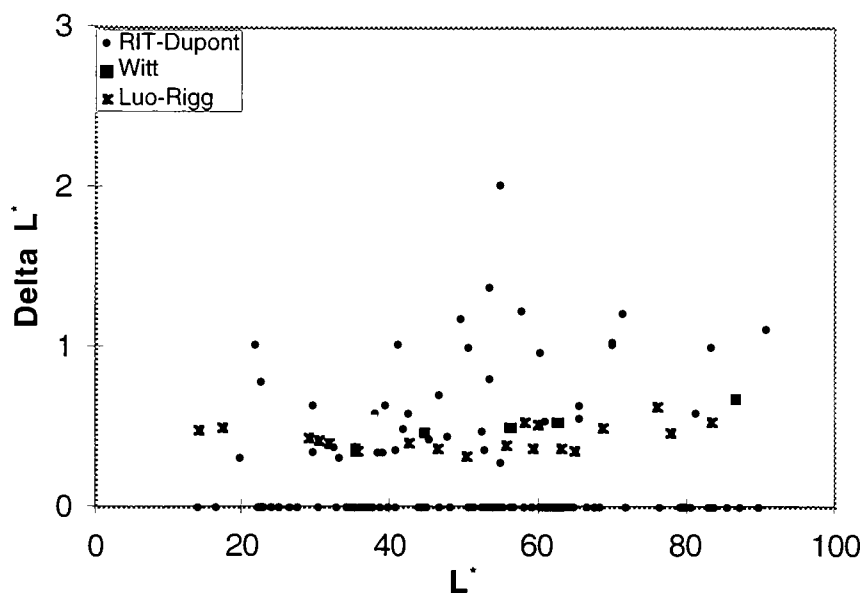


Fig. 17. Equal visual lightness differences.¹⁹

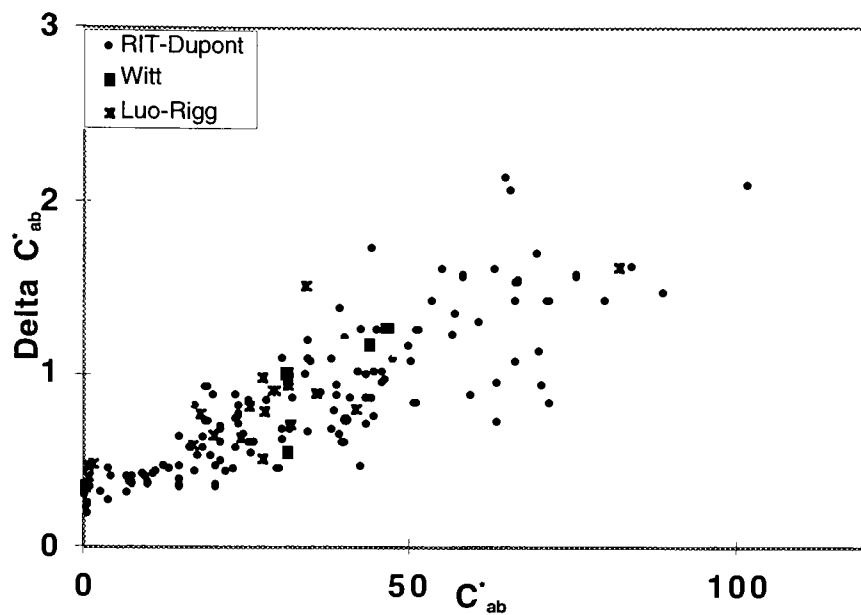


Fig. 18. Equal visual chroma differences.¹⁹

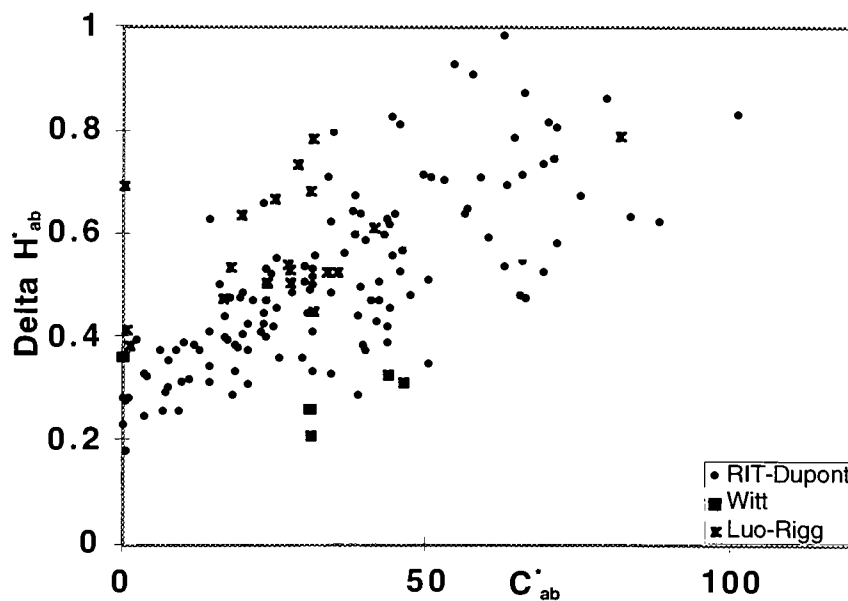


Fig. 19. Equal visual hue differences.¹⁹

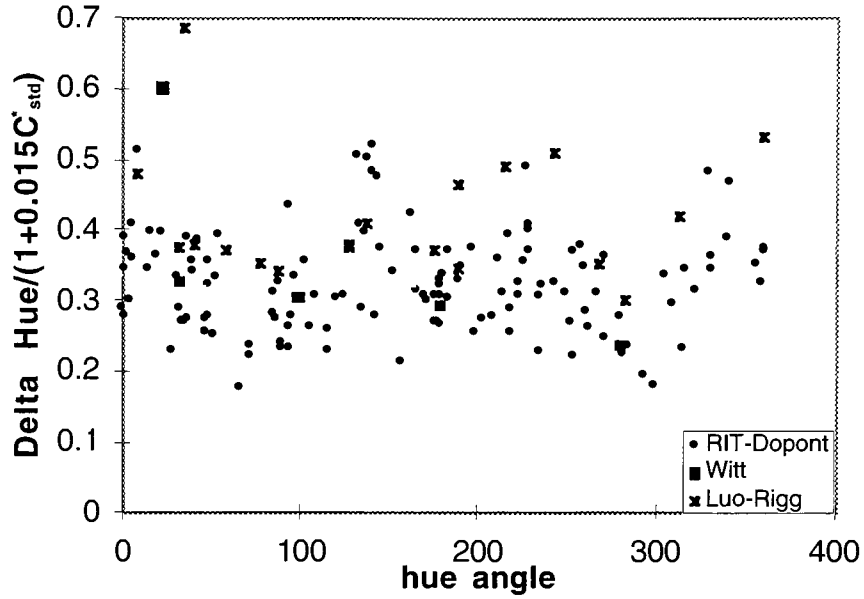


Fig. 20. Equal visual hue differences corrected for chroma position.¹⁹

From the plots, it is clear that the dependence of lightness difference on lightness varied significantly among the three datasets. These inconsistencies may be due to different parametric factors, such as different viewing conditions, different samples, and different visual assessments. The plot is not consistent with the CMC lightness correction. The CMC lightness weighting function was unsupported. The chroma trends were consistent among datasets. The chroma position strongly correlated with ΔC_{ab}^* and weakly correlated with ΔH_{ab}^* . The trends of the data indicate that it was appropriate to model these relationships by linear equation. The dependence of chroma-difference and hue-difference sensitivities on chroma is the key

element of the CMC(l:c) equation leading to improved correlation with visual perception. Fig. 19 shows that there is no clear indication of the relationship between hue angle and hue difference. The random nature of the data indicates that the practice of hue angle dependent weighting functions as derived in the CMC and the BFD equations, was questionable. The CMC equation has hyperbolic functions dependent on lightness and chroma describing the S_L , S_C , and S_H weights and a cosine function dependent on h_{ab} . The plots suggest that these nonlinear functions are not suitable for the three datasets tested.

Based on the results of testing the three datasets, the following general equation was defined.

$$\Delta E = \left[\left(\frac{\Delta L^*}{\beta_{0,L}} \right)^2 + \left(\frac{\Delta C_{ab}^*}{\beta_{0,c} + \beta_{1,c} C_{ab}^*} \right)^2 + \left(\frac{\Delta H_{ab}^*}{\beta_{0,h} + \beta_{1,h} C_{ab}^*} \right)^2 \right]^{1/2}$$

where the coefficients, $\beta_{0,L}$, ... $\beta_{1,h}$, would be optimized using reliable datasets. The RIT-Dupont and Luo and Rigg datasets were used and resulted in the CIE94 equation.

A sensitivity analysis was also performed¹⁹ to test the effectiveness of the various component of the CMC equation in predictivity the RIT-Dupont

dataset. Only the S_C function resulted in significant improvement. The S_C function decreased performance while the S_H hue angle component had an insignificant effect.

$$\Delta E^*_{94} = \left[\left(\frac{\Delta L^*}{K_L S_L} \right)^2 + \left(\frac{\Delta C^*}{K_C S_C} \right)^2 + \left(\frac{\Delta H^*}{K_H S_H} \right)^2 \right]^{1/2} \quad (11)$$

where

$$S_L = 1.0, \quad S_C = 1.0 + 0.045 C_{ab}^*, \quad S_H = 1.0 + 0.015 C_{ab}^*$$

$K_L = K_C = K_H = 1$ under reference conditions

$K_L = 2; K_C = K_H = 1$ for the textile industry

The CIE94 equation is simple and easily understood. It is believed that this equation is a superior model that can correct the limitation of CIELAB in correlating with industrial tolerances. It has been recommended by CIE for testing and further improvement.

It is critical to point out that current tolerance equations such as the CMC(l:c) and the CIE94 equations do not model many of the important factors affecting tolerance judgments. These include sample geometric attributes such as texture and gloss and viewing conditions such as sample separation,

illuminance level, and background luminance factor.¹ They also are constrained to orient along CIELAB constant hue loci.

Purpose of Current Thesis

One of the disagreements between CMC and CIE94 is the hue weighting function. Evaluating the relevance and significance of hue weights found in CMC and CIE94 could be a key to improve a perceptually nearly uniform color-difference equation. It is felt that more research needs to be performed. In particular, additional visual experiments are needed focusing on possible hue-angle dependencies and in quantifying parametric effects. Moreover, the datasets that we have do not completely sample the gamut of surface-color space. There are still some regions in color space that have not been adequately tested by visual experimentation such as the purple-blue region. Thus more experimental data are required to validate this lack of effect.²⁰

The current thesis topic was identified by the Munsell Color Science Laboratory's Industrial Color Difference Evaluation Consortium. The purposes of this thesis are to develop more experimental data to describe consumers' color-difference judgment behavior along hue direction that add to the RIT-Dupont dataset and to test hue-weighting functions of current color-difference formulae.

The thesis is outlined in Table I.

Table I. Thesis outline.

outline	purposes	details
Experiments on Background and surround effect	Testing the significance of the change in background and surround from the background with $L^*=38$ used in Phase I and II to CIE TC1-29 reference background with $L^*=50$.	<ol style="list-style-type: none"> 1. Samples used in Phase I and II were mounted on two different backgrounds. 2. Conducting psychophysical experiments on background effect. 3. Probit analysis on data.
Fuji printer testing	Samples used in Main experiments were printed from Fuji printer	<ol style="list-style-type: none"> 1. Tested the uniformity and gamut of the Fuji printer. 2. Tested mathematical model and lookup table for Fuji printer.
Sample design	Determining color centers studied in the main experiments.	<p>39 color centers were chosen,</p> <p>--3 of CIE recommended colors, red, green and blue.</p> <p>--3 complete hue circles at $L^*=60$, $C_{ab}^*=20$; $L^*=40$, $C_{ab}^*=20$; and $L^*=40$, $C_{ab}^*=35$.</p>
Sample preparation	Preparing samples for the main experiments.	<ol style="list-style-type: none"> 1. Printed samples from Fuji printer. 2. Selected 10 pairs of samples around each color center in the hue direction. 3. Mounted samples on background.
Psychophysical experiments on hue discrimination	Testing the perception of color differences in hue direction.	Conducted two-session psychophysical experiments.
Statistical Analysis	Analyzing visual data.	Applied logic program with 3-d normit function and calculated T50 values and fiducial limits.
Model the hue weighting function	Fitting data with possible functions.	<ol style="list-style-type: none"> 1. Tested current available hue weighting function of color-difference formulae. 2. Fit data with proper function.

EXPERIMENTS ON BACKGROUND AND SURROUND EFFECT

Under the recommendations from the first meeting of the color-difference consortium, the experiment was carried out under the reference condition of CIE TC1-29. Comparing these reference conditions with those used in Phase I and Phase II, the lightness of the background should be changed from 38 to 50. It was necessary, therefore, to perform visual assessments to test the significance of the change in background. Thus, the consistency of the dataset on hue-discrimination developed in this research with previous RIT-Dupont dataset was tested.

Experiments

All samples used in this experiment were chosen from those used in Phase I and Phase II in order to test the significance of the change in only background. The materials used to produce the anchor pairs and samples were glossy acrylic paints sprayed on an aluminum substrate. Two color centers were chosen. They were neutral gray with $L^*=58.2$, $a^*=-0.3$, $b^*=0.8$ and cyan with $L^*=49.1$, $a^*=-16.2$, $b^*=-11.5$. Cyan was chosen because the lightness of cyan was close to the lightness of the CIE recommended background ($L^*=50$). Crispening effect was expected to occur.²¹ The crispening occurs

when the lightness of the sample pairs are close to the lightness of the background. The crispening effect enhances the sensitivity of the observer to the lightness difference between the sample pair.

The colors were sampled along three directions for each color center. The three vectors were chosen from the eight vectors studied in Phases I and II.¹² One was along the lightness direction, $-L^*$ to $+L^*$, which was called vector A; one was along chromaticness direction, $-a^* - b^*$ to $+a^* + b^*$, which was called vector D; and one was along $-L^* + a^* - b^*$ to $+L^* - a^* + b^*$, which was called vector G representing the interaction between lightness and chromaticness. The names of these three vectors were also the same as those used in Phases I and II.

Samples were mounted on two different backgrounds. One was the same as used in Phases I and II, which was a 4"x6" aluminum gray panel with lightness around $L^*=38$. This background is called the RIT-background. The other was the same size, but made from gray cardboard with a lightness around $L^*=50$. This background will be referred to as the CIE-reference background. From the results of the Phase II research, 5-7 sample pairs for each vector were a sufficient number for statistical reliability. Accordingly, six sample pairs were chosen for each vector on each background. The samples on the RIT background were chosen from those used in Phases I and II. Sample pairs on the CIE-reference background were carefully chosen from the

materials left over from Phases I and II. They were measured to make sure that the colors of each sample pair were close enough to those of each sample pair of the RIT background. They then were cut into 2"x2.5" rectangles, the same size as used previously, by the bench sheer located in the College of Fine and Applied Arts metal shop at RIT. The pieces were attached to the CIE-reference background using thin, double sided carpet tape. The Milton Roy ColorScan 45/0 spectrophotometer was used for the sample measurements.

The anchor pair used in Phase I and Phase II was missing. The new anchor pairs were made from the remaining materials in Phase I and Phase II. One of the new anchor pair was mounted on the RIT background. One sample was $L^*=48.50$, $a^*=0.25$, $b^*=4.24$; the other was $L^*=47.96$, $a^*=0.56$, $b^*=3.42$. The ΔE_{ab}^* color difference was 1.02. The other anchor pair was mounted on the CIE-reference background. One sample was $L^*=48.52$, $a^*=0.24$, $b^*=4.21$; the other was $L^*=47.96$, $a^*=0.57$, $b^*=3.45$. The ΔE_{ab}^* color difference was 1.00. The colors of the two anchor pairs could not be identical because of the slight nonuniformity among the samples.

The visual assessments were performed in a Macbeth Spectralight booth using its daylight simulator (D65) in a darkened room. The CCT of the filtered tungsten light source was 6550K with an illuminance of 1840 lux; the chromaticities were $x=0.3129$, $y=0.3212$. Black velvet covered on the back of

the lightbooth to prevent specular reflections. The spectral radiance of the light source measured off a pressed PTFE sample placed in the bottom of the booth is shown in Fig. 21.

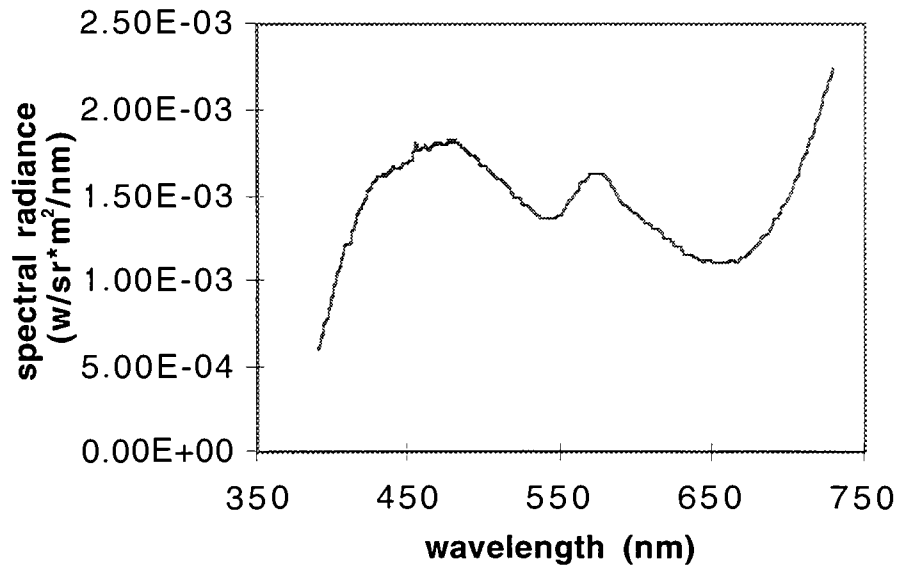


Fig. 21. Spectral radiance of the Macbeth lightbooth.

Twenty-five observers participated in the twenty-minute pass/fail visual experiment. At the beginning of the experiment, observers were instructed to judge the color difference against the anchor pair by example. They were told to put each sample pair at the bottom of the light booth parallel to the anchor pair and look at the samples at 45° degrees to the normal of the surface with more than 4 degree visual subtended angle. If they thought the color

difference of the sample pair was greater than the anchor pair, then put it in the “greater than” pile. Otherwise they put it in the “less than” pile. The demonstration also insured that each observer was fully adapted to the lighting conditions. There were two parts in the experiment. In the first segment observers made pass/fail decisions on the samples mounted on the RIT background. The surround was a gray cardboard with the same lightness as the RIT background. In the second segment observers made pass/fail decisions on the samples mounted on the CIE-reference background. The surround was changed to the same cardboard of the CIE-reference background. The sample pairs were arranged in random order. The order of the two-part visual experiment was changed for every other observer. Between the two parts of the experiment, observers stepped back and waited for the experimenter to change the samples, the anchor pairs, and the surround. A total of 1,800 pass/fail decisions were made.

Results and Discussion of Background and Surround Experiments

The SAS probit program was used for data analysis. Probit analysis fits a cumulative normal distribution to the frequency of rejection data for increasing color difference values. Medium tolerance, T50, values and their corresponding fiducial limits were listed in the output of the program. The results of the two-part experiment were compared and are listed in Table II. T50 values and the corresponding fiducial limits for each vector on the two backgrounds are plotted in Fig. 22.

Table II. The comparison of probit analysis results for each vector on different backgrounds.

colors		Gray			Cyan		
vectors		A	D	G	A	D	G
RIT-background	T50	1.37	0.83	0.93	1.15	1.83	1.06
L [*] =38	Fiducial	1.26-1.51	0.74-0.91	0.84-1.00	1.06-1.25	1.44-2.41	0.99-1.13
	χ^2	1.70	1.39	2.81	1.68	9.50	3.46
CIE reference	T50	1.14	0.80	0.95	1.08	1.80	1.11
L [*] = 50	Fiducial	1.05-1.26	0.72-0.87	0.86-1.03	1.00-1.16	1.64-1.98	1.03-1.19
	χ^2	4.89	0.28	1.32	3.47	3.16	4.20
%ΔT50		16.8	3.6	2.2	6.1	1.6	4.7

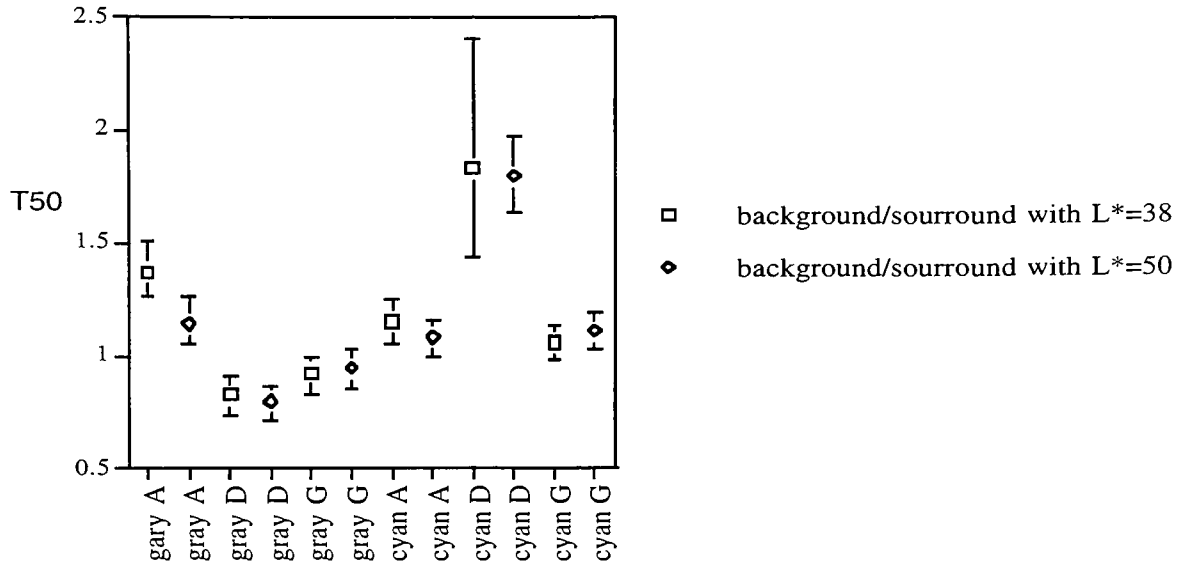


Fig. 22. Results of background and surround experiments.

Table II and Fig. 22 show that the differences between T50 values for each vector on the two different backgrounds are small except vector A for both colors. The fiducial limits are from 1.26-1.51 for the gray samples along the vector A on the RIT background with lightness of 38, and are from 1.05-1.26 for those on the CIE-reference background with lightness of 50. There is no overlap between these two intervals. The Chi-square values for these two vectors are relatively small. They are 1.69 and 4.89, respectively. Thus the difference of the T50 values of vector A for the gray sample due to different background is significant. The Chi-square values for the remaining vectors of both colors are small except for the vector D of cyan on the RIT background

with lightness of 38. This was also reported in the Phase I and Phase II experiments. There is a great deal of overlap between the fiducial limits of each vector for the two colors. Thus, there is no significance of change in background for the rest of the vectors of both colors.

The large chi-square value for cyan samples along chroma direction (vector D) on the RIT background was due to noisy data and poor sampling. The color difference values and rejection frequencies for this vector for each background are listed in Table III.

Table III. Comparison of the data of cyan D vector on the two different backgrounds

background sample pairs	RIT background		CIE-reference background	
	ΔE_{ab}^*	OBSFALL	ΔE_{ab}^*	OBSFALL
1	0.58	0	0.53	0
2	0.98	1	1.00	2
3	1.32	6	1.35	6
4	1.49	10	1.56	11
5	2.10	20	2.14	20
6	2.66	19	2.63	22

Table III shows that the trends of the two datasets are very similar except the rejection frequency at $\Delta E_{ab}^* = 2.66$. As the T50 values for cyan color along D direction on both backgrounds are around 1.80, there were not enough samples with color differences around or greater than the threshold. A small

degree of noise for these points can result in large deviation from the probit model.

The reason why the T50 value of the gray samples along the lightness direction (vector A) on the RIT background was significantly higher than that of the CIE-reference background is not fully understood. These results contradict the crispening theory derived by Semmelroth. According to the theory, if the lightness of an anchor pair is around 50, the difference of the visual response of the anchor pair on the CIE-reference background with lightness of 50, thus, is larger than that on the background with lightness of 38 because of the crispening effect. The lightness of gray samples are around 60. According to the plot that Judd and Wyszecki²¹ made and shown in Fig. 23, which describes the relationship between lightness of a sample and the lightness of visual response of the samples on different background, the visual differences between the two colors of each gray sample pair on the CIE-reference background with lightness of 50 are almost the same as those on the RIT backgrounds with lightness of 38, respectively. The visual rejection frequency of each sample pair judged against the anchor pair on the RIT background are relatively larger than that on the CIE-reference background, respectively. The T50 value of these gray samples on the RIT background with lightness of 38, thus, is smaller than that of the gray samples on the CIE-reference background with lightness of 50.

The result that the T50 value of the cyan samples in the lightness direction on the RIT background was larger than that on the CIE-reference background also contradicts the theory. The lightness of the cyan samples is close to the lightness of the CIE-reference background. The crispening effect occurred for both the anchor pair and cyan sample pairs on the CIE-reference background with lightness of 50. Since crispening effect is more significant for the chroma of samples close to the chroma of the background, the crispening effect of the anchor pair on the CIE-reference background is more severe than that of the cyan sample pairs on the same background. Comparing with the situation that both the anchor pair and sample pairs on the RIT background with lightness of 38, the visual response of the color difference of the anchor pair is relatively larger on the CIE-reference background with lightness of 50. So the T50 value of cyan sample along vector A on the CIE-reference background with lightness of 50 is greater than that of cyan samples on the RIT background with lightness of 38.

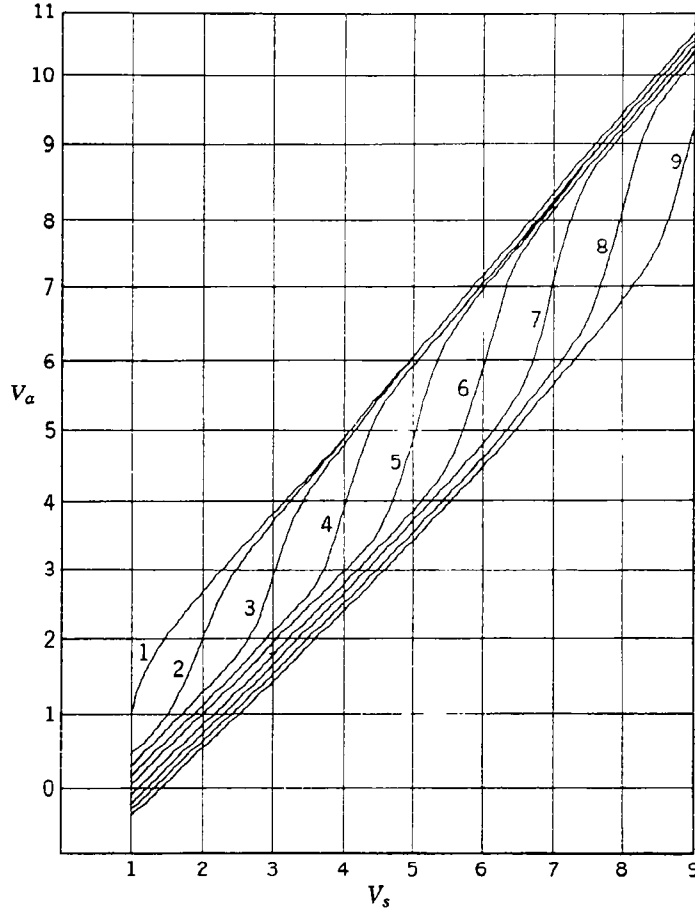


Fig. 23. Background adjusted Munsell value V_a plotted against nominal Munsell value V_s for backgrounds of nominal Munsell value 1/, 2/,...,9/. (Prepared by Judd and Wyszecki, 1975 from a table by Semmelroth, 1971).²¹

Since we are interested in testing color differences in the chromatic plane and the hue direction, the significance of the change in background in vector A are not taken into account.

Overall, changing lightness of the gray background results in significant change in T50 values along lightness direction (vector A) for gray color and

insignificant change in this direction for the colors away from the neutral. There is no significant change for those vectors in the chromaticness plane (vector D) and vectors representing the interaction between the chromaticness and lightness (vector G) on the change of the lightness of the gray background. The dataset on hue-discrimination developed in this thesis is consistent with RIT-Dupont dataset. Therefore, it can be added to the RIT-Dupont dataset.

MAIN EXPERIMENTS

Printer Testing and Calibration

Samples were prepared using a Fuji Pictography 3000 digital printer. This technology uses a laser to expose a silver halide donor material. Following water activated color development, color dyes are transferred to a glossy receiver material using heat and pressure. The print medium consists of a dye receiver layer composed of soluble polyester and silicone, a compliant layer, a base layer, and a backing layer.²⁰ The glossy coating of the paper well simulated the glossy automotive coating used in Phase I and Phase II research.

The spatial uniformity of the printer was tested by printing a medium gray color on 10x17 grids on a half page of the paper in the “landscape” orientation. The color of each grid was measured three times using a Gretag spectrophotometer. It was found that the color varied along the width and was nearly constant along its height. The mean of the colors in height was plotted with the position of the grid in width. The results are shown in Figs. 24-26.

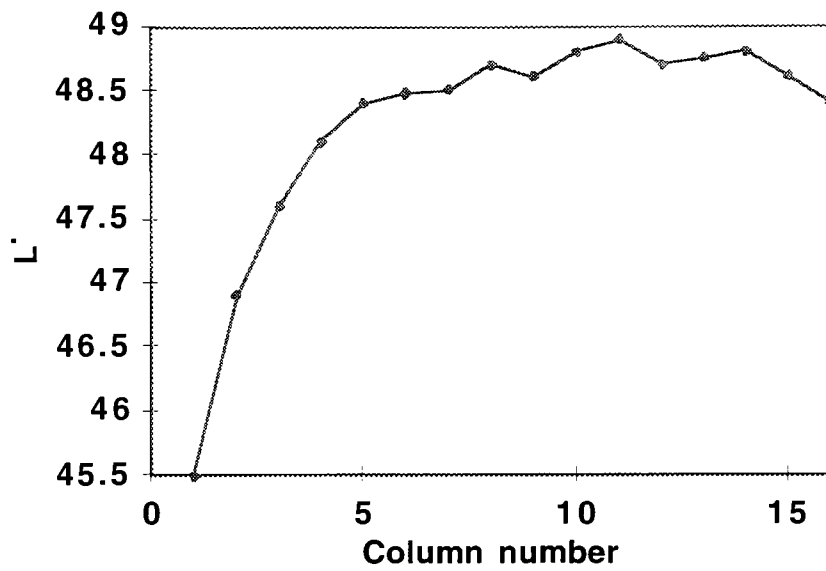


Fig. 24. The lightness change with the position in width.

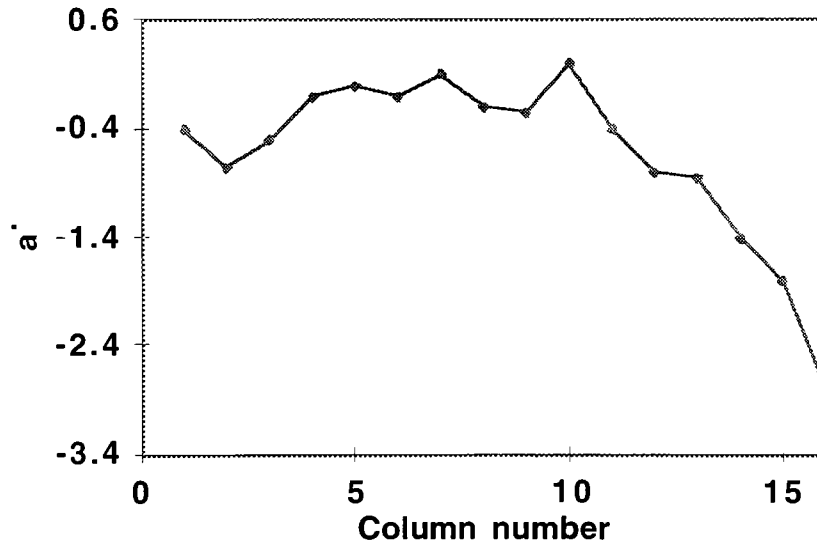


Fig. 25. Color coordinate a^* change with the position in width.

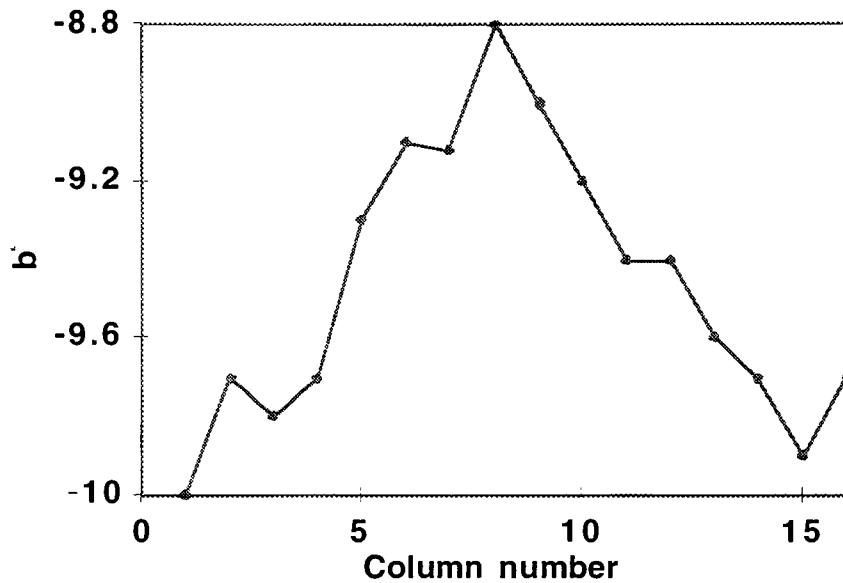


Fig. 26. Color coordinate b' change with the position in width.

The plots show that the printer does not have as good spatial uniformity as expected. The middle area of the paper ranging from Column 4 to Column 12, which is about the inner five inches of the width of the paper, was chosen as the printing area. Because of the poor uniformity of the printer, it is impossible to produce colors in an expected direction. Since we are interested in testing color-difference in hue direction, the colors produced from the printer change in hue direction with unwanted variation in chroma and lightness direction. Fig. 27 shows an example in the chromatic plane.

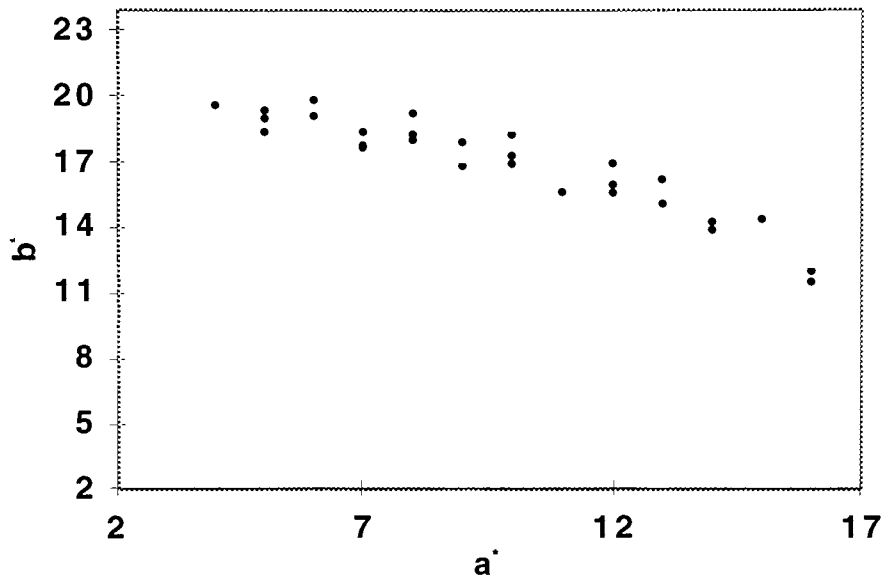


Fig. 27. An example of color sampling in hue direction.

The gamut of the printer was tested by printing $17 \times 17 \times 17$ colors. Each color was measured three times by BYK-Gardner Color View 45/0 spectrophotometer with small optical aperture. The results are shown in Fig. 28. The results show that the printer has the largest gamut at lightness around 40.

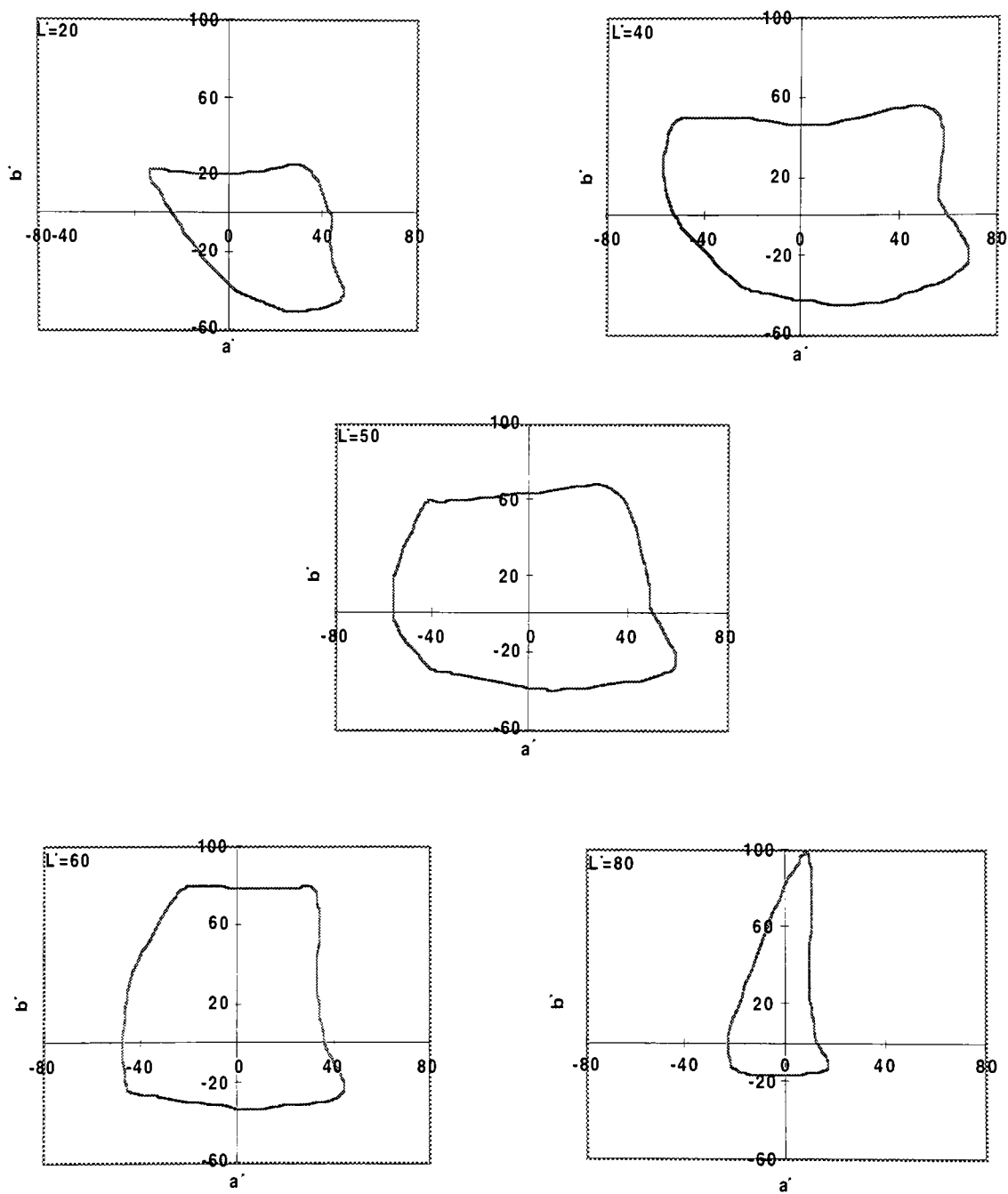


Fig. 28. The gamut of the Fuji printer located in Munsell Color Science Laboratory.

Two existing calibration techniques were used to convert L^* , a^* , b^* values to digital counts, R, G, and B. One was a 17*17*17 look-up table based on statistical regression; one was a theoretical model based on the Kubelka-Munk turbid media theory.²⁰ The look up table method was found to be the more accurate method for prediction of the digital values for a specified color and was subsequently used for this research. The average ΔE_{ab}^* values using the Macbeth Color Checker as a verification target was around 2.0. It was also found that the ability to produce samples varying in one CIELAB dimension was limited due to the variability within the page and from page to page and donor to donor. The look up table was adequate to produce samples with minor changes by the experimenter for the different color centers.

Determination of Statistical Analysis

1. The logit Program with 3-D Normit Function

Because of the printer variability, color-difference pairs were not able to be produced in one CIELAB dimension. Sample pairs were scattered along the hue direction with small variation in chroma and lightness. This required a change of the statistical analysis method from uni-dimensional to multi-dimensional. The SAS multi-dimensional logit program with 3-D normit

function was chosen to accomplish the task. The 3-D normit function is a three dimensional normal distribution function. Different from the probit analysis which was applied in Phase I and Phase II research, the 3-D normit function fits a cumulative normal distribution to the frequency of rejection visual data in ΔL^* , ΔC_{ab}^* and ΔH_{ab}^* directions instead of one direction as shown in Equation 11.

Variables are added to the normit function with stepwise regression are ΔL^* , ΔC_{ab}^* , and ΔH_{ab}^* .

$$Z = \beta_0 + \beta_1 * |\Delta L^*| + \beta_2 * |\Delta C_{ab}^*| + \beta_3 * |\Delta H_{ab}^*| \quad (11)$$

where Z is the z-score converted from the frequency of rejection visual data.

ΔL^* , ΔC_{ab}^* and ΔH_{ab}^* are measured color difference of each pair in lightness, chroma, and hue directions. β 's are parameters estimated by a maximum likelihood method. Equation (11) shows that instead of fitting Z-scores to a straight line in one dimension, the logistic program with normit function fits z-scores to a 3-dimensional super plane. This 3-D super plane is changed to a special 3-D surface by inverting z-scores to frequencies. If we keep any two of the three independent variables constant, the shape of the line in this space is

sigmoid, which is the same as fitting a cumulative normal distribution to the frequency of rejection data in one dimension. Stepwise selection was also used so that only statistically significant parameters are estimated.

The interaction between the independent variables are not considered by the logistic analysis. It is assumed that the visual response of color-difference around a center is linearly related to the local color space of ΔL^* , ΔC_{ab}^* and ΔH_{ab}^* . In order to apply the logit analysis properly, a C++ program was written for selecting color-difference pairs with constrained conditions in ΔL^* and ΔC_{ab}^* direction. The constrained conditions were

$$\begin{aligned}
 |\Delta L^*| &< 0.6 \\
 |\Delta C_{ab}^*| &< 0.6 \\
 |\Delta H_{ab}^*| / |\Delta E_{ab}^*| &> 0.90
 \end{aligned} \tag{12}$$

It is reasonable to assume that the interactions between ΔL^* , ΔC_{ab}^* ; ΔL^* , ΔH_{ab}^* ; and ΔC_{ab}^* , ΔH_{ab}^* are statistically insignificant. The joint effects of the

explanatory variables included in the model also could be tested by the logit program.

2. Criteria for Assessing Model Fit²²

Criteria for assessing model fit in the Logistic procedure are -2.log likelihood, AIC, SC and Score. The first three criteria are based on the maximum likelihood for fitting a model with intercepts only and for fitting a model with intercepts and explanatory variables. The Score statistic tests the joint effects of the explanatory variables included in the model. These statistics should be used when comparing different models of the same data. Lower value of the statistics indicates a more desirable model.

The overall model fit should be assessed by chi-square value which can be calculated from expected probability printed from the output of the logistic procedure.

$$\chi^2 = \sum \frac{(r - np)^2}{np(1 - p)} \quad (13)$$

where r is the number of the rejection for each color pair of one color center, n is the number of observations, and p is the expected proportion of the rejection for each color pair for one color center.

If the probability of chi-square distribution is less than 0.1, then the heterogeneity factor should be applied.

$$h = \frac{\chi^2}{n - 2} \quad (14)$$

3. Determination of T50 Values and Fiducial Limits²³

One of the disadvantage of the logit program is that the overall model fit of χ^2 value as well as T50 value and its fiducial limits could not be obtained automatically from the output of the logit analysis. A C++ program was attached to the output to accomplish this task, as described by Finney.²³

The variations in lightness and chroma directions are considered to be noise. If $\Delta L^* = 0$ and $\Delta C_{ab}^* = 0$ in equation (11), then the equation (11) is changed to

$$Z_H = \beta_0 + \beta_3^* |\Delta H_{ab}^*| \quad (15)$$

where Z_H is considered as the new z-score which can be converted to the frequency of rejection visual data only in hue direction, P_H . When the z-score is equal to zero, the T50 value is

$$m = -\frac{\beta_0}{\beta_3} \quad (16)$$

The 95% fiducial limits are

$$m + \frac{g}{(1-g)}(m - \bar{\Delta H_{ab}^*}) \pm h \sqrt{\frac{1-g}{\sum nw} + \frac{(m - \bar{\Delta H_{ab}^*})^2}{S\Delta H_{ab}^* \Delta H_{ab}^*}} \quad (17)$$

$$\text{where } g = \frac{3.84}{\beta^2 S\Delta H_{ab}^* \Delta H_{ab}^*}$$

$$w \text{ is a weighting coefficient, } w = \frac{Z^2}{P(1-P)}$$

$\bar{\Delta H_{ab}^*}$ is expected mean value of ΔH_{ab}^* , $\bar{\Delta H_{ab}^*} = \sum nw \Delta H_{ab}^* / \sum nw$

$S\Delta H_{ab}^* \Delta H_{ab}^*$ is variance, $S\Delta H_{ab}^* \Delta H_{ab}^* = \sum nw (\Delta H_{ab}^* - \bar{\Delta H_{ab}^*})^2$

If the χ^2 value obtained from normit model is very large, i.e. $P > \chi^2 < 0.1$, the heterogeneity factor will be applied. Otherwise $h=1$.

4. Testing of the Logit Program with 3-D Normit Function

The cyan center with sample pairs varying in lightness direction (vector A) was used to test the significance of the logit program with 3-D normit function and the probit analysis used in Phase I and Phase II research. This center was tested in Phase II research and the background and surround effect experiment of this research. Instead of fitting ΔE_{ab}^* with the rejection frequency in the probit program, the corresponding ΔL^* , Δa^* and Δb^* values of each sample pair with the rejection frequency were used as the input of the logit program. The output of the logit program is listed below. The results were compared with the probit analysis.

Part I. The Printing output of the SAS logit program with normit function.

1

The SAS System

Testing logit program with normit function using cyan center

OBS	OBSFAIL	TOTOBS	ΔL^*	Δa^*	Δb^*
1	0	25	0.46260	0.009901	0.037100
2	4	25	0.74470	0.046799	0.011400
3	8	25	0.91450	0.044500	0.024500
4	14	25	1.20620	0.080200	0.017700
5	16	25	1.32930	0.033499	0.097100
6	23	25	1.64610	0.079901	0.066000

The LOGISTIC Procedure

Data Set: WORK.MAIN

Response Variable (Events): OBSFAIL

Response Variable (Trials): TOTOBS

Number of Observations: 6

Link Function: normit

Response Profile

Ordered Binary		
Value	Outcome	Count
1	EVENT	65
	NO EVENT	85

Part II. The printing output of the SAS logit program with normit function.

2

Stepwise Selection Procedure

Step 0. Intercept entered:

Analysis of Maximum Likelihood Estimates

Variable	DF	Estimate Parameter	Standard Error	Wald Chi-Square	Pr > Chi-Square	Standardized Estimate
INTERCEPT	1	-0.1679	0.1029	2.6643	0.1026	

Residual Chi-Square = 57.9140 with 3 DF (p=0.0001)

Analysis of Variables Not in the Model

Variable	Score Chi-Square	Pr > Chi-Square
ΔL^*	57.875	0.0001
Δa	0.3237	0.0001
Δb	19.6162	0.0001

Step 1. Variable DL entered:

The LOGISTIC Procedure

Criteria for Assessing Model Fit

Criterion	Intercept only	Intercept and Covariates	Chi-Square for Covariates
AIC	207.270		140.628
SC	210.280		146.649
-2 LOG L	205.270		136.628 68.642 with 1 DF (p=0.0001)
Score			57.876 with 1 DF (p=0.0001)

Analysis of Maximum Likelihood Estimates

Variable	DF	Parameter Estimate	Standard Error	Wald Chi-Square	Pr > Chi-Square	Standardized Estimate
INTERCEPT	1	-3.1321	0.4463	49.2482	0.0001	
ΔL^*	1	2.7279	0.3868	49.7467	0.0001	1.068467

Association of Predicted Probabilities and Observed Responses

Concordant = 80.4%	Somers' D = 0.710	Discordant = 9.4%	Gamma = 0.791
Tied = 10.2%	Tau-a = 0.351 (5525 pairs)	c = 0.855	

Residual Chi-Square = 1.3453 with 2 DF (p=0.5104)

Analysis of Variables Not in the Model

Variable	Score Chi-Square	Pr > Chi-Square
Δa	0.4081	0.5229
Δb	0.6221	0.4303

NOTE: No (additional) variables met the 0.3 significance level for entry into the model.

Part III. The Printing output of the SAS logit program with normit function.

3

The SAS System

Testing logit program with normit function using cyan center

Parameter Estimates and Covariance Matrix

OBS	_LINK_	_TYPE_	_NAME_	INTERCEPT	ΔL^*	Δa	Δb	_LNLIKE_
1	NORMIT	PARMS	ESTIMATE	-3.13213	2.72791			-68.3139
2	NORMIT	COV	INTERCEPT	0.19920	-0.16594			-68.3139
3	NORMIT	COV	ΔL^*	-0.16594	0.14959			-68.3139
4	NORMIT	COV	Δa					-68.3139
5	NORMIT	COV	Δb					-68.3139

Part IV. The Printing output of the SAS logit program with normit function.

4	Predicted Probabilities and 95% confidence Limits							
OBS	OBSFAIL	TOTOBS	ΔL	Δa	Δb	PHAT	LCL	UCL
1	0	25	0.46260	0.009901	0.037100	0.03073	0.00784	0.09277
2	4	25	0.74470	0.046799	0.011400	0.13552	0.07113	0.23150
3	8	25	0.91450	0.044500	0.024500	0.26191	0.17874	0.36139
4	14	25	1.20620	0.080200	0.017700	0.56288	0.46265	0.65921
5	16	25	1.32930	0.033499	0.097100	0.68937	0.57962	0.78443
6	23	25	1.64610	0.079901	0.066000	0.91281	0.81200	0.96647

The first part of the printed output was listed the original input data of the logit program. These input data were the same as the data used in the experiment of background and surround in this research. It is the cyan center with samples varying in lightness direction on the RIT-background. The second part of the output was the stepwise regression on the input data. As sample pairs were designed to vary only in lightness direction, the change in a^* and b^* direction did not meet the 0.3 significance level for entry into the model. The joint effects of the three variables was tested by the criteria of the Score. The probability value of 0.0001 shows the joint effects of these three variables are statistically insignificant. The results of the logit program are listed in the output of Part III. The intercept and the parameter in lightness direction were estimated by the maximum likelihood method. The goodness fit of the model was calculated by the predicted probability listed in Part IV.

The T50 value and its fiducial limits were calculated by running the C++ program in Appendix C. The results are :

$$T50=1.148,$$

$$\text{Fiducial limits: } 1.058-1.245$$

$$\chi^2=1.658$$

These results are exactly the same as what we obtained in the background and surround effect experiments shown in Table II. The consistency of the results indicates that logit program with 3-D normit function is an extended probit program in multiple dimensions (as expected). The results of this research thus could be combined with the dataset obtained in Phase I and Phase II research .

Sample Design

Thirty nine color centers were chosen. Three of them were the red, green, and blue centers recommended by the CIE TC-1.3. Because the gamut of the printer, CIE recommended yellow center could not be produced. There are two lightness levels and two chroma levels for the remaining centers. At each lightness level and chroma level, twelve centers were chosen to span the complete hue circle. The three circles are $L^*=60, C_{ab}^*=20$; $L^*=40, C_{ab}^*=20$; $L^*=40, C_{ab}^*=40$. Lightness 40 was chosen because the printer has its largest gamut around this level. The thirty nine centers are plotted in Fig. 29.

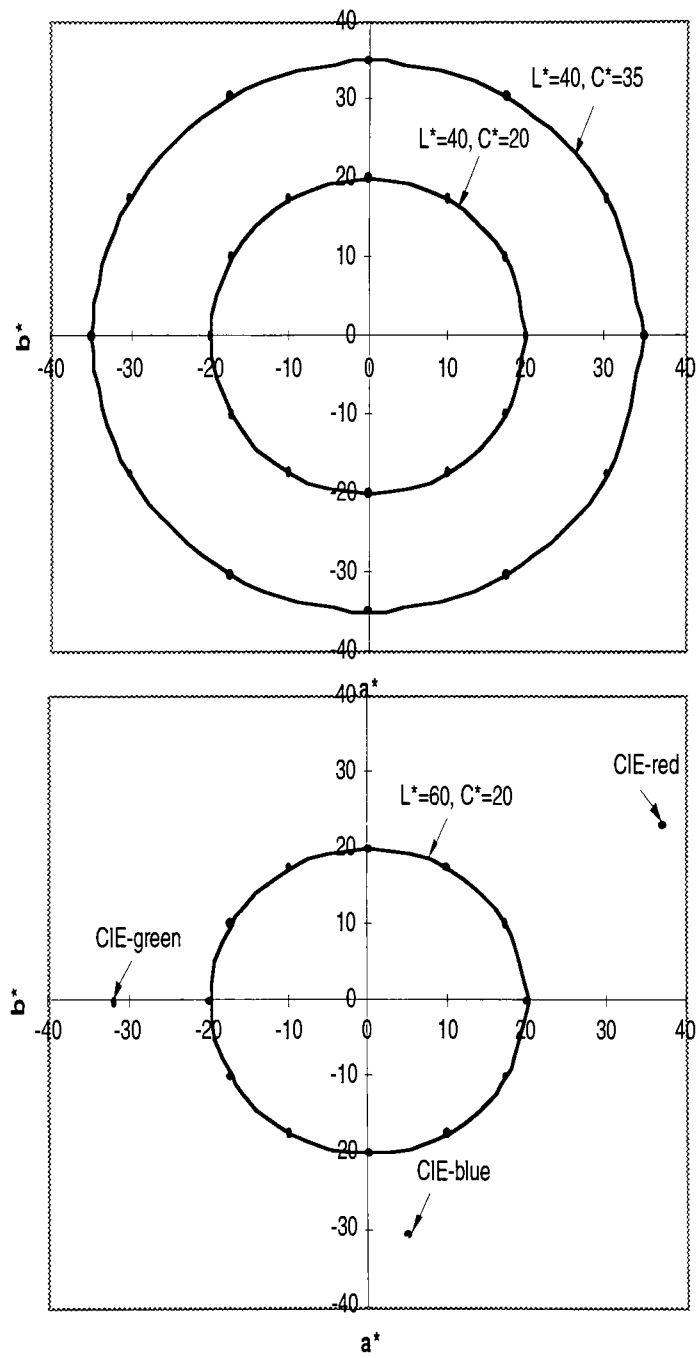


Fig. 29. The thirty nine color centers studied.

Because of the change of statistical analysis method from uni-dimensional to three-dimensional, three parameters were needed to be fit by the maximum likelihood method. Therefore, 9-10 sample pairs were produced for each color center. A total of 393 color-difference pairs were produced around the 39 color centers sampling hue direction.

Preparation of Samples

Each color sample was cut into a 2.5"x 2.0" rectangle using a Roller cutter. Color-difference samples were placed on gray cardboard in adjacent fashion. In order to avoid a white gap between the adjacent edges, these two edges of each sample pair were cut by an Art Mate Mat Cutter with 45 degree blade. 3M positionable Mounting Adhesive was used to tape the two color patches to the background. The great advantage of this adhesive is to let one position and reposition prints for alignment before applying pressure and permanently affixing the sample. The gray cardboard was cut into 6"x 4" rectangles using the Art Mate Mat Cutter. The 45 degree blade was used so that there were no dark shade and black edges. The CIELAB values of the cardboard are $L^*=50.6$, $a^*=0.5$, $b^*=0.1$. The size of the sample and background materials are consistent with the previous RIT experiment, which agrees with

the recommendation, greater than four degrees subtended visual angle with no sample separation. The sample arrangement is shown in Fig. 30.

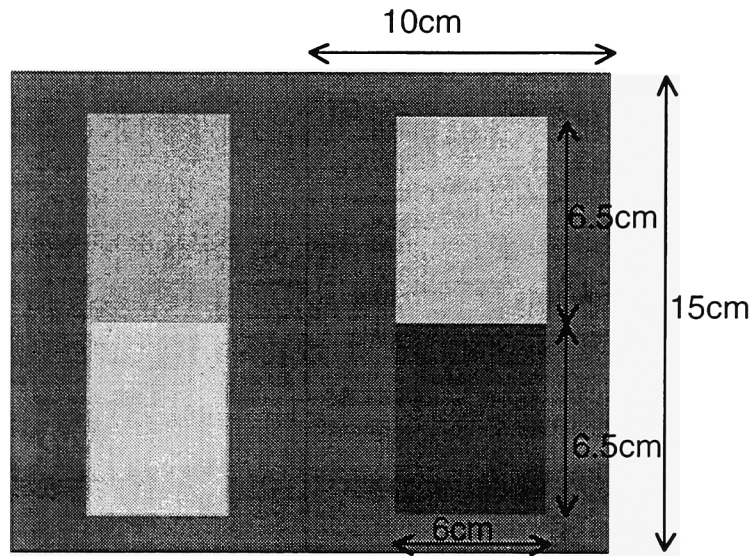


Fig. 30. The arrangement of the sample pair.

Viewing Conditions

The observer judged the color difference pairs in a Macbeth Spectralight booth with simulated daylight illumination in a darkened room. The light source had a correlated color temperature of 6550K, an illuminance level of 1840 lux, and chromaticities of $x=0.3134$, $y=0.3320$. The source was measured by an LMT colorimeter model C 1200.

The viewing geometry was 0/45 with the sample and anchor pair positioned flat on the bottom of the lightbooth and observers viewed the

samples at 45 degrees to the normal. The material and CIELAB values of the surround are the same as the background. The back of the booth was lined with black velvet to prevent specular reflections from being viewed on the samples. Observers wore a neutral smock to prevent reflections from colorful clothing.

Sample Measurements

A BYK-Gardner 45/0 Colorview spectrophotometer was first used to choose color-difference pairs. Because of the poor uniformity of the printer resulting in some degree of sinusoidal variance in the color samples, each color sample was measured three places from edge to edge with three measurements at each position. The large aperture of the spectrophotometer was used. A C++ program was written to convert spectral reflectance data to CIELAB LCH data with illuminant D65 and the 10 degree observer, take the average of three measurements of each sample, and calculate ΔE_{ab}^* values between each possible sample pair.

The final sample pairs were measured with a Milton Roy ColorScan 45/0 spectrophotometer. The instrument is an abridged double beam scanning spectrophotometer which was calibrated using an NIST calibrated white

porcelain tile. Eight NIST standards were measured four times during the sample measurements. They were white porcelain, pale gray, middle gray, deep gray, cyan, green, deep pink, and red BCRA Series II tiles. The red tile measurements were only used in the spectrum region of 380nm to 580nm due to thermochromic properties of the tile. The measurements were used to correct the systematic errors inherent in the instrument.^{24,25}

There was some concern about the difference in spectral power distribution between the Macbeth spectralight and the Milton Roy ColorScan because of the optical brighteners used to whiten the Fuji paper. The results of the measurements of the lightbooth showed that there is not enough ultraviolet in the light source. Therefore, it was assumed that there is little fluorescent emission occurring. No extra treatment on the spectrophotometer, thus, was needed.

Psychophysical Experiments

The psychophysical design was similar to the visual assessments performed in Phase I and Phase II, i.e. a pass/fail experiment with a mid-gray anchor pair. The 393 samples were randomly ordered by running a C program using a random number generator. The random number and sample number of each sample were written at the back of the sample. In order to prevent

observer fatigue, samples were divided into two sets. There was a 45-minute experimental session for each set. In each session, the experimenter randomly presented a set for the observer either in backward order or forward order of the random number order to minimize bias due to learning. There were a total of four possible orders for each observer. The experimenter put six training samples at the beginning of each session without informing the observer. Before the beginning of the experiment, the observer was given a verbal and written instruction:

"You are going to judge the color difference of each sample pair against the color difference of the anchor pair. If the color difference of the sample pair is greater than the color difference of the anchor pair, put the sample pair in the **"greater than"** basket. If the color difference of the sample pair is less than the color difference of the anchor pair, put the sample pair in the **"less than"** basket. The two baskets will not necessarily have an equal number."

Observers were also instructed to put each sample pair parallel to the anchor pair at the bottom of the light booth, look at the samples at 45 degree to the normal of the surface of the sample pair using greater than a 4° degree subtended angle. They were also told that if the adjacent edge of each sample

pair was not straight or had a dark or white color, they could flip the sample. If they had a hard time making the pass/fail decisions, they should look away and then look back to prevent local adaptation to the color-difference pair.

Forty five color-normal observers participated in the experiment. There were ten female observers among them. The observers' ages ranged from 17 to 58 with an average of 34. The observers were comprised of graduate students, faculty members, visiting scholars, and secretaries at RIT. Among graduate students, many of them were part-time students who were involved in color science in industry. Some of the observers were very experienced in judging color and some were naive. Thirty seven observers participated in both sessions and eight observers took part in a single session. Thus, a total of 41 observations for each different pair were collected. Thirty nine vectors consisted of 9-10 samples each. Three vectors exceeded 10 pairs due to unexpected low visual discrimination. 393 color difference pairs were tested. A total of 32,226 pass/fail decisions were made.

RESULTS AND DISCUSSION

Sample Measurements

A total of 393 color-difference pairs around 39 color centers were measured. The color center was determined by taking the average of the samples produced around it in CIELAB space. Different from the expected chroma and lightness values for a certain hue circle, the actual values of color-difference centers and standard deviation of chroma and lightness for the samples around each center are listed in Table IV. Examples of good and poor sample distributions around several color centers are shown in Fig. 31 and Fig. 32, respectively. Most of the sample pairs were produced along the hue direction with small variations in lightness and chroma as shown in Fig. 31. There were still some color centers, like the CIE red center, that had relatively large variations in chroma and lightness directions. The CIE-red center is shown in Fig. 32.

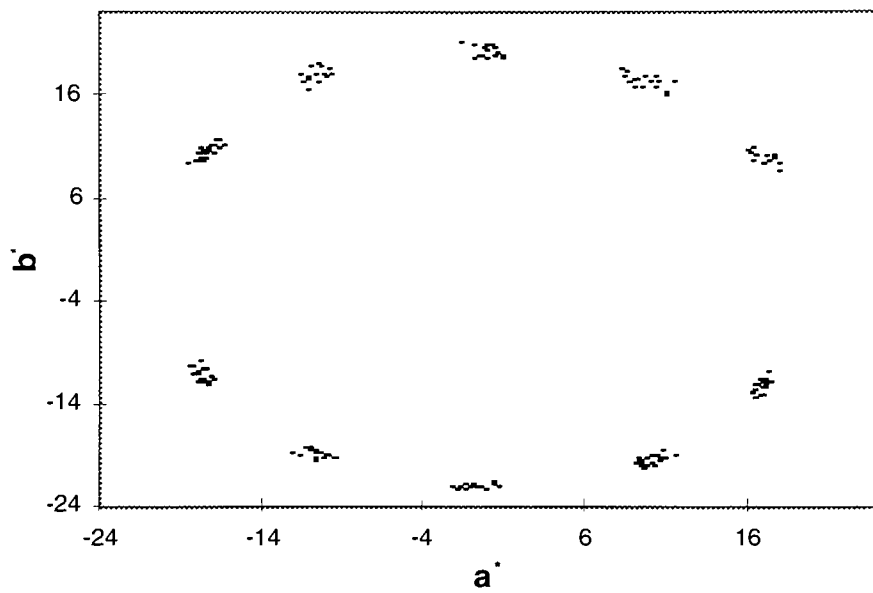


Fig. 31. Typical desirable sampling about a given color center.

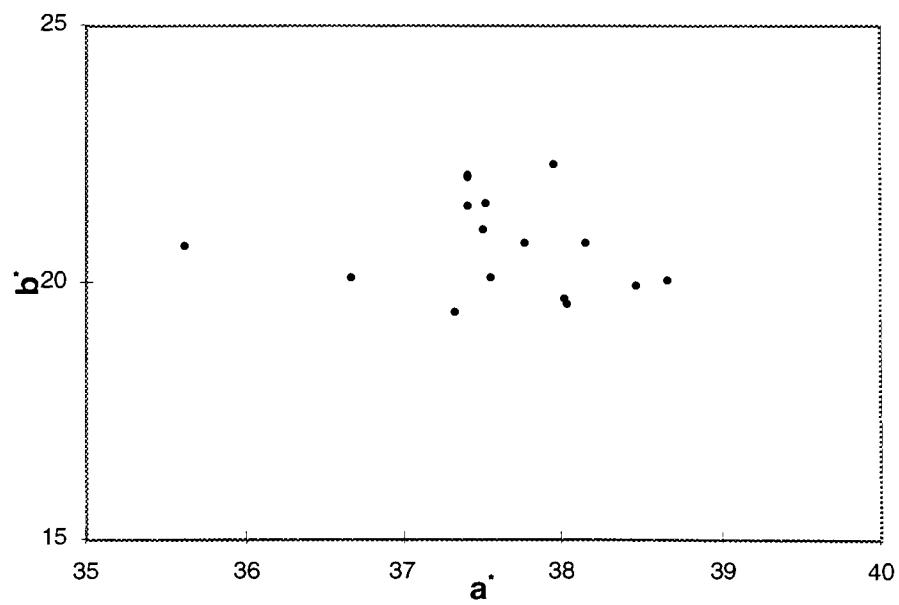


Fig. 32. Typical undesirable sampling about a given color center.

The colors of the anchor pair were $L^*=49.03$, $a^*=0.927$, $b^*=2.27$, $L^*=49.35$, $a^*=0.10$, $b^*=2.79$. The color difference in CIELAB was 1.02 with lightness difference 0.31, chroma difference 0.34, and hue difference 0.92. Since the main interest is in testing hue-dependence of hue discrimination in CIELAB space, the color difference of the anchor pair varied mainly in the hue direction.

Table IV. Coordinates of all color centers in CIELAB space and variation in lightness and chroma directions.

centers	L^*	C_{ab}^*	h_{ab}	stdev. of L^*	stdev. of C_{ab}^*
L40C20H0	38.64	19.32	-1.91	0.40	0.37
L40C20H30	38.51	19.31	27.83	0.49	0.54
L40C20H60	38.39	18.63	57.33	0.66	0.72
L40C20H90	38.30	19.02	87.95	0.46	0.67
L40C20H120	38.55	19.86	123.34	0.36	0.44
L40C20H150	37.90	21.50	153.14	0.47	0.50
L40C20H180	37.82	21.67	180.36	0.34	0.50
L40C20H210	38.45	21.36	209.00	0.37	0.34
L40C20H240	38.69	21.75	238.77	0.46	0.40
L40C20H270	38.99	20.90	266.99	0.35	0.20
L40C20H300	38.96	20.74	296.30	0.24	0.45
L40C20H330	38.84	19.90	325.22	0.35	0.43
L40C35H0	37.62	33.91	0.53	0.90	0.49
L40C35H30	37.11	34.83	32.24	0.39	0.38
L40C35H60	37.14	34.09	59.23	0.51	0.41
L40C35H90	36.97	34.40	88.85	0.57	0.44
L40C35H120	37.32	35.35	119.72	0.52	0.67
L40C35H150	37.86	35.97	151.17	0.61	0.65

Table IV Continued

L40C35I80	38.25	35.83	176.12	0.43	0.30
L40C35H210	39.61	37.10	210.63	0.43	0.28
L40C35H240	38.78	36.72	239.06	0.44	0.26
L40C35H270	38.58	36.52	270.46	0.49	0.25
L40C35H300	36.72	36.69	296.99	0.40	0.25
L40C35H330	37.94	34.84	328.69	0.38	0.37
L60C20H0	60.74	18.39	-1.58	0.53	0.38
L60C20H30	59.51	19.55	30.01	0.46	0.39
L60C20H60	59.69	19.74	61.35	0.57	0.41
L60C20H90	59.94	20.34	90.54	0.35	0.48
L60C20H120	60.09	20.98	121.25	0.41	0.47
L60C20H150	60.06	20.44	148.87	0.43	0.26
L60C20H180	60.05	20.49	179.93	0.39	0.31
L60C20H210	60.39	21.02	212.43	0.33	0.34
L60C20H240	60.65	21.86	240.30	0.33	0.37
L60C20H270	60.54	22.13	267.43	0.35	0.22
L60C20H300	59.87	21.94	296.74	0.73	0.32
L60C20H330	60.27	20.71	323.76	0.54	0.42
CIE-red	42.60	42.61	28.77	0.57	0.82
CIE-green	55.25	33.68	180.49	0.45	0.25
CIE-blue	34.96	32.75	276.85	0.46	0.27

Observer Variability

The visual experiment was designed to test perceptibility matching on the magnitude of color differences of surface colors. It is necessary to test the reliability of the observers' visual performances. This includes testing each observer's variance compared to the majority decision, overall observers' performance on each color center studied, and inter-observer variance. A C++ program was written to analyze the data.

1. Observer Variance

In order to get an error free pass/fail formula, it is important to know the reliability of the observers. Some researchers, like Davidson and Freide,²⁶ tried to deduce the percentage errors by using the average observer in relation to the corporate decision of the matching panel.

For each sample pair, if the majority decision (above 50% observer agreed on) was taken as the correct one and each observer's decision was compared with the majority decision, then the disagreement of each observer with the 'corporate panel observer'³ was obtained. The results are listed in Table V. The mean variance is 18.6% with the standard deviation of 4.0%, the maximum variance of 28.0%, and minimum variance of 10.8%. The

percentage disagreements range of McDonald's acceptability matching experiments was from 10.2% to 16.4% with a mean of 13.2%. The variance of our results is higher than that of McDonald's because of the observers' leniency.

Leniency³ is defined as pass rate for each observer, i.e. the number of pass decisions expressed as a percentage of the number of the assessments. The relationship between the percentage of disagreements with majority decision and leniency for each observer is plotted in Fig. 33. It forms a V shape, which means that the most and the least lenient observers agree less with the corporate panel observer than those observers with average leniency. As mentioned before, the observers varied a great deal of experience in judging colors. It is interesting to find that the most lenient observers were inexperienced observers, and the least lenient observers were very experienced observers. For example, observer 22 works in the color science field in industry and has been involved in color painting for a long time. He has very sensitive color discrimination. Observer 27, on the other hand, never had experience in judging colors before. The eight observers in McDonald's experiments were all professional experienced observers. The variance of the current results is higher than that of McDonald's, thus, is due to the large observer variation in experience in these experiments.

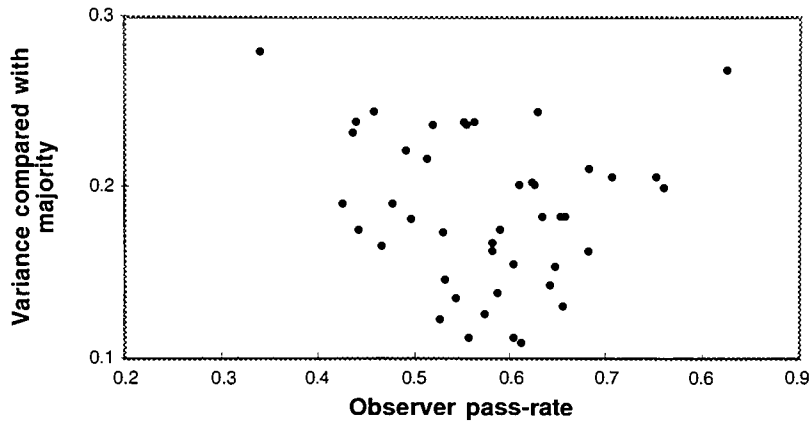


Fig. 33. Influence of matching leniency on disagreements of each observer compared with majority decision.

Table V. Variance of each observer comparing with majority decision.

Observers	Number of Assessments	Disagreement with majority decision	Percentage of disagreements	Average Pass Rate (leniency)
0	205	37	0.18	0.50
1	205	39	0.19	0.48
2	205	39	0.19	0.48
3	394	94	0.24	0.55
4	205	41	0.20	0.76
5	394	85	0.22	0.51
6	205	43	0.21	0.68
7	206	23	0.11	0.60
8	394	96	0.24	0.46
9	394	93	0.24	0.52
10	394	94	0.24	0.44
11	394	65	0.16	0.47
12	394	66	0.17	0.58
13	205	25	0.12	0.53
14	394	57	0.14	0.53
15	394	64	0.16	0.68

Table V. Continued

16	394	69	0.18	0.59
17	394	44	0.11	0.56
18	394	72	0.18	0.66
19	394	81	0.20	0.75
20	394	80	0.20	0.62
21	190	39	0.21	0.71
22	393	110	0.28	0.34
23	394	94	0.24	0.56
24	394	96	0.24	0.63
25	394	53	0.13	0.54
26	394	87	0.22	0.49
27	379	102	0.27	0.83
28	394	72	0.18	0.63
29	379	49	0.14	0.65
30	379	76	0.20	0.61
31	394	56	0.14	0.64
32	394	79	0.20	0.62
33	379	41	0.11	0.61
34	394	69	0.18	0.44
35	394	72	0.18	0.65
36	394	54	0.14	0.59
37	394	49	0.12	0.57
38	394	61	0.15	0.60
39	394	68	0.17	0.53
40	394	75	0.19	0.43
41	394	91	0.23	0.44
42	394	60	0.15	0.65
43	394	64	0.16	0.58
44	394	93	0.24	0.55

2. Mean Variance of Each Color Center

The average of the observers' variance in comparison with the majority decision was also calculated for each color center. The results could provide information on observers' sensitivity for small color differences. Therefore, the uniformity of the CIELAB space for small color difference could be tested. The results are listed in Table VI. The maximum variance for each vector is 0.22, and the minimum variance for each vector is 0.13. Fig. 34 shows the relationship between mean variance and hue angle for the three complete hue circles. Data points on each circle have the same chroma and lightness.

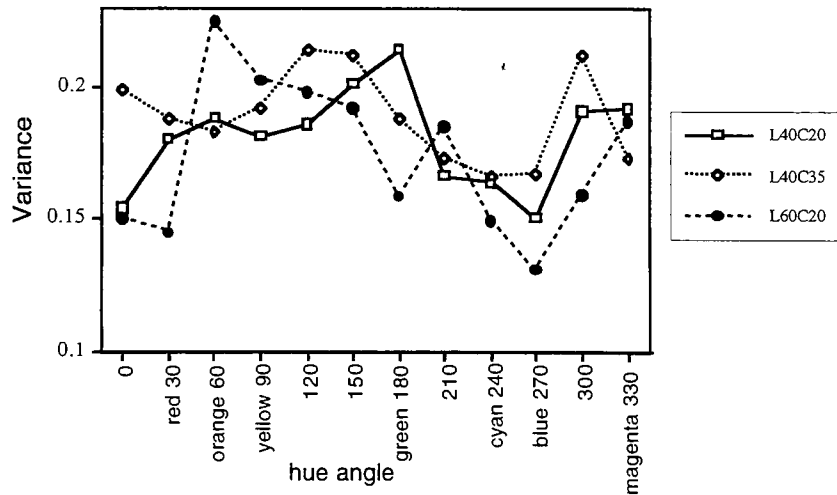


Fig. 34. Mean variance compared with majority decision as a function of hue angles.

Table VI. The mean and standard deviation of observers' disagreements in comparison with majority decision for each color center.

Centers	mean	Standard Deviation
L40C20H0	0.15	0.11
L40C20H30	0.18	0.16
L40C20H60	0.19	0.14
L40C20H90	0.18	0.16
L40C20H120	0.19	0.15
L40C20H150	0.20	0.16
L40C20H180	0.21	0.17
L40C20H210	0.17	0.12
L40C20H240	0.16	0.14
L40C20H270	0.15	0.13
L40C20H300	0.19	0.15
L40C20H330	0.19	0.15
L40C35H0	0.20	0.17
L40C35H30	0.19	0.15
L40C35H60	0.18	0.17
L40C35H90	0.19	0.16
L40C35H120	0.21	0.19
L40C35H150	0.21	0.17

Table VI. Continued

L40C35H180	0.19	0.16
L40C35H210	0.17	0.14
L40C35H240	0.17	0.15
L40C35H270	0.17	0.12
L40C35H300	0.21	0.15
L40C35H330	0.17	0.13
L60C20H0	0.15	0.12
L60C20H30	0.14	0.11
L60C20H60	0.22	0.17
L60C20H90	0.20	0.16
L60C20H120	0.20	0.15
L60C20H150	0.19	0.14
L60C20H180	0.16	0.14
L60C20H210	0.19	0.13
L60C20H240	0.15	0.13
L60C20H270	0.13	0.11
L60C20H300	0.16	0.13
L60C20H330	0.19	0.15
CIE-RED	0.18	0.15
CIE-GREEN	0.21	0.18
CIE-BLUE	0.15	0.11

There is a systematic trend shown in Fig. 34. The average variance is very low in the blue region, and is higher in green-yellow, cyan, and magenta regions. These results indicate that the sensitivity of visual perceptions is varied with hue angle and therefore, CIELAB space for small color difference is not uniform.

3. Inter-Observer Variance

The goodness of fit of the logistic model for each color center is greatly influenced by inter-observer variance. The inter-observer variance was calculated by comparing each possible pair of observers' decision on the same color pairs that they both judged. It is expressed as the number of disagreements of each two observers as a percentage of the number of assessments which they both had. The disagreements between observers ranges from 0 to 52.9%, with average inter-observer variance 26.6% and the standard deviation of 5.0% inter-observer variance. As would be expected, the inter-observer variance also highly depends on the difference of the two observers' leniency. The inter-observer variance increases with the difference of the two observers' leniency. This is shown in Fig. 35.

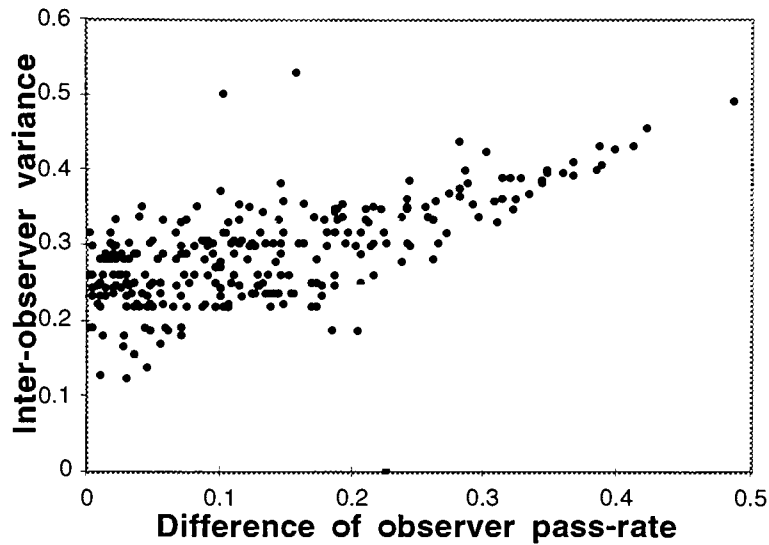


Fig. 35. Influence of matching leniency on inter observer variance.

Comparing these results with McDonald's acceptability matching experiments; where the disagreements between observers ranged from 9.5% to 25.2%, with a mean of 17.3, inter-observer variance in the current experiments is much higher. Again, the reason is due to the large differences in observer population.

Results of Logit Analysis

The results of logit analysis showed that the joint effects of the three variables ΔL^* , ΔC_{ab}^* , and ΔH_{ab}^* were statistically insignificant. A C++ program was written to calculate T50 values, fiducial limits of color-difference in hue direction, goodness of fit chi-square value for logit model with 3-D normit function, and heterogeneity factor for each test color center from the output of the logit program. The logit program was run three times for each center in order to exclude the outliers and to narrow down the 95% confidence intervals without altering the T50 values. The outliers could be, for example, some of the data points did not fit the constrain conditions (12) according to the final measurements and the frequency of the rejection was unreasonably far off the predicted probability at a certain color difference level. The results are listed in Table VII. It shows that the heterogeneity factor was very large for the centers close to the red and cyan regions. But for the rest of the centers, the heterogeneity factor was either unnecessary or small. The large fiducial interval and high heterogeneity factor were due to noisy data. The noise might come from the poor color uniformity of sample pairs. Because of the poor uniformity of the printer, it was very hard to produce uniform color patches despite efforts to minimize this limitation. In

addition, sinusoidal variations were unavoidably produced in some color patches. These sample defects led to increased observer uncertainty.

Table VII. Results of logit Analysis and T50 Values with 95% Fiducial Limits.

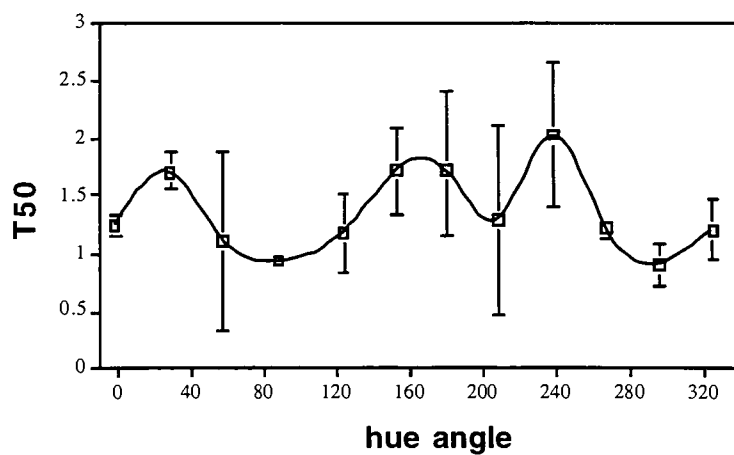
centers	Hue angle	T50	95%UCL	95%LCL	χ^2	heterogeneity
L40C20H0	-1.91	1.24	1.33	1.14	8.32	no
L40C20H30	27.83	1.70	1.88	1.56	9.43	no
L40C20H60	57.34	1.11	1.88	0.33	75.37	9.42
L40C20H90	87.95	0.92	0.98	0.85	2.71	no
L40C20H120	123.35	1.17	1.50	0.83	22.50	4.5
L40C20H150	153.14	1.71	2.09	1.34	21.65	4.33
L40C20H180	180.33	1.71	2.31	1.15	26.65	3.80
L40C20H210	208.99	1.28	2.12	0.47	53.53	6.69
L40C20H240	238.77	2.02	2.65	1.34	15.95	1.77
L40C20H270	266.99	1.21	1.29	1.12	10.37	no
L40C20H300	296.30	0.90	1.08	0.71	21.07	3.01
L40C20H330	325.23	1.20	1.32	0.88	20.59	2.94
L40C35H0	0.53	2.36	3.07	2.10	6.85	no
L40C35H30	32.24	1.05	2.19	0.00	50.97	7.28
L40C35H60	59.23	1.64	1.84	1.45	9.27	1.85
L40C35H90	88.85	2.17	2.70	1.95	6.38	no
L40C35H120	119.72	2.11	2.48	1.88	2.52	no
L40C35H150	151.17	3.05	3.55	2.78	8.50	no
L40C35H180	176.12	2.58	3.24	2.24	7.73	no
L40C35H210	210.63	2.34	3.34	1.43	22.19	3.69
L40C35H240	239.06	3.52	3.99	3.08	21.96	1.99
L40C35H270	270.46	1.31	1.38	1.23	10.99	no
L40C35H300	296.99	1.21	1.38	1.05	20.84	2.60
L40C35H330	328.70	1.64	1.77	1.52	2.16	no

Table VII Continued

L60C20H0	-1.58	1.57	1.93	1.24	17.11	2.85
L60C20H30	30.01	1.08	1.15	0.99	6.90	no
L60C20H60	61.35	0.78	1.14	0.38	18.26	3.04
L60C20H90	90.55	0.87	1.04	0.69	26.88	3.36
L60C20H120	121.26	1.42	1.51	1.33	3.54	no
L60C20H150	148.87	1.70	2.01	1.39	18.80	1.69
L60C20H180	179.93	1.48	1.56	1.42	18.50	no
L60C20H210	212.44	1.29	1.77	0.80	44.66	5.58
L60C20H240	240.31	2.13	2.57	1.78	10.66	1.77
L60C20H270	267.43	1.16	1.56	0.75	22.15	4.43
L60C20H300	296.74	1.34	1.42	1.27	4.29	no
L60C20H330	323.76	1.44	1.60	1.30	18.82	2.35
CIE-red	28.78	2.52	3.77	2.08	3.77	no
CIE-green	180.50	1.66	1.99	1.34	37.78	4.72
CIE-blue	276.85	1.24	1.33	1.14	6.70	no

The T50 values and fiducial limits as a function of CIELAB hue angle for each color center are plotted in Figs. 36-38.

Fig. 36. T50 values vs. CIELAB hue angle for the hue circle at chroma close to 20, lightness close to 40.



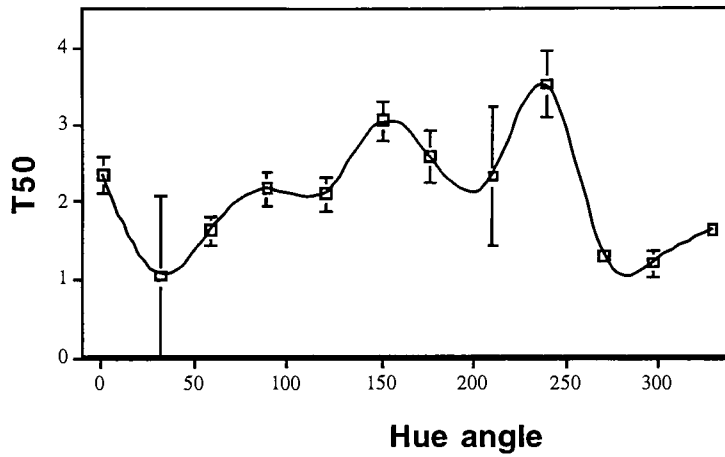


Fig. 37. T50 values vs. CIELAB hue angle for the hue circle at chroma close to 35, lightness close to 40.

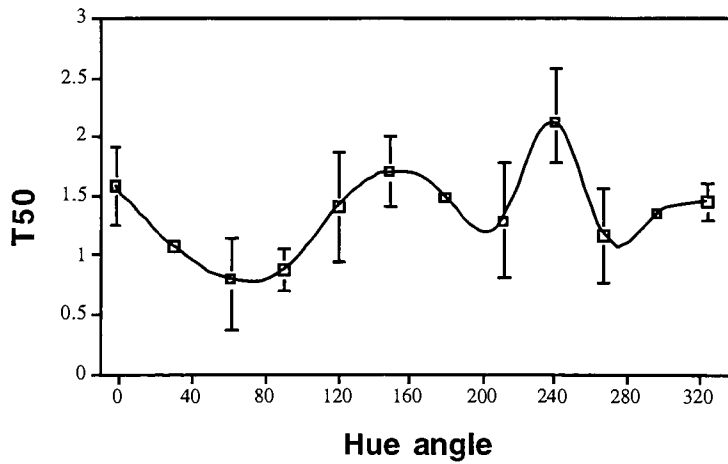


Fig. 38. T50 values vs. CIELAB hue angle for the hue circle at chroma close to 20, lightness close to 60.

The T50 values as a function of hue angle for the three complete circles and CIE red, green, blue centers are plotted in Fig. 39.

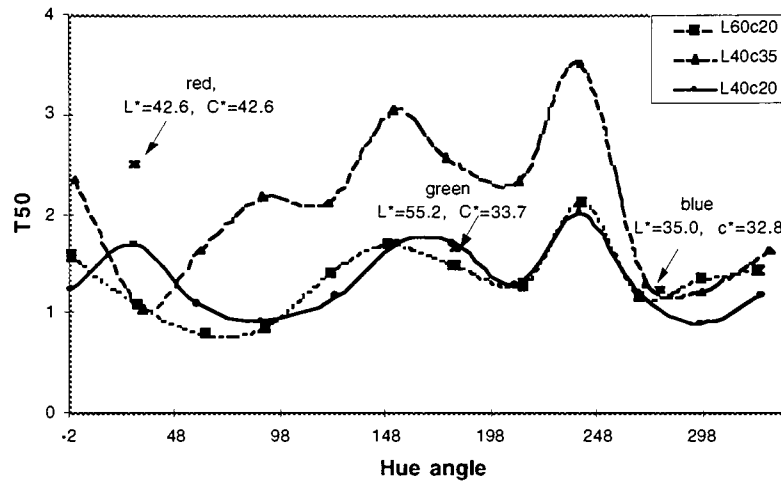


Fig. 39. T50 values as function of CIELAB hue angle for all color centers.

The plots show that T50 values vary with hue angle and have very similar trends for the three hue circles at different chroma and lightness levels. The results are summarized below.

First, The T50 values highly depend on chroma, which is shown clearly in Fig. 39. At the same lightness level ($L^*=40$), the colors at the hue circle with higher chroma ($C_{ab}^*=35$) have higher thresholds than those with lower chroma ($C_{ab}^*=20$). The chroma dependency is also shown in the three CIE recommended colors. The T50 value of the CIE-red center with chroma around 42 is significantly higher than the color centers at the same hue angle. The T50 value of the CIE-green center with lightness 55 and chroma 33 is

higher than the color with the same hue angle at the hue circle with lightness 60 and chroma 20. The T50 value of the CIE-blue center with chroma 32 and lightness 35 is higher than the colors with the same hue angles at the two hue circles with chroma 20. It is also higher than the color at the hue circle with chroma 35. This may indicate experimental error in the hue circle with chroma 35.

Ideally, constant hue is a radial line on the chromaticness plane of CIELAB color space. The distance between the two constant hue (ΔH_{ab}^*) increases with chroma. In other words, we need to increase the hue difference (ΔH_{ab}^*) in order to distinguish the two constant hue lines at higher chroma level. This is why it is easier to notice the hue differences of neutral gray samples than those of most chromatic colors. The hue discrimination thresholds of most of the color centers in the current experiments are greater than 1.

Because the color difference of the anchor pair in hue direction is about 0.9. For many inexperienced observers, they thought the color difference of the anchor pair was very large because of the hue difference of the anchor pair. The thresholds of their visual perception therefore were very high. For some experienced observers, because of the good knowledge of color science, they were aware that the magnitude of the color difference of the anchor pair was

around one unit. The overall results of T50 values in our research could be systematically higher than other research.

Second, Comparing the two hue circles with the same chroma level ($C_{ab}^*=20$) and different lightness levels ($L^*=60$, $L^*=40$), the trends of the data are very similar and the T50 values of these two hue circles are in the same level. The difference between these two circles is that it seems to have some hue angle shift.

Third, as mentioned above, the T50 values of this research were systematically higher than those in current available formulae. In order to compare the systematic trends in our research with others, we need to bring them on to the same level. Commercial factors, thus, were applied. They were determined by comparing the magnitudes of T50 values in this research with those in the CMC, the BFD and the CIE94 formulae. Comparing the present results with the CMC, the BFD and the CIE94 equations, which are shown in Fig. 40 to Fig. 42, it is clear that there are some similarities among CMC, BFD and this research, especially at hue angles of 60 and 270. The RMS values by comparing each data point with CMC, BFD, and CIE94 are listed in TABLE VIII.

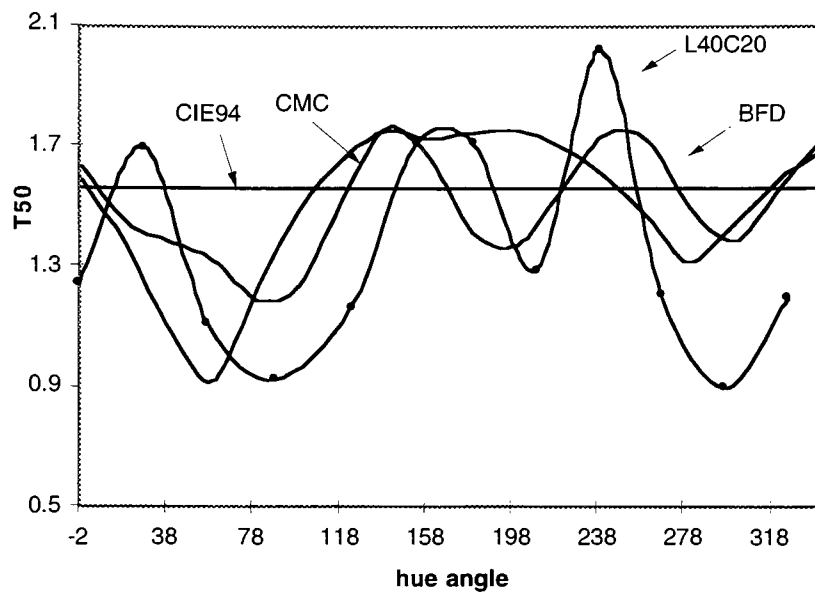


Fig. 40. Comparing L40C20 data with CMC, CIE94 and BFD.

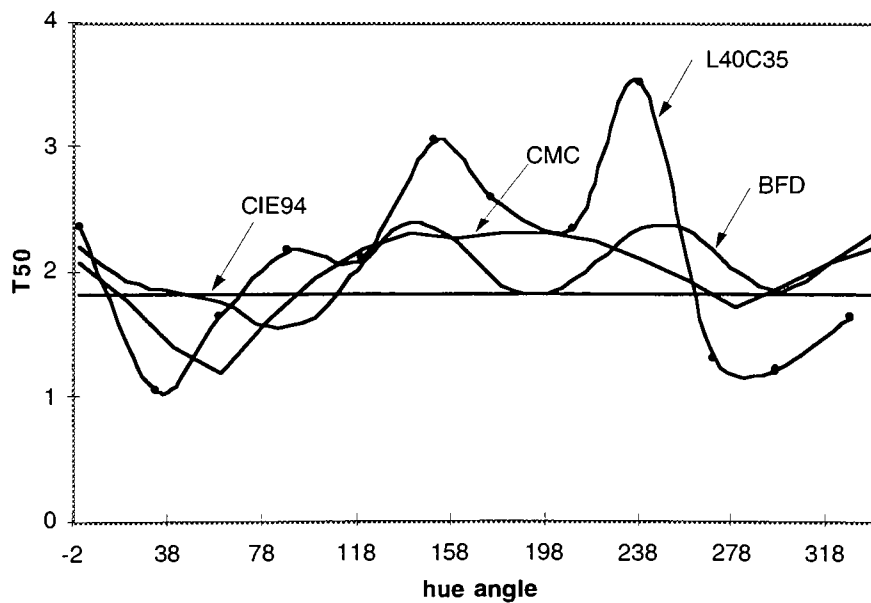


Fig. 41. Comparing L40C35 data with CMC, CIE94 and BFD.

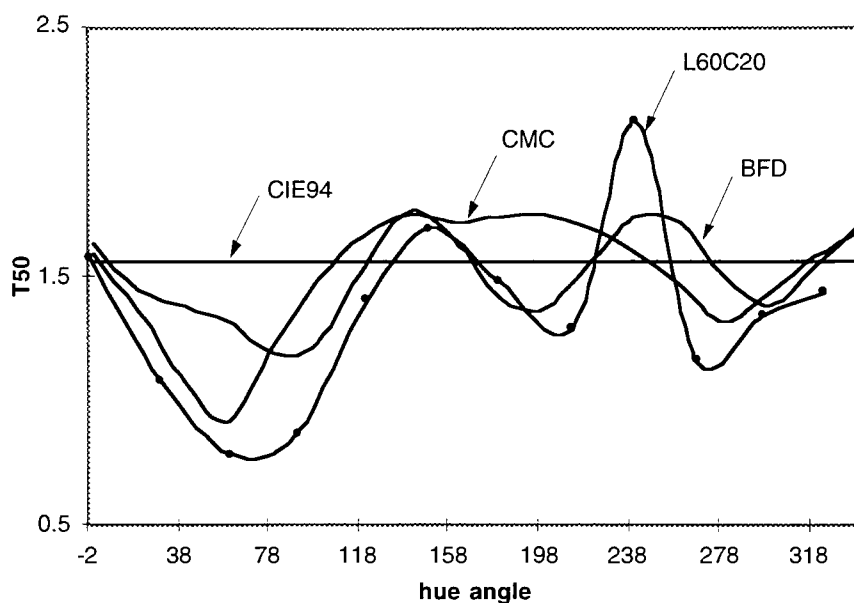


Fig. 42. Comparing L60C20 data with CMC, CIE94 and BFD.

Table VIII The RMS values by comparing experimental data with CMC, BFD, and CIE94 equations.

	CMC	BFD	CIE94
L40C20	0.39	0.35	0.42
L40C35	0.62	0.67	0.80
L60C20	0.30	0.29	0.42
overall	0.45	0.45	0.56

Overall, CMC and BFD are quantitatively equally good at modeling the hue discrimination after applying the commercial factors 1.4 and 2.0, respectively.

The plots show that the trend of the experimental data are best approximated by the BFD formula. It seems that after applying the commercial factor of 1.2, the CIE94 formula averages out the hue discrimination.

Model Fit

1. Testing CMC Model Fit

The previous discussion showed that the CMC formula did not model the results of this research well. It is necessary to compare these results with the original data from which the CMC equation was derived and to check how the CMC equation fits its original data. This is shown in Fig. 43.

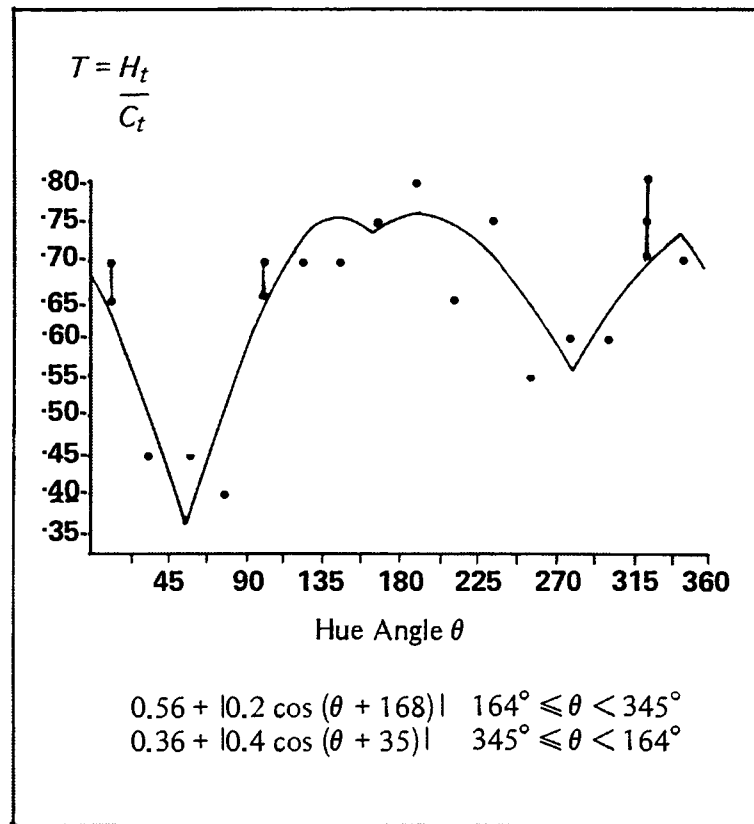


Fig. 43. The CMC model fit with its original data.⁵

The plot indicates that the CMC equation failed to model two local maximum peaks which occurred around hue angles of 180 and 240, and one local minimum peak which occurred around hue angle of 210. They are marked in the plot. Comparing these results with McDonald's original data, it is found that the trends of critical numbers in McDonald's data, which occurred at hue angles of 60, 150, 180, 210, 240, 270 and 330 are very consistent with the present results. It further proves that the CMC hue weighting function does not model the experimental data well.

2. Testing the BFD Equation

The results of the present experiments show that the BFD equation has better correlation with these data compared with the CIE94 and CMC formulae. It is necessary to optimize the BFD equation for the experimental data, and to check the goodness of fit. SYSTAT nonlinear optimization was used to adjust the parameters in the BFD equation. The starting values was carefully chosen by adding the cosine function in the BFD equation piece by piece from time to time. The optimized BFD equation is

$$D_{H_opt} = D_{c_opt}(G_{opt} * T_{opt} + 1 - G_{opt}) \quad (18)$$

where,

$$D_{c_opt} = \frac{0.045 * C^*}{1 - 0.018 * C^*} + 1.181$$

$$G_{opt} = \frac{C^{*4}}{(C^{*4} + 171022.066)^{1/2}}$$

$$T'_{opt} = 0.349 + 0.071 * \cos(h + 3.005) - 0.054 * \cos(2 * h + 3.262) + 0.088 * \cos(3 * h - 0.142) \\ + 0.071 * \cos(4 * h - 1.723) - 0.066 * \cos(5 * h + 4.389)$$

where h has units of arc.

The results are compared with the optimized BFD model, and are shown in Figs. 44-46.

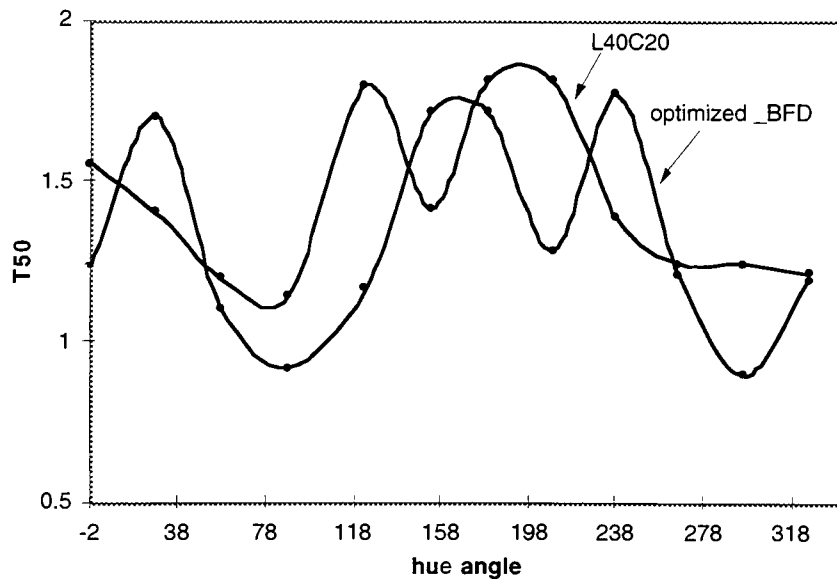


Fig. 44. Comparing the optimized BFD equation with the data L40C20.

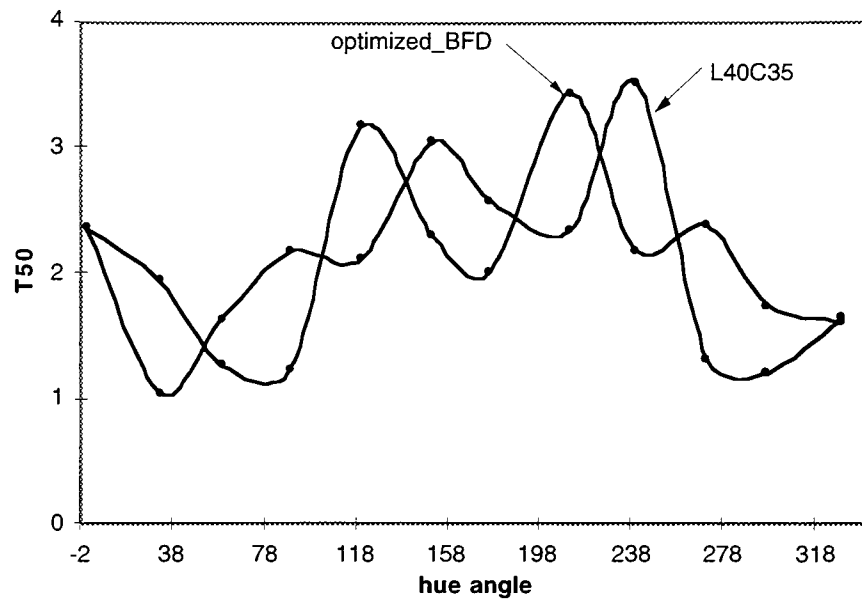


Fig. 45. Comparing the optimized BFD equation with the data L40C35.

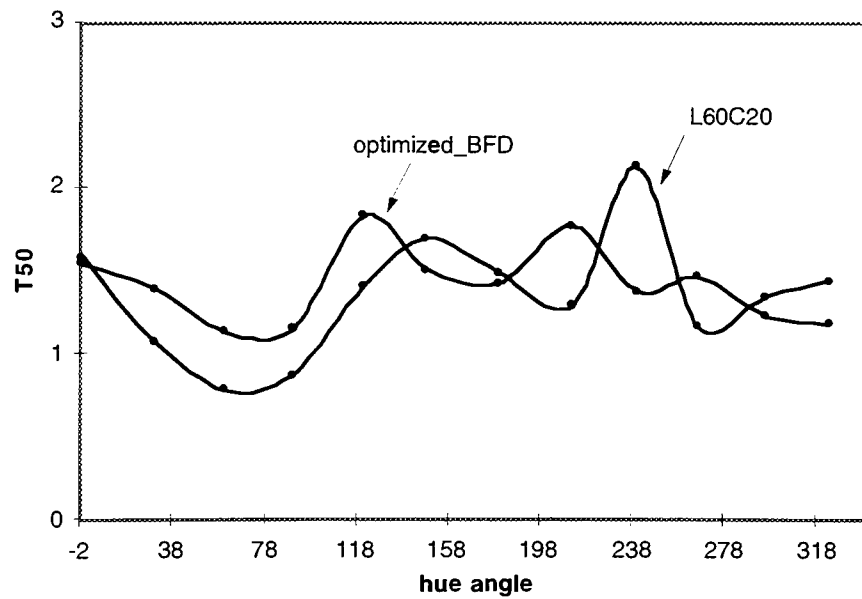


Fig. 46. Comparing the optimized BFD equation with the data L60C20.

The plots show that the BFD has similar trend with our dataset, but has a large hue angle shift, which produces great differences.

The original data from which that the BFD was derived are compared with these experimental data. The goodness of the fit of the BFD equation are shown in Fig. 47. The trend of the original BFD data, especially, the perceptibility data, are very similar with the present experimental data. Both sets of data showed that a strong cosine wave occurred. The frequency changed with hue angle.

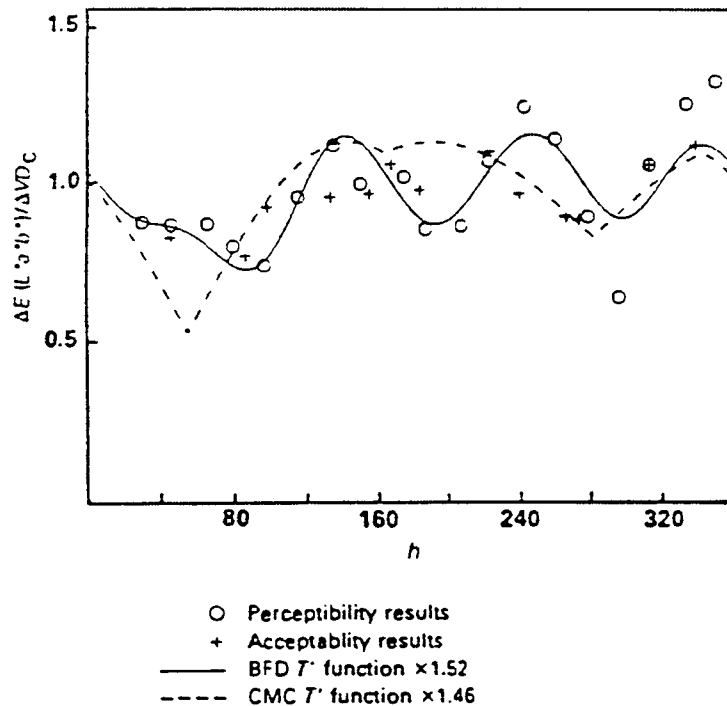


Fig. 47. The BFD model fit with its original data.¹⁸

The plot shows that there are two local maximum peaks occurred around hue angle of 150 and 240. The peak at 240 is higher than that around 150. There are three local minimum peaks occurred. Two of them occurred around hue angle of 210 and 290. The local minimum peak around 290 is lower than that occurred at 210. Fig. 47 also shows that the BFD equation did not accurately model the peak around 240 and the peak around 290 well.

3. Model Derived from Current Dataset

The results of testing the CMC and the BFD formulae showed that both models did not fit the experimental data well. The outline shapes shown in Fig. 20 and Fig. 39 are “~” shape, which could be modeled by the fourth order polynomial. Periodic waves are clearly shown in our results. The frequency of the wave is increasing with hue angle. These could be modeled by cosine wave, $\cos(x)$, and higher order cosine wave, $\cos(x^2)$. The two function multiply each other, thus will get similar trend as shown in the present data.

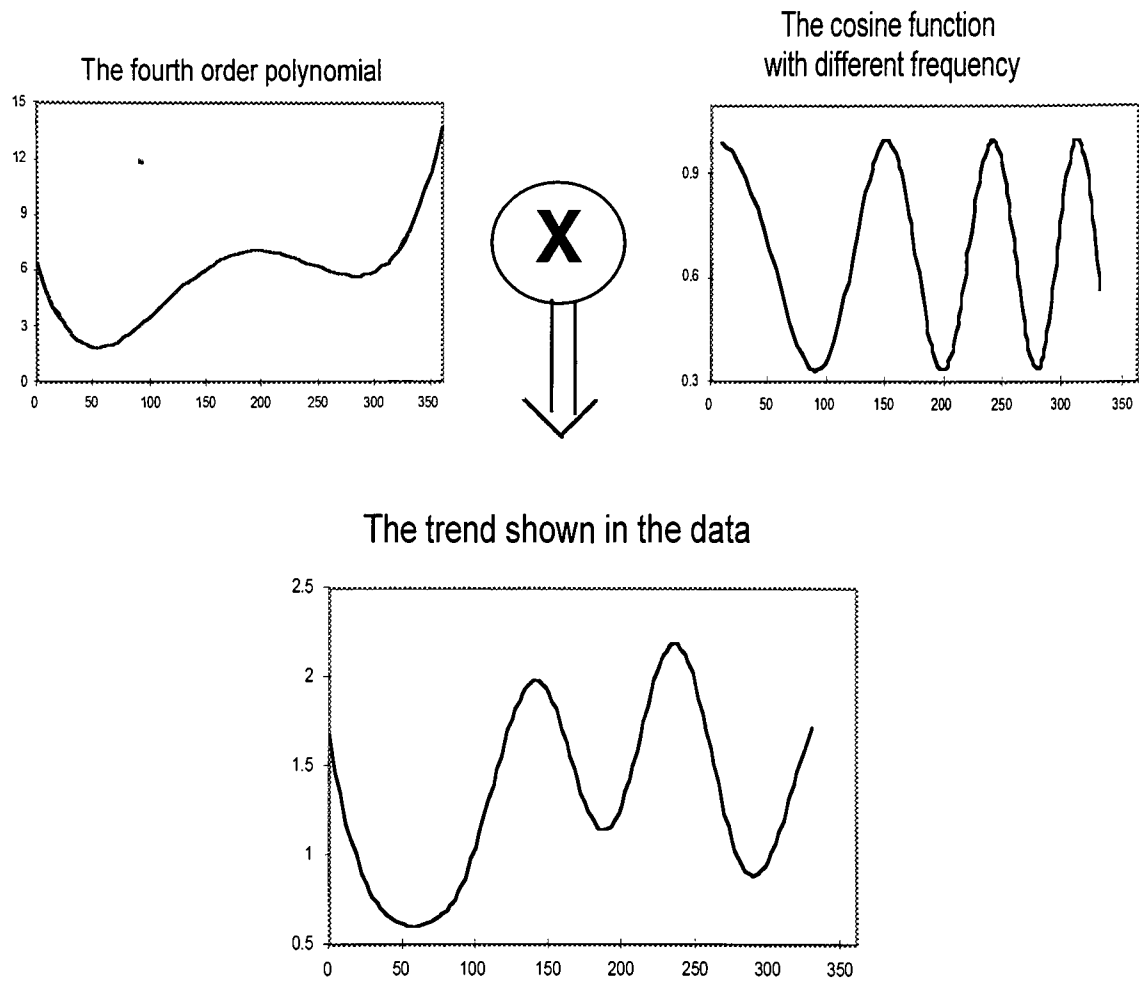


Fig. 48. Derivation of the model.

The fourth order polynomial and cosine functions were derived based on basic calculus theory. The overwhelming trend in the data shows that the fourth order polynomial has two local minimum peaks and one local maximum peak. These peaks occurred around hue angle of 60, 180 and 270. This means that the derivative of this polynomial function at these critical points are zeros. The derivative of this function could be the following

$$P' = A(h - 60)(h - 180)(h - 270) \quad (19)$$

where h is CIELAB hue angle in units of degrees.

Integrating equation (19) with hue angle and adding a constant term adjusted by the experimental data, the fourth order polynomial function is

$$P = 2.13 \times 10^{-9} (h^4/4 - 550h^3/3 + 42600h^2 - 259200h) + 0.233 \quad (20)$$

Studying the cosine function trends in the data, it is found that the frequency increased with hue angle. It seems that $\cos(h^2)$ plays a role. The general function of this cosine wave is $\cos(ah^2+bh+c)$, where a,b, c are parameters obtained by solving a 3-equation system with critical values, such as hue angle 60, 210, 240, 270. The cosine function is

$$T = \cos[\pi / 27000 * (h^2 + 210h)] + 2 \quad (21)$$

The mathematical expression of the hue weighting function derived from this research therefore is

$$F_H = f(C_{ab}^*)(PT + 0.56) \quad (22)$$

The function is differentiable at any points. where $f(C_{ab}^*)$ is a linear function of chroma, which is expressed as

$$f(C_{ab}^*) = 0.029 + 0.047 * C_{ab}^* \quad (23)$$

The equal visual hue differences corrected for chroma position ($T50/f(C_{ab}^*)$) is plotted below.

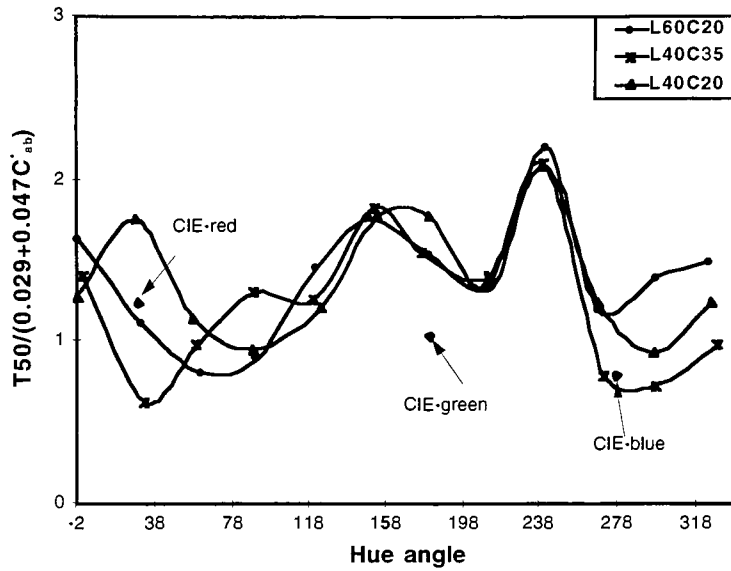


Fig. 49. Equal visual hue differences corrected for chroma position.

Fig. 49 shows that the equal visual hue differences corrected for the chroma position for the three hue circles are very similar. The CIE red and blue centers are in reasonable positions. The equal visual hue difference corrected for the CIE-green center is too low. The average hue differences corrected for chroma position of the three hue circles weighted by fiducial limits is plotted in FIG. 50. Since there were only several chroma levels in this research, the chroma function needs to be tested.

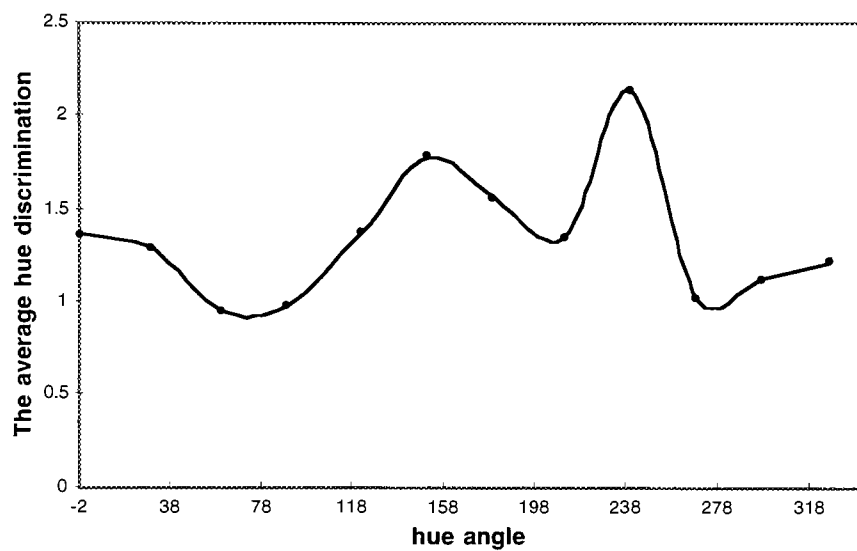


Fig. 50. The average hue discrimination corrected for chroma position.

The calculated data from the model and the experimental data with the fiducial limits of the three complete hue circles are shown in Figs. 51-53.

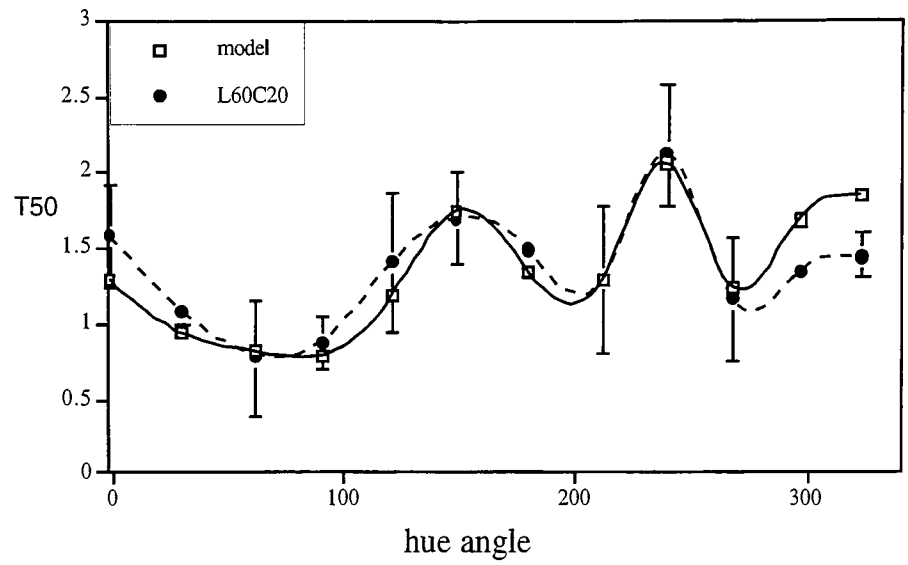


Fig. 51. Testing the model fit for L60C20 hue circle.

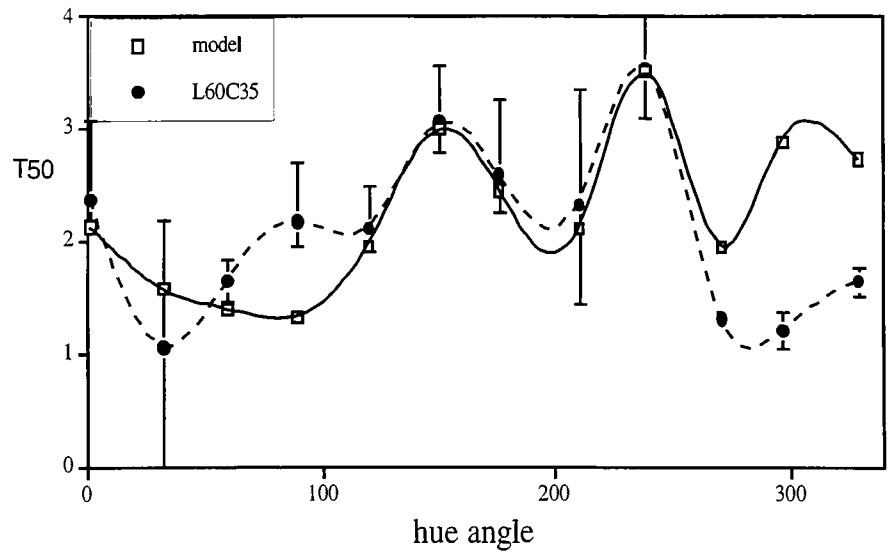


Fig. 52. Testing the model fit for L40C35 hue circle.

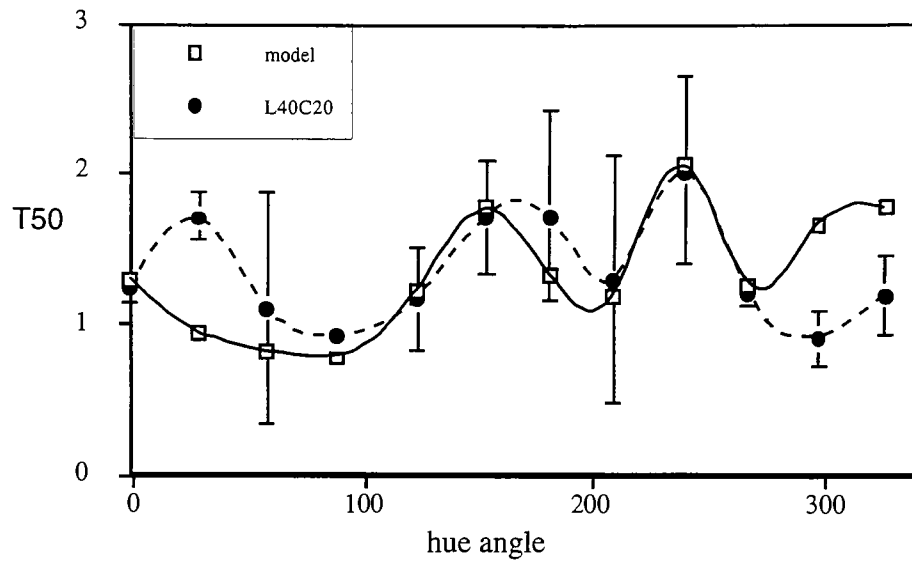


Fig. 53. Testing the model fit for L40C20 hue circle.

The plots show that the model interpolates the overwhelming trends in the current experimental data very well.

The RMS values by comparing experimental data with the present model, CMC, BFD, and CIE94 are listed in TABLE IX.

Table IX. The RMS values by comparing experimental data with the present model, CMC, BFD, and CIE94 equations.

	CMC	BFD	CIE94	model
L40C20	0.39	0.35	0.42	0.40
L40C35	0.62	0.67	0.80	0.71
L60C20	0.30	0.29	0.42	0.21
overall	0.45	0.45	0.56	0.22

Table IX shows that the present model fits the experimental data better than the other three formulae. This model was derived from the three complete hue circles at two different lightness levels and chroma levels. The model is only good at the hue angle range $0 \leq h_{ab} < 360$. 360° will be considered as 0 degree. More visual data should be collected to improve the model and to test the significance of the parameters.

CONCLUSIONS

The purpose of this thesis was to develop more experimental data to describe consumers' color-difference judgment behavior along hue direction under the reference condition of CIE TC1-29. Comparing these reference conditions with previous research performed at R.I.T, the lightness of the background and surround was changed from 38 to 50 L^* . The visual assessments were conducted to test the significance of the change in background and surround. The results showed that changing lightness of the gray background and surround resulted in significant change in T50 values along lightness direction for gray color and insignificant change in this direction for colors away from the origin. There was no significant change for those vectors in chromaticness plane and vectors representing the interaction between the chromaticness and lightness on the change of the lightness of gray background and surround. The viewing condition of this thesis, thus, is equivalent with the previous research.

Forty-five observers participated in the pass/fail experiments. Thirty nine color centers including three complete hue circle at different lightness or chroma levels and three CIE recommended colors (Red, green, blue) were tested for hue discrimination. A total of 32,226 visual observations were made. Observers' variability was analyzed and compared with McDonald's

acceptability matching experiments. The variability of our observers were reasonable though larger than found by McDonald's. However, McDonald's observers were only eight very experienced observers rather than 45 observers with a wide range of experiments.

In contrast to previous research, the statistical analysis method was changed from uni-dimensional to multi-dimensional due to the printer's variability. The SAS logit program with three dimensional normit function was chosen. The program was tested by the cyan center in previous Phase I and Phase II research and the background and surround experiments. The results of the probit analysis and the results of the logit with 3-dimensional normit analysis were compared. The identical results indicated that the logit program with 3-D normit function was an extended probit analysis in multiple dimensions. The results of this research are statistically consistent with previous Phase I and Phase II research. The chi-squared value was also calculated for testing the model fit of each color center, and were of reasonable range. Therefore, the logit program with normit function is a proper method for analyzing the experimental data.

The experimental results indicated that the hue discrimination thresholds of observers vary with CIELAB hue angle. The suprathresholds increase with the chroma values of the standard points. The CMC, BFD and CIE94 equation were tested by the present dataset. The dataset were also compared with the

original data used to derive the CMC and BFD formulae. These data showed that the CMC equation did not fit both its original data and the present data well. Thus the complicated CMC hue weighting function is questionable. Compared to the CMC equation, the BFD equation has a better fit to its original data and the current data. However, it is not accurate enough to model the trends in some critical points. A mathematical equation was derived from the present results. It well models the trends of the experimental data.

It is felt that more visual experiments need to be conducted in testing hue discrimination at different lightness and chroma levels. A new method of producing samples should be adopted due to the difficulties of the Fuji printer.

REFERENCES

1. R.S. Berns, *Proposal: Industrial Color-Difference Evaluation Consortium*, (1994).
2. D.H. Alman, R.S. Berns, G.D. Snyder, and W.A. Larsen, Performance metrics using a color tolerance dataset, *Color Res. Appl.* **14**, 139-150 (1989).
3. R. McDonald, Industrial pass/fail color matching, Part I Preparation of visual color-matching data, *J. Soc. Dyers Colorists* **96**, 372-376 (1980).
4. R. McDonald, Industrial pass/fail color matching, Part II - Methods of fitting tolerance ellipsoids, *J. Soc. Dyers Colorists* **96**, 418-422 (1980).
5. R. McDonald, Industrial pass/fail color matching, Part III Development of a pass/fail formula for use with instrumental measurement of color difference, *J. Soc. Dyers Colorists* **96**, 486-497 (1980).
6. A.R. Robertson, Guidelines for coordinated research on color-difference evaluation, *Color Res. Appl.* **3**, 149-151 (1978).
7. K. Witt and G. Doring, Parametric variations in a threshold color-difference ellipsoid for green painted samples, *Color Res. Appl.* **8**, 153-163 (1983).

8. K. Witt, Three-dimensional threshold of color-difference perceptibility in painted samples: variability of observers in four CIE color regions, *Color Res. Appl.* **12**, 128-134 (1987).
9. M.R. Luo and B. Rigg, Chromaticity-discrimination ellipses for surface colors, *Color Res. Appl.* **11**, 25-42 (1986).
10. G.D. Snyder, *Visual Determination of Industrial Color-Difference Tolerances Using probit Analysis*, RIT Master Thesis (1991).
11. R.S. Berns, D.H. Alman, L. Renniff, G.D. Snyder, and M.R. Balonon-Rosen, Visual determination of suprathreshold color-difference tolerances using probit analysis, *Color Res. Appl.* **16**, 297-316 (1991).
12. L. Reniff, *Visual Determination of Color Differences Using probit Analysis: Phase II*, RIT Master Thesis (1989).
13. R.M. McDonald, A review of the relationship between visual and instrumental assessment of color difference, part 1, *J. Oil Col. Chem. Assoc.* **65**, 93-106 (1982).
14. R.M. McDonald, Acceptability and perceptibility decisions using the CMC color difference formula, *J. Oil Chem. Assoc.* **20**, 31-37 (1988).

- performance using LUTCHI color appearance data, *Color Res. Appl.* **16**, 181-183 (1991).
16. R.G. Kuehni, Advances in color-difference formulas, *Color Res. Appl.* **7**, 19-23 (1982).
17. CIE publication 116, *Industrial color-difference evaluation*, p.116, (1995).
18. M.R. Luo and B. Rigg, BFD(l:c) color-difference formula part I-development of the formula, *J. Soc. Dyers Colorist* **103**, 86-92 (1987).
19. R.S. Berns, The mathematical development of CIE TC1-29 proposed color difference equation: CIELCH, *Proceedings AIC Colour 93*, Vol. B, C19-1-4, 1993.
20. R. S. Berns, Cathode-ray-tube to reflection-print matching under mixed chromatic adaptation using RLAB, *Journal of Electronic Imaging*, **4**, 347-359 (1995).
21. G. Wyszecki and W.S. Stiles, *Color Science: Concepts and Methods, Quantitative Data and Formulae, 2nd Edition*, John Wiley & Sons, NewYork, 496-497 (1982).
22. *SAS/STAT User's Guide, Version 6, 4th Edition* , Volume 2, SAS Institute Inc. (1990).
23. D.J. Finney, *Probit Analysis, 3rd Edition*, Cambridge Univ. Press, Cambridge (1971).

24. Lisa Reniff, Transferring the 45/0 spectral reflectance factor scale, *Color Res. Appl.* **19**, 332-340 (1994).
25. R. S. Berns, Empirical modeling of systematic spectrophotometric error, *Color Res. Appl.* **13**, 243-256 (1988).
26. K. McLaren, An introduction to instrumental shade passing and sorting and a review of recent developments, *J. Soc. Dyers Colorist* **92**, 317-326 (1976).

APPENDIX A

The measurements of the 393 color sample pairs

	L [*]	a [*]	b [*]	C _{ab} [*]	hue angle
c2h0	39.07	19.27	-0.97	19.30	-2.89
	39.21	19.18	-0.64	19.19	-1.90
	38.20	19.54	-1.21	19.58	-3.56
	38.16	19.60	-0.67	19.61	-1.94
	38.90	19.45	-0.56	19.45	-1.65
	38.65	19.56	0.31	19.56	0.90
	38.52	18.64	-0.76	18.65	-2.34
	38.43	18.59	-1.68	18.67	-5.15
	38.15	19.58	0.45	19.58	1.33
	38.59	19.66	-0.60	19.67	-1.75
	38.66	18.97	-0.75	18.99	-2.27
	39.14	18.90	-2.18	19.03	-6.57
	39.18	19.17	-0.53	19.17	-1.59
	39.09	19.20	0.99	19.23	2.95
	38.45	19.17	-1.56	19.23	-4.64
	38.78	19.07	0.06	19.07	0.19
	38.07	19.72	0.48	19.72	1.40
	38.06	20.07	-1.74	20.14	-4.95
average	38.63	19.30	-0.64	19.33	-1.91
c2h30	38.83	17.08	9.64	19.61	29.44
	38.89	17.13	9.31	19.49	28.53
	37.58	17.59	8.76	19.65	26.47
	37.66	17.24	9.19	19.54	28.04
	38.81	16.79	9.18	19.14	28.66
	38.59	17.11	8.56	19.13	26.57
	38.90	16.73	8.10	18.59	25.84
	39.19	16.20	8.98	18.52	28.99
	38.92	17.09	8.91	19.28	27.53
	38.60	16.93	9.86	19.59	30.21
	38.73	17.55	8.83	19.65	26.72

	38.34	17.21	10.22	20.02	30.70
	37.98	17.09	9.99	19.80	30.32
	38.33	18.06	8.99	20.18	26.47
	39.08	15.99	9.39	18.54	30.43
	39.08	16.83	7.66	18.49	24.49
	37.99	17.08	7.67	18.72	24.19
	38.75	16.42	9.17	18.81	29.18
	37.72	18.33	7.97	19.98	23.50
	38.31	16.90	9.95	19.61	30.50
average	38.51	17.07	9.02	19.32	27.84
c2h60	38.85	9.28	15.88	18.39	59.69
	38.84	9.21	16.60	18.99	60.98
	37.73	10.40	14.43	17.79	54.22
	37.82	9.64	14.43	17.35	56.25
	37.90	10.00	15.05	18.07	56.40
	37.70	9.69	15.75	18.49	58.41
	38.70	10.23	14.75	17.95	55.24
	38.67	9.57	15.51	18.22	58.32
	38.49	10.44	16.12	19.21	57.07
	37.71	10.50	15.10	18.39	55.19
	39.25	9.45	16.85	19.32	60.71
	39.36	8.42	17.52	19.44	64.33
	37.21	12.16	15.46	19.67	51.81
	37.50	10.87	15.93	19.29	55.70
	39.14	9.07	15.50	17.96	59.67
	38.52	10.29	14.20	17.53	54.08
	39.34	9.82	16.61	19.29	59.41
	38.55	11.04	15.60	19.12	54.71
	38.20	10.54	16.38	19.48	57.24
average	38.39	10.03	15.67	18.63	57.34
c2h90	38.52	8.88	17.77	19.87	63.46
	38.25	-0.64	18.64	18.65	91.98
	38.20	-0.32	18.56	18.57	90.98
	37.83	1.24	18.09	18.13	86.09
	37.99	0.48	18.48	18.48	88.52

	38.53	-0.09	18.13	18.13	90.30
	38.48	-1.30	17.75	17.80	94.19
	38.58	-0.37	19.34	19.35	91.08
	38.63	0.48	19.63	19.63	88.59
	38.63	0.96	19.82	19.84	87.22
	38.60	-0.38	20.14	20.15	91.07
	39.09	0.26	19.31	19.31	89.22
	38.94	-1.07	19.21	19.24	93.17
	37.73	1.91	19.59	19.68	84.43
	38.02	0.20	19.23	19.23	89.40
	37.64	-0.03	18.91	18.91	90.10
	37.34	1.86	19.30	19.39	84.51
	37.96	1.50	18.35	18.41	85.34
	38.66	-0.43	18.64	18.65	91.32
average	38.30	0.69	18.89	19.02	87.95
c2h120	38.39	-10.31	16.79	19.71	121.55
	38.51	-10.6	16.59	19.69	122.57
	38.90	-11.16	16.47	19.89	124.12
	38.83	-11.51	16.15	19.83	125.46
	38.29	-10.23	16.97	19.81	121.09
	38.03	-10.91	16.59	19.86	123.33
	38.74	-10.13	17.04	19.83	120.74
	38.76	-10.91	16.52	19.79	123.44
	39.09	-11.07	15.48	19.03	125.56
	38.05	-11.11	16.7	20.06	123.62
	38.43	-10.87	17.26	20.40	122.2
	38.51	-11.9	16.43	20.29	125.92
	39.27	-12.36	16.72	20.79	126.48
	38.78	-10.82	17.52	20.59	121.7
	38.49	-11.58	16.07	19.81	125.79
	38.11	-9.79	16.70	19.35	120.38
	38.58	-11.44	15.71	19.44	126.06
	38.04	-9.74	16.72	19.35	120.23
average	38.55	-10.91	16.58	19.86	123.35
c2h150	37.31	-18.73	9.91	21.19	152.11

	37.19	-19.17	9.55	21.42	153.52
	38.38	-19.35	10.83	22.17	150.78
	38.34	-19.56	10.06	22.00	152.77
	37.82	-19.04	10.33	21.66	151.53
	37.79	-19.33	9.62	21.59	153.55
	37.31	-18.54	9.49	20.83	152.90
	37.38	-18.66	8.34	20.44	155.93
	38.73	-19.76	9.04	21.73	155.42
	38.76	-19.32	10.20	21.85	152.18
	37.50	-18.93	8.46	20.73	155.93
	37.52	-18.62	9.91	21.09	151.98
	38.34	-19.97	9.26	22.02	155.12
	37.99	-19.03	10.94	21.95	150.11
	38.00	-19.77	9.03	21.74	155.46
	37.97	-18.96	10.80	21.82	150.34
	37.79	-19.18	8.53	20.99	156.04
	37.98	-18.99	10.56	21.72	150.93
average	37.90	-19.16	9.71	21.50	153.14
c2h180	38.07	-22.58	-0.54	22.59	181.36
	38.14	-22.57	-0.85	22.59	182.16
	37.69	-21.37	-0.03	21.37	180.08
	37.57	-21.07	-1.25	21.11	183.39
	37.62	-21.62	1.13	21.65	177.02
	37.77	-21.65	0.58	21.66	178.47
	37.70	-21.48	-0.04	21.48	180.11
	37.89	-21.71	-0.96	21.73	182.53
	37.50	-21.37	-1.25	21.40	183.35
	37.43	-21.62	-0.13	21.62	180.34
	38.11	-21.82	-0.75	21.83	181.97
	37.62	-21.75	0.43	21.76	178.87
	37.37	-20.73	-0.46	20.74	181.26
	37.71	-21.03	0.99	21.05	177.30
	37.97	-21.52	1.08	21.55	177.12
	38.21	-21.47	-0.99	21.49	182.64
	38.29	-22.40	-0.87	22.41	182.22

	38.17	-22.07	1.39	22.12	176.40
	37.82	-21.66	-0.14	21.67	180.37
average	37.82	-21.66	-0.14	21.67	180.37
c2h210	38.15	-18.28	-10.66	21.16	210.26
	38.16	-18.57	-10.1	21.13	208.54
	38.58	-19.04	-10.12	21.56	207.99
	38.68	-18.85	-9.59	21.15	206.96
	38.37	-18.77	-10.8	21.65	209.91
	38.72	-19.19	-10.11	21.69	207.79
	39.00	-18.10	-11.02	21.19	211.34
	38.69	-18.54	-10.34	21.23	209.15
	38.69	-18.52	-10.83	21.45	210.32
	38.23	-18.95	-9.83	21.35	207.41
	38.64	-18.95	-10.32	21.58	208.58
	38.49	-19.04	-9.19	21.14	205.77
	37.77	-17.52	-10.66	20.51	211.31
	37.73	-18.61	-9.66	20.97	207.44
	38.93	-18.58	-11.1	21.64	210.86
	38.84	-19.53	-9.58	21.75	206.13
	37.93	-19.06	-9.93	21.50	207.53
	38.32	-17.68	-11.41	21.04	212.83
	38.24	-18.09	-11.57	21.48	212.61
	38.90	-19.63	-10.00	22.03	207.00
average	38.45	-18.67	-10.34	21.36	208.99
c2h240	38.80	-11.70	-18.39	21.79	237.54
	38.80	-11.98	-18.01	21.63	236.38
	38.56	-10.28	-18.76	21.40	241.28
	38.41	-10.74	-18.47	21.36	239.82
	39.30	-11.47	-18.33	21.62	237.96
	39.43	-12.26	-17.96	21.74	235.67
	38.54	-10.58	-19.15	21.88	241.08
	38.30	-11.05	-18.50	21.55	239.15
	38.63	-12.22	-18.03	21.78	235.87
	38.42	-11.23	-18.71	21.83	239.03
	38.86	-11.96	-18.46	22.00	237.06

	39.26	-10.75	-18.97	21.80	240.46
	38.55	-11.52	-18.32	21.64	237.85
	38.39	-10.01	-18.68	21.19	241.80
	39.02	-11.71	-18.31	21.74	237.40
	38.88	-10.27	-19.24	21.81	241.91
	39.51	-12.40	-17.95	21.82	235.35
	39.21	-10.90	-19.29	22.16	240.52
	38.23	-12.20	-18.74	22.36	236.95
	37.97	-10.55	-20.11	22.71	242.32
	38.92	-10.48	-19.72	22.33	242.01
	39.27	-12.72	-18.32	22.30	235.23
	37.94	-10.41	-18.38	21.12	240.47
	37.92	-12.25	-16.73	20.74	233.80
	38.92	-11.25	-18.34	21.51	238.48
	39.05	-9.23	-19.85	21.89	245.07
	38.28	-12.82	-17.47	21.67	233.73
	38.10	-10.26	-18.91	21.51	241.52
average	38.69	-11.26	-18.57	21.75	238.77
c2h270	38.28	0.03	-20.99	20.99	270.07
	38.47	-0.16	-20.76	20.77	269.55
	38.62	0.04	-21.10	21.10	270.11
	38.47	-0.62	-20.8	20.81	268.30
	39.06	-0.97	-20.78	20.80	267.32
	38.95	-1.72	-20.87	20.94	265.30
	38.74	-1.63	-20.84	20.90	265.53
	38.49	-0.68	-20.86	20.87	268.15
	38.75	-0.82	-20.64	20.65	267.73
	38.93	-1.89	-21.04	21.12	264.87
	39.17	-2.23	-20.65	20.77	263.84
	39.40	-0.75	-20.56	20.58	267.90
	38.91	-2.16	-20.99	21.10	264.12
	39.03	-0.56	-20.68	20.69	268.44
	39.86	-0.17	-20.99	20.99	269.54
	39.21	-1.99	-20.99	21.09	264.59
	39.63	-2.73	-20.82	21.00	262.54

	39.75	-0.52	-21.33	21.33	268.61
	39.08	-2.34	-20.86	20.99	263.60
	39.05	-0.09	-20.57	20.57	269.75
	38.99	-1.10	-20.86	20.90	266.99
average	38.99	-1.10	-20.86	20.90	266.99
c2h300	39.11	9.26	-17.92	20.17	297.33
	39.08	8.98	-18.23	20.32	296.22
	39.27	8.67	-18.78	20.68	294.77
	39.10	8.94	-18.37	20.43	295.96
	38.62	9.71	-18.78	21.14	297.34
	38.87	10.31	-18.93	21.55	298.59
	39.39	9.52	-18.85	21.12	296.79
	39.34	8.66	-19.08	20.95	294.42
	38.72	9.28	-17.96	20.22	297.32
	39.10	8.34	-18.16	19.98	294.66
	38.76	8.81	-18.99	20.94	294.90
	38.83	9.92	-18.31	20.83	298.44
	38.96	8.15	-18.74	20.43	293.50
	39.07	9.57	-18.33	20.68	297.56
	38.99	9.82	-17.77	20.30	298.94
	38.76	8.72	-18.98	20.89	294.67
	38.65	8.47	-19.50	21.26	293.48
	38.59	10.20	-18.76	21.35	298.54
average	38.96	9.19	-18.58	20.74	296.30
c2h330	38.92	16.43	-10.45	19.47	327.56
	38.88	16.28	-10.8	19.53	326.44
	38.62	16.33	-11.41	19.92	325.04
	38.58	16.53	-10.84	19.76	326.75
	39.05	16.18	-12.44	20.40	322.44
	38.98	16.19	-11.66	19.95	324.23
	39.35	15.09	-11.62	19.05	322.41
	39.04	15.82	-11.08	19.31	325.00
	39.15	16.07	-12.50	20.36	322.12
	38.77	16.52	-11.66	20.22	324.78
	38.08	17.57	-10.64	20.54	328.81

	38.07	16.89	-11.71	20.55	325.26
	39.01	16.26	-11.41	19.86	324.95
	39.03	17.03	-10.34	19.93	328.74
	38.49	16.65	-10.60	19.74	327.51
	38.89	16.21	-12.34	20.37	322.72
	38.99	16.52	-10.35	19.49	327.93
	39.27	15.45	-12.31	19.75	321.45
average	38.84	16.33	-11.34	19.90	325.23
c35h0	37.44	34.39	-2.60	34.49	-4.32
	37.37	34.65	-2.28	34.72	-3.77
	37.33	33.61	0.76	33.61	1.30
	37.50	33.45	1.46	33.48	2.50
	37.54	33.42	0.86	33.43	1.47
	38.00	33.38	-0.28	33.38	-0.48
	36.60	34.45	0.48	34.45	0.80
	36.97	34.30	1.45	34.33	2.42
	37.24	33.59	1.14	33.61	1.94
	36.86	34.00	0.19	34.00	0.32
	37.37	34.08	1.12	34.10	1.88
	36.90	34.46	-0.23	34.46	-0.38
	36.65	34.40	0.02	34.40	0.03
	37.12	34.14	1.91	34.19	3.20
	39.81	32.86	-0.72	32.87	-1.25
	39.17	33.33	1.26	33.35	2.17
	37.46	33.82	1.44	33.86	2.43
	37.22	33.98	-0.34	33.99	-0.58
	39.25	33.51	1.02	33.52	1.75
	38.70	33.93	-0.44	33.93	-0.74
average	37.62	33.89	0.31	33.91	0.53
c35h30	36.88	29.70	18.66	35.07	32.14
	37.14	29.37	18.93	34.95	32.80
	36.71	29.08	18.35	34.38	32.25
	36.81	29.44	17.77	34.38	31.11
	37.12	29.31	18.51	34.67	32.28
	37.08	29.35	17.46	34.15	30.75

	36.85	29.02	18.82	34.59	32.96
	37.26	29.65	18.12	34.75	31.42
	37.96	29.10	18.48	34.47	32.42
	37.73	28.59	19.50	34.61	34.30
	36.54	30.40	17.63	35.14	30.12
	36.78	30.13	19.12	35.69	32.40
	36.85	29.59	19.26	35.30	33.06
	36.7	29.89	17.59	34.68	30.48
	37.24	29.84	18.77	35.25	32.17
	37.61	28.82	19.97	35.06	34.72
	37.09	30.10	17.98	35.06	30.85
	37.58	28.73	19.45	34.69	34.09
average	37.11	29.45	18.58	34.83	32.24
c35h60	36.57	18.12	28.45	33.73	57.50
	36.78	18.36	28.24	33.69	56.98
	37.57	17.41	29.67	34.40	59.60
	37.65	17.87	29.61	34.58	58.88
	37.10	16.53	29.51	33.83	60.74
	36.86	15.89	29.80	33.77	61.93
	36.68	17.47	29.33	34.14	59.22
	36.44	16.56	29.68	33.99	60.84
	36.77	17.07	29.46	34.05	59.91
	36.77	18.22	29.00	34.25	57.86
	38.04	17.72	28.78	33.79	58.38
	38.00	16.86	29.86	34.29	60.55
	36.79	17.79	29.07	34.08	58.53
	36.63	18.98	28.07	33.88	55.94
	37.69	16.27	30.53	34.60	61.94
	37.51	18.23	30.24	35.31	58.91
	37.71	16.50	29.90	34.15	61.10
	37.56	18.27	28.93	34.22	57.73
	36.74	16.40	29.35	33.62	60.81
	36.92	18.12	28.21	33.53	57.29
average	37.14	17.43	29.28	34.09	59.23
c35h90	37.31	2.12	34.03	34.10	86.43

	37.11	1.83	33.92	33.97	86.92
	37.33	0.93	35.02	35.04	88.48
	37.14	0.18	35.03	35.03	89.71
	36.84	0.73	34.37	34.37	88.78
	37.02	0.09	34.67	34.67	89.85
	36.16	1.23	33.74	33.77	87.91
	36.05	0.32	33.37	33.37	89.46
	36.22	0.93	34.18	34.19	88.44
	36.56	-0.02	34.75	34.75	90.03
	36.62	0.67	34.23	34.24	88.87
	36.29	1.91	34.13	34.18	86.80
	36.86	0.97	34.17	34.18	88.38
	37.23	-0.33	34.53	34.53	90.55
	37.61	-0.47	34.79	34.80	90.78
	37.47	1.32	34.92	34.95	87.83
	37.47	0.84	34.51	34.52	88.60
	38.15	-0.84	34.61	34.62	91.40
average	36.97	0.69	34.39	34.40	88.85
c35h120	37.32	-16.93	30.50	34.88	119.03
	37.22	-17.18	30.08	34.64	119.72
	37.04	-17.96	30.99	35.82	120.09
	37.19	-18.52	31.32	36.38	120.60
	36.59	-17.94	29.63	34.64	121.20
	36.47	-17.02	29.93	34.43	119.64
	37.53	-17.21	31.01	35.47	119.04
	37.71	-18.16	30.85	35.80	120.48
	37.92	-18.67	31.02	36.20	121.03
	37.82	-17.82	31.58	36.26	119.44
	37.35	-17.43	31.47	35.97	118.99
	37.48	-18.34	30.37	35.48	121.13
	36.77	-18.16	29.79	34.89	121.37
	36.56	-16.63	29.86	34.18	119.11
	36.68	-17.58	30.40	35.12	120.03
	36.93	-15.82	30.84	34.66	117.16
	37.90	-16.31	31.63	35.58	117.28

	37.88	-18.29	30.84	35.86	120.66
	38.01	-16.08	30.75	34.70	117.61
	37.95	-18.44	30.87	35.96	120.86
average	37.32	-17.52	30.69	35.35	119.72
c35h150	37.39	-31.35	17.64	35.98	150.63
	37.45	-31.08	17.90	35.86	150.06
	37.07	-30.85	17.11	35.28	150.98
	37.13	-30.89	16.67	35.10	151.65
	38.12	-32.12	17.37	36.51	151.59
	38.23	-31.70	17.82	36.37	150.66
	37.95	-31.97	16.75	36.09	152.36
	37.67	-31.47	17.60	36.06	150.79
	38.44	-31.51	18.27	36.42	149.89
	38.22	-32.25	17.46	36.67	151.56
	37.29	-31.40	18.53	36.46	149.45
	37.42	-31.85	17.18	36.19	151.66
	37.05	-31.39	15.93	35.20	153.09
	37.47	-30.98	17.07	35.37	151.15
	37.14	-31.28	18.41	36.29	149.52
	37.27	-31.85	16.91	36.06	152.03
	38.11	-31.65	18.62	36.72	149.53
	38.60	-32.55	16.81	36.64	152.70
	38.17	-31.95	16.92	36.16	152.09
	37.89	-31.73	19.22	37.09	148.79
	39.18	-31.09	18.33	36.09	149.48
	39.38	-32.42	16.66	36.45	152.80
	38.29	-31.37	15.14	34.83	154.24
	38.03	-29.79	17.29	34.45	149.88
	37.87	-32.00	15.57	35.59	154.05
	37.62	-30.44	17.69	35.21	149.84
average	37.86	-31.50	17.34	35.97	151.17
c35h180	38.51	-35.54	1.62	35.58	177.39
	38.49	-35.64	2.17	35.71	176.51
	38.67	-35.96	3.21	36.10	174.90
	38.34	-35.87	2.68	35.97	175.72

	38.61	-36.25	3.38	36.41	174.68
	38.80	-36.04	2.58	36.13	175.91
	38.75	-35.90	3.83	36.10	173.92
	38.97	-35.92	3.02	36.05	175.19
	37.69	-35.26	3.54	35.44	174.27
	37.40	-35.13	2.33	35.21	176.20
	37.82	-35.59	3.44	35.75	174.49
	37.78	-35.50	2.16	35.56	176.53
	37.96	-35.25	4.05	35.48	173.44
	38.06	-35.64	2.72	35.74	175.63
	38.24	-35.82	-2.04	35.88	183.27
	38.13	-36.01	-0.25	36.01	180.41
	38.01	-35.64	1.46	35.67	177.65
	38.36	-35.91	3.78	36.11	174.00
average	38.25	-35.72	2.43	35.83	176.12
c35h210	39.74	-32.22	-18.77	37.29	210.22
	39.73	-32.59	-18.35	37.40	209.39
	39.76	-31.71	-17.99	36.45	209.57
	40.02	-31.56	-18.48	36.57	210.35
	39.26	-31.67	-19.04	36.95	211.01
	39.66	-32.18	-18.41	37.07	209.78
	39.97	-32.20	-18.90	37.34	210.42
	39.72	-31.82	-19.52	37.33	211.53
	39.41	-31.53	-19.65	37.16	211.93
	39.33	-32.06	-18.43	36.98	209.89
	38.74	-30.96	-19.88	36.79	212.72
	39.02	-31.59	-18.83	36.78	210.80
	39.44	-32.04	-18.99	37.24	210.65
	39.31	-32.82	-17.69	37.28	208.33
	40.16	-32.50	-17.18	36.76	207.86
	40.73	-31.84	-18.80	36.98	210.56
	39.61	-32.04	-18.78	37.14	210.38
	39.15	-30.88	-20.45	37.04	213.51
	39.75	-31.14	-20.76	37.43	213.69
	39.75	-32.41	-18.67	37.40	209.95

average	39.61	-31.89	-18.88	37.07	210.63
c35h240	38.25	-18.71	-31.92	37.00	239.62
	38.31	-19.02	-31.64	36.92	238.99
	38.85	-19.57	-31.27	36.89	237.96
	38.85	-20.20	-31.04	37.04	236.94
	37.97	-18.25	-31.95	36.79	240.26
	38.07	-17.61	-32.25	36.74	241.36
	39.15	-18.64	-31.82	36.88	239.64
	38.97	-19.55	-31.35	36.95	238.05
	38.71	-19.50	-31.39	36.96	238.15
	38.22	-18.61	-31.93	36.96	239.77
	38.71	-19.34	-31.46	36.93	238.41
	38.49	-18.09	-32.03	36.78	240.54
	39.33	-19.46	-31.66	37.17	238.42
	38.76	-18.02	-32.03	36.75	240.63
	39.01	-19.45	-31.03	36.62	237.92
	39.07	-17.88	-32.01	36.67	240.82
	38.40	-18.25	-31.98	36.82	240.29
	38.62	-20.13	-31.02	36.98	237.02
	38.43	-19.13	-31.28	36.66	238.55
	38.47	-17.21	-32.46	36.74	242.07
	38.84	-19.83	-30.77	36.61	237.19
	39.08	-17.72	-31.98	36.56	241.00
	38.36	-19.42	-30.82	36.43	237.78
	38.56	-17.13	-32.21	36.48	242.00
	39.46	-18.06	-32.07	36.81	240.62
	39.15	-20.47	-30.59	36.80	236.22
	39.58	-18.15	-31.80	36.62	240.29
	39.76	-21.00	-30.44	36.98	235.39
	39.11	-17.61	-32.10	36.61	241.25
	38.97	-20.36	-30.37	36.57	236.16
	39.30	-17.75	-32.26	36.82	241.17
	39.38	-20.80	-30.41	36.85	235.63
	38.26	-20.28	-30.15	36.33	236.07
	38.69	-16.91	-32.00	36.19	242.14

	38.56	-16.59	-31.84	35.90	242.49
	38.35	-20.65	-29.76	36.23	235.24
average	38.78	-18.87	-31.47	36.72	239.06
c35h270	38.89	-0.13	-36.46	36.46	269.80
	38.84	0.20	-36.48	36.48	270.32
	37.74	1.37	-36.96	36.99	272.12
	37.73	2.01	-36.8	36.85	273.13
	39.42	0.75	-36.59	36.60	271.17
	39.59	-0.05	-36.57	36.57	269.91
	38.40	0.81	-36.62	36.63	271.27
	38.39	1.85	-36.47	36.52	272.90
	38.36	0.59	-36.64	36.64	270.92
	38.52	-0.58	-36.49	36.49	269.10
	39.03	-0.63	-36.14	36.15	269.00
	38.66	0.60	-36.39	36.40	270.95
	38.85	-1.24	-36.33	36.35	268.04
	38.90	0.20	-36.03	36.03	270.32
	38.43	0.87	-36.26	36.27	271.38
	38.95	-0.66	-36.39	36.39	268.96
	38.48	-0.66	-36.37	36.37	268.96
	38.04	0.96	-37.07	37.08	271.48
	38.08	0.85	-36.56	36.57	271.33
	38.23	-1.16	-36.54	36.55	268.18
average	38.58	0.30	-36.51	36.52	270.46
c35h300	36.60	15.91	-32.96	36.60	295.76
	36.57	16.21	-32.78	36.57	296.32
	37.41	15.34	-32.86	36.27	295.02
	37.47	15.63	-32.81	36.34	295.47
	36.81	17.59	-32.24	36.73	298.61
	36.65	16.88	-32.34	36.48	297.56
	37.07	16.52	-32.82	36.74	296.72
	36.84	17.36	-32.53	36.87	298.10
	36.93	15.67	-33.11	36.63	295.32
	36.83	16.88	-32.73	36.83	297.28
	37.10	16.52	-32.51	36.47	296.94

	36.63	17.64	-32.21	36.73	298.71
	36.19	17.80	-32.55	37.10	298.67
	36.22	16.46	-33.17	37.02	296.39
	37.29	15.81	-32.76	36.37	295.76
	36.63	17.30	-32.32	36.66	298.15
	36.31	17.56	-32.19	36.67	298.61
	36.01	15.61	-33.18	36.67	295.20
	36.47	18.18	-32.54	37.27	299.20
	36.45	16.11	-33.02	36.74	296.01
average	36.72	16.65	-32.68	36.69	296.99
c35h330	38.01	29.14	-19.25	34.92	326.55
	37.93	29.36	-18.96	34.95	327.15
	38.07	29.65	-18.53	34.96	327.99
	38.04	29.26	-18.83	34.80	327.24
	38.29	29.24	-19.24	35.00	326.65
	37.82	29.85	-18.50	35.12	328.21
	38.54	29.34	-17.68	34.25	328.92
	38.12	29.29	-18.41	34.59	327.85
	38.09	29.58	-18.71	35.00	327.68
	38.53	30.36	-17.63	35.11	329.86
	38.36	29.28	-19.25	35.04	326.67
	37.74	30.08	-18.26	35.19	328.74
	37.29	30.86	-17.11	35.28	330.99
	37.75	30.03	-18.44	35.24	328.45
	37.61	30.13	-15.61	33.94	332.62
	38.09	29.89	-17.32	34.55	329.92
	37.61	30.25	-17.26	34.83	330.29
	37.05	29.71	-18.93	35.22	327.50
	38.14	30.41	-15.87	34.30	332.44
	37.66	29.35	-18.17	34.52	328.23
average	37.94	29.75	-18.10	34.84	328.70
L6h0	61.50	18.03	0.14	18.03	0.45
	61.56	17.89	-0.41	17.89	-1.30
	61.13	18.29	-0.63	18.30	-1.98
	60.84	18.37	-0.03	18.37	-0.11

	60.76	18.50	-1.15	18.54	-3.54
	60.51	18.39	-0.35	18.39	-1.10
	60.87	17.66	0.28	17.66	0.92
	60.71	17.96	-1.14	18.00	-3.63
	61.21	18.18	-1.04	18.21	-3.27
	60.63	18.01	0.23	18.01	0.73
	60.37	18.62	0.19	18.62	0.58
	60.40	18.04	-1.2	18.08	-3.82
	60.20	18.67	1.37	18.72	4.18
	59.86	18.62	-0.37	18.63	-1.14
	59.73	18.94	1.10	18.97	3.32
	60.29	18.75	-0.83	18.76	-2.55
	60.10	18.93	1.05	18.96	3.18
	59.97	18.72	-1.19	18.75	-3.62
average	60.74	18.37	-0.52	18.39	-1.59
L6h30	59.61	17.30	9.24	19.61	28.12
	59.54	17.03	9.38	19.44	28.85
	59.37	17.05	9.57	19.55	29.30
	59.54	16.92	10.16	19.74	30.99
	58.83	17.78	9.20	20.02	27.35
	58.80	17.34	10.02	20.03	30.02
	60.11	16.13	9.64	18.79	30.86
	60.28	15.78	10.63	19.03	33.97
	59.95	16.79	9.28	19.19	28.93
	60.20	15.97	10.37	19.04	33.01
	59.28	16.50	10.22	19.41	31.78
	58.94	17.76	9.25	20.03	27.52
	59.79	16.11	10.96	19.49	34.23
	59.36	17.46	9.78	20.01	29.25
	59.87	16.40	9.98	19.20	31.33
	59.46	17.66	8.65	19.66	26.11
	59.40	16.53	10.39	19.53	32.14
	58.86	18.05	8.99	20.17	26.49
average	59.51	16.92	9.76	19.55	30.01
L6h60	60.25	8.19	17.71	19.51	65.19

	60.10	8.54	17.32	19.31	63.76
	60.08	8.13	17.92	19.68	65.60
	59.75	8.68	17.47	19.51	63.58
	59.93	9.42	17.86	20.19	62.20
	59.95	10.30	17.34	20.17	59.28
	58.57	11.26	17.19	20.55	56.76
	58.87	10.19	17.71	20.43	60.09
	59.05	8.97	17.52	19.68	62.89
	59.26	10.18	16.84	19.68	58.84
	59.35	8.85	17.49	19.60	63.18
	59.78	10.13	16.69	19.52	58.74
	59.44	10.86	16.09	19.41	55.99
	58.83	9.35	16.89	19.30	61.03
	59.30	8.85	16.74	18.94	62.15
	59.90	10.74	16.17	19.41	56.42
	60.66	9.82	17.33	19.92	60.46
	60.19	8.02	18.51	20.17	66.58
	60.51	10.17	16.86	19.69	58.91
	59.97	8.39	18.34	20.17	65.42
average	59.69	9.45	17.30	19.74	61.35
L6h90	59.76	0.17	20.45	20.45	89.53
	59.97	-0.26	20.43	20.43	90.74
	60.37	0.40	20.04	20.04	88.85
	60.57	-0.22	20.31	20.31	90.61
	59.93	0.25	20.44	20.44	89.29
	60.08	-0.32	20.49	20.49	90.90
	59.59	0.06	20.70	20.70	89.84
	59.71	-0.88	20.73	20.75	92.44
	59.83	-0.21	19.58	19.58	90.62
	59.48	0.70	19.83	19.84	87.98
	59.51	-0.95	19.62	19.64	92.78
	59.48	0.27	19.91	19.91	89.23
	60.57	-0.58	19.81	19.82	91.67
	60.08	0.76	19.68	19.70	87.78
	60.33	-0.13	20.71	20.71	90.35

	59.99	-1.74	20.99	21.07	94.73
	59.92	-1.22	21.19	21.23	93.29
	60.16	0.37	20.48	20.48	88.95
	60.13	-1.31	20.95	20.99	93.58
	59.43	0.79	20.24	20.25	87.76
average	59.94	-0.20	20.33	20.34	90.55
L6h120	59.98	-10.69	18.98	21.79	119.39
	60.00	-11.09	18.78	21.81	120.55
	59.91	-10.61	17.30	20.30	121.51
	59.96	-10.12	17.86	20.53	119.54
	60.37	-11.37	17.47	20.85	123.07
	60.24	-10.79	18.12	21.09	120.78
	59.57	-11.22	17.92	21.14	122.04
	59.47	-10.27	17.91	20.64	119.83
	59.47	-11.28	17.75	21.04	122.44
	59.82	-10.53	18.76	21.51	119.30
	60.66	-11.10	18.24	21.35	121.32
	60.87	-11.90	16.67	20.48	125.52
	60.50	-11.67	17.35	20.91	123.94
	60.72	-10.38	18.19	20.94	119.71
	59.83	-11.46	17.27	20.73	123.56
	60.30	-10.27	18.78	21.40	118.68
	60.55	-11.71	18.05	21.51	122.99
	60.00	-9.90	18.57	21.05	118.07
	59.84	-9.82	18.16	20.64	118.40
	59.85	-11.35	16.53	20.05	124.49
average	60.10	-10.88	17.93	20.99	121.26
L6h150	59.31	-16.54	11.19	19.97	145.93
	59.36	-16.79	10.85	20.00	147.13
	60.12	-17.40	10.52	20.33	148.83
	60.13	-17.08	11.11	20.38	146.96
	60.41	-17.71	10.61	20.64	149.07
	60.50	-17.90	9.91	20.46	151.03
	60.49	-17.33	11.11	20.58	147.34
	60.27	-17.63	10.36	20.45	149.56

	59.36	-17.18	10.47	20.12	148.65
	59.56	-17.87	9.53	20.26	151.93
	60.72	-18.14	9.55	20.50	152.22
	60.64	-17.89	10.97	20.98	148.49
	59.91	-16.88	11.67	20.52	145.34
	60.29	-17.97	10.47	20.80	149.77
	60.24	-16.97	11.26	20.37	146.43
	59.64	-17.71	9.91	20.30	150.76
	59.71	-17.49	10.90	20.61	148.07
	60.25	-18.65	9.30	20.84	153.50
	60.19	-16.96	11.69	20.60	145.42
	60.18	-17.67	9.78	20.20	151.05
average	60.06	-17.49	10.56	20.45	148.87
L6h180	60.3	-20.37	0.33	20.37	179.06
	60.21	-20.49	0.15	20.49	179.59
	60.18	-20.55	0.71	20.56	178.03
	60.45	-20.56	0.38	20.56	178.93
	59.43	-20.32	0.93	20.34	177.37
	59.42	-20.11	0.45	20.12	178.73
	59.82	-20.28	0.82	20.30	177.68
	59.62	-20.02	-0.18	20.02	180.52
	60.3	-20.20	0.06	20.2	179.84
	59.81	-20.45	-1.22	20.48	183.43
	60.47	-21.03	-0.91	21.05	182.49
	60.64	-20.79	0.38	20.79	178.96
	59.70	-20.07	-1.03	20.10	182.94
	59.52	-20.17	0.53	20.17	178.50
	59.79	-20.50	0.27	20.50	179.24
	59.93	-20.71	-1.36	20.76	183.76
	60.25	-20.55	0.96	20.58	177.34
	60.50	-20.97	-1.03	20.99	182.81
	60.64	-21.04	-0.87	21.06	182.36
	60.11	-20.37	1.01	20.40	177.16
average	60.06	-20.48	0.02	20.49	179.94
L6h210	60.44	-17.45	-11.63	20.97	213.67

	60.42	-17.25	-11.58	20.78	213.88
	60.55	-18.01	-11.15	21.19	211.77
	60.68	-17.85	-11.71	21.35	213.25
	60.99	-17.97	-11.87	21.53	213.46
	60.85	-18.30	-11.08	21.39	211.19
	60.61	-17.67	-10.58	20.59	210.92
	60.25	-17.28	-11.44	20.73	213.49
	60.10	-17.52	-11.96	21.21	214.32
	59.93	-18.02	-11.01	21.12	211.42
	60.39	-18.39	-10.40	21.13	209.49
	60.78	-17.81	-11.85	21.39	213.64
	59.68	-17.01	-11.98	20.80	215.16
	60.29	-17.63	-10.39	20.46	210.51
	59.88	-17.10	-11.65	20.69	214.28
	60.39	-17.89	-9.97	20.48	209.14
	60.47	-17.61	-12.19	21.41	214.70
	60.48	-17.90	-10.38	20.69	210.10
	60.63	-18.51	-10.46	21.26	209.46
	60.05	-17.47	-12.17	21.29	214.87
average	60.39	-17.73	-11.27	21.02	212.44
L6h240	60.80	-10.85	-18.73	21.64	239.92
	60.67	-11.21	-18.57	21.69	238.88
	60.85	-11.20	-19.56	22.53	240.21
	61.24	-11.43	-19.09	22.25	239.09
	60.00	-10.88	-18.58	21.53	239.66
	59.84	-10.16	-19.09	21.63	241.98
	60.49	-10.46	-18.87	21.58	241.00
	60.64	-9.61	-19.37	21.63	243.61
	60.73	-11.77	-19.07	22.41	238.31
	61.09	-10.78	-19.60	22.37	241.18
	60.56	-11.10	-18.36	21.46	238.84
	60.45	-9.96	-19.15	21.58	242.52
	60.93	-11.49	-18.30	21.61	237.87
	60.69	-10.25	-19.26	21.82	241.99
	60.85	-10.81	-19.48	22.28	240.97

	60.86	-12.28	-18.77	22.43	236.80
	60.63	-11.11	-18.44	21.53	238.93
	60.19	-9.47	-19.38	21.57	243.95
	60.86	-9.80	-19.17	21.53	242.92
	60.69	-11.91	-18.69	22.16	237.50
average	60.65	-10.83	-18.98	21.86	240.31
L6h270	60.28	-1.37	-22.32	22.36	266.49
	60.17	-1.50	-22.29	22.34	266.14
	60.85	-0.81	-22.05	22.06	267.91
	60.76	-1.42	-22.28	22.32	266.35
	61.04	-1.76	-22.06	22.13	265.45
	61.17	-1.11	-22.07	22.10	267.12
	60.51	0.21	-21.69	21.69	270.56
	60.84	-0.88	-21.77	21.79	267.67
	60.16	-0.25	-22.36	22.36	269.36
	60.35	-1.37	-22.31	22.36	266.48
	60.17	-0.35	-22.06	22.06	269.08
	60.80	-1.65	-21.82	21.88	265.69
	60.90	-2.32	-21.99	22.11	263.97
	60.81	-0.57	-22.23	22.24	268.54
	60.87	-2.18	-22.15	22.25	264.38
	60.10	-0.27	-22.29	22.29	269.30
	60.43	-1.36	-21.85	21.89	266.45
	59.96	0.63	-22.13	22.14	271.63
	60.25	-1.89	-22.39	22.47	265.16
	60.47	0.33	-21.85	21.85	270.87
average	60.54	-0.99	-22.10	22.14	267.43
L6h300	59.45	10.40	-19.66	22.24	297.89
	59.28	10.06	-19.96	22.35	296.76
	59.27	10.12	-20.02	22.44	296.82
	59.05	9.45	-20.41	22.49	294.84
	60.05	9.20	-19.95	21.97	294.77
	60.24	9.71	-19.48	21.77	296.49
	60.26	9.22	-19.32	21.41	295.51
	60.49	10.04	-19.07	21.56	297.77

	61.35	9.35	-19.8	21.90	295.28
	61.08	10.06	-19.22	21.69	297.62
	60.42	10.42	-19.43	22.05	298.20
	60.06	9.15	-19.71	21.73	294.90
	60.02	9.30	-20.09	22.14	294.83
	60.32	10.37	-19.24	21.85	298.32
	60.04	10.58	-18.61	21.41	299.61
	59.80	9.28	-19.74	21.81	295.17
	59.76	10.73	-19.28	22.07	299.11
	59.40	8.93	-19.78	21.70	294.30
	58.36	11.48	-19.02	22.22	301.11
	58.73	9.58	-20.03	22.20	295.57
average	59.87	9.87	-19.59	21.95	296.74
L6h330	60.70	16.90	-11.63	20.52	325.46
	60.82	16.74	-11.82	20.49	324.79
	60.98	16.69	-11.76	20.42	324.83
	60.74	16.28	-12.15	20.31	323.27
	59.28	16.87	-12.33	20.90	323.85
	59.21	16.69	-13.19	21.28	321.68
	60.40	16.32	-12.64	20.64	322.24
	60.64	16.93	-12.15	20.84	324.32
	59.55	16.55	-12.11	20.51	323.81
	59.86	16.99	-10.93	20.21	327.25
	60.17	17.14	-11.93	20.89	325.16
	60.02	16.17	-12.97	20.74	321.27
	60.11	16.11	-12.99	20.69	321.13
	60.19	16.26	-11.00	19.63	325.92
	60.53	17.11	-11.81	20.79	325.38
	60.91	16.33	-13.54	21.21	320.34
	61.12	16.33	-12.87	20.79	321.75
	60.46	17.60	-11.55	21.05	326.72
	59.88	17.33	-11.64	20.88	326.11
	59.97	16.50	-13.90	21.57	319.90
average	60.28	16.69	-12.25	20.72	323.76
cie-red	43.21	35.97	20.20	41.26	29.32

	43.18	35.61	20.63	41.15	30.09
	42.42	37.56	20.06	42.58	28.10
	42.57	38.04	19.57	42.78	27.23
	43.13	36.67	20.07	41.80	28.69
	42.79	37.33	19.38	42.06	27.43
	42.10	37.77	20.71	43.08	28.73
	42.38	38.67	20.00	43.53	27.35
	41.66	37.41	22.02	43.41	30.48
	41.44	37.51	20.95	42.96	29.19
	42.91	36.51	20.87	42.06	29.75
	42.36	36.77	19.73	41.73	28.22
	42.92	38.16	20.72	43.42	28.51
	42.65	37.96	22.26	44.00	30.39
	42.87	37.44	19.67	42.29	27.71
	43.10	36.03	20.77	41.59	29.96
	43.14	38.47	19.93	43.33	27.38
	43.48	37.54	21.48	43.25	29.78
	42.20	37.41	21.44	43.12	29.82
	41.61	38.02	19.67	42.81	27.36
average	42.61	37.34	20.51	42.61	28.78
Cie-green	55.59	-33.90	-0.29	33.90	180.48
	55.68	-33.80	-0.80	33.81	181.36
	55.90	-33.87	-0.99	33.89	181.67
	55.86	-34.14	-0.21	34.14	180.35
	54.73	-33.56	-1.08	33.58	181.84
	54.84	-33.44	-0.06	33.44	180.10
	55.64	-33.87	-1.44	33.90	182.44
	55.69	-33.70	-0.21	33.70	180.35
	55.51	-33.43	0.30	33.43	179.48
	55.06	-33.76	-0.80	33.77	181.35
	54.69	-33.63	-0.37	33.63	180.63
	55.31	-33.53	0.94	33.54	178.39
	55.67	-33.75	-0.58	33.76	180.99
	55.21	-33.48	1.16	33.50	178.02
	55.42	-33.68	-1.15	33.70	181.96

	54.80	-33.23	0.78	33.24	178.65
	55.08	-33.77	-1.08	33.79	181.83
	55.52	-33.31	0.97	33.33	178.34
	54.62	-34.22	-1.58	34.25	182.64
	54.36	-33.45	0.53	33.46	179.09
average	55.26	-33.68	-0.30	33.69	180.50
cie-blue	35.32	3.10	-32.93	33.07	275.39
	35.34	2.54	-32.91	33.01	274.41
	34.60	4.81	-32.41	32.76	278.44
	34.52	5.54	-32.26	32.73	279.75
	35.30	4.38	-32.09	32.39	277.77
	35.30	3.56	-32.43	32.62	276.26
	34.56	3.87	-32.85	33.07	276.72
	34.87	5.03	-32.42	32.81	278.82
	35.85	2.04	-32.29	32.36	273.61
	35.66	3.31	-32.52	32.69	275.80
	34.72	3.37	-32.67	32.85	275.90
	34.36	4.80	-32.16	32.52	278.49
	34.84	2.49	-32.47	32.56	274.38
	35.41	3.99	-32.11	32.36	277.08
	34.95	4.30	-32.36	32.64	277.56
	34.95	4.27	-32.37	32.65	277.51
	34.52	3.50	-33.16	33.34	276.03
	34.20	5.44	-32.60	33.05	279.48
average	34.96	3.91	-32.50	32.75	276.85

APPENDIX B

The measurement of Color-difference pairs

samples	ΔE_{ab}^*	ΔL^*	ΔC_{ab}^*	ΔH_{ab}^*
c2h0	0.37	-0.14	0.10	0.33
	0.55	0.04	0.03	0.55
	0.91	0.25	0.11	0.87
	0.92	0.09	0.02	0.91
	1.15	-0.44	0.09	1.05
	1.51	-0.48	0.04	1.43
	1.53	0.09	0.05	1.52
	1.66	-0.34	0.16	1.61
	2.25	0.01	0.42	2.21
c2h30	0.34	-0.06	0.12	0.31
	0.56	-0.08	0.11	0.54
	0.73	0.22	0.01	0.70
	1.06	-0.29	0.07	1.02
	1.01	0.32	0.31	0.91
	1.48	0.39	0.37	1.37
	1.44	-0.34	0.38	1.34
	1.92	-0.01	0.05	1.92
	1.80	-0.76	0.09	1.63
	2.52	-0.59	0.38	2.42
c2h60	0.73	0.01	0.59	0.42
	0.77	-0.09	0.44	0.62
	0.79	0.20	0.42	0.64
	1.01	0.03	0.27	0.97
	1.29	0.78	0.82	0.61
	1.23	-0.11	0.12	1.22
	1.40	-0.29	0.38	1.32
	1.89	0.61	0.43	1.73
	1.77	0.80	0.17	1.57
	2.19	-0.32	0.39	2.13

c2h90	0.34	0.05	0.08	0.32
	0.87	-0.16	0.35	0.78
	1.26	0.04	0.33	1.22
	0.90	-0.05	0.29	0.85
	1.38	0.03	0.31	1.34
	1.34	0.15	0.08	1.33
	1.77	-0.29	0.45	1.69
	1.95	0.31	0.48	1.87
	2.07	-0.69	0.24	1.93
c2h120	0.37	-0.12	0.02	0.35
	0.47	0.06	0.06	0.47
	0.82	0.26	0.05	0.77
	0.94	-0.02	0.04	0.94
	1.61	1.04	1.03	0.66
	1.33	-0.08	0.11	1.32
	1.80	0.48	0.20	1.72
	1.94	0.38	0.45	1.85
	2.05	0.53	0.09	1.97
c2h150	0.58	0.12	0.23	0.52
	0.79	0.04	0.18	0.77
	0.77	0.03	0.06	0.76
	1.16	-0.08	0.39	1.09
	1.24	-0.03	0.12	1.23
	1.48	-0.02	0.35	1.44
	1.95	0.34	0.06	1.92
	1.95	0.03	0.08	1.94
	2.05	-0.19	0.73	1.91
c2h180	0.32	-0.07	0.00	0.31
	1.26	0.11	0.26	1.23
	0.57	-0.15	0.01	0.55
	0.97	-0.19	0.26	0.91
	1.15	0.06	0.22	1.13
	1.28	0.49	0.07	1.18
	1.51	-0.33	0.31	1.44
	1.82	0.21	0.85	1.59

	2.09	-0.24	0.06	2.07
	2.28	0.12	0.30	2.26
c2h210	0.64	-0.02	0.03	0.64
	0.57	-0.10	0.41	0.38
	0.87	-0.35	0.03	0.80
	0.87	0.31	0.04	0.81
	1.19	0.46	0.11	1.09
	1.15	0.15	0.44	1.05
	1.48	0.04	0.46	1.40
	1.80	0.09	0.11	1.79
	2.06	-0.40	0.45	1.97
	2.30	-0.66	0.55	2.13
c2h240	0.47	0.01	0.17	0.44
	0.57	0.16	0.03	0.54
	0.88	-0.13	0.12	0.87
	0.84	0.24	0.33	0.73
	1.22	0.21	0.05	1.20
	1.37	-0.39	0.19	1.30
	1.55	0.15	0.45	1.48
	1.72	0.14	0.07	1.71
	2.03	0.30	0.34	1.98
	2.16	0.26	0.35	2.11
	2.66	-0.35	0.03	2.64
	2.46	0.02	0.39	2.43
	2.53	-0.13	0.38	2.49
	2.94	0.18	0.16	2.93
c2h270	0.35	-0.19	0.23	0.19
	0.74	0.15	0.29	0.66
	0.76	0.11	0.14	0.74
	0.99	0.25	0.03	0.95
	1.16	-0.18	0.47	1.04
	1.50	-0.22	0.19	1.47
	1.63	-0.13	0.41	1.57
	1.93	0.65	0.09	1.82
	2.27	-0.13	0.33	2.24

	2.27	0.03	0.41	2.23
c2h300	0.42	0.03	0.16	0.39
	0.52	0.17	0.25	0.43
	0.67	-0.26	0.42	0.47
	0.89	0.05	0.17	0.87
	1.03	-0.38	0.23	0.93
	1.30	-0.07	0.11	1.29
	1.48	-0.12	0.24	1.46
	1.66	0.23	0.59	1.53
	1.89	0.07	0.09	1.88
c2h330	0.39	0.03	0.06	0.38
	0.61	0.04	0.16	0.59
	0.78	0.07	0.45	0.63
	0.96	0.31	0.27	0.87
	1.03	0.38	0.14	0.94
	1.27	0.01	0.01	1.27
	1.32	-0.02	0.06	1.32
	1.83	-0.40	0.63	1.68
	2.25	-0.28	0.26	2.22
c35h0	0.41	0.07	0.23	0.33
	0.73	-0.17	0.14	0.70
	1.23	-0.46	0.05	1.14
	1.05	-0.37	0.13	0.97
	1.10	0.38	0.39	0.96
	1.48	0.47	0.36	1.35
	1.97	-0.47	0.21	1.90
	2.13	0.65	0.48	1.97
	1.80	0.23	0.13	1.78
	1.61	0.55	0.41	1.46
c35h30	0.50	-0.26	0.12	0.41
	0.69	-0.10	0.00	0.68
	1.05	0.04	0.52	0.91
	1.03	-0.41	0.16	0.93
	1.17	0.23	0.13	1.13
	1.53	-0.24	0.54	1.41

	1.70	0.15	0.62	1.57
	1.62	-0.37	0.19	1.56
	2.06	-0.49	0.36	1.97
c35h60	0.37	-0.21	0.04	0.31
	0.48	-0.07	0.18	0.43
	0.74	0.24	0.06	0.70
	1.00	0.24	0.15	0.96
	1.23	0.00	0.19	1.22
	1.38	0.04	0.5	1.29
	1.56	0.17	0.2	1.54
	1.99	0.18	0.71	1.85
	2.02	0.15	0.07	2.01
	2.07	-0.18	0.09	2.06
c35h90	0.37	0.20	0.13	0.29
	0.78	0.19	0.01	0.75
	0.73	-0.18	0.29	0.65
	0.99	0.12	0.40	0.90
	1.16	-0.34	0.55	0.96
	1.28	0.33	0.06	1.24
	1.40	-0.38	0.34	1.30
	1.81	0.15	0.15	1.79
	1.82	-0.68	0.10	1.68
c35h120	0.50	0.10	0.24	0.42
	0.66	-0.15	0.56	0.32
	0.97	0.12	0.21	0.94
	0.98	-0.19	0.33	0.90
	1.02	0.09	0.06	1.01
	1.43	-0.13	0.49	1.34
	1.55	0.21	0.71	1.36
	1.83	-0.25	0.46	1.75
	2.13	0.02	0.27	2.11
	2.37	0.07	1.26	2.00
c35h150	0.38	-0.07	0.11	0.36
	0.45	-0.06	0.18	0.41
	0.62	-0.10	0.14	0.59

	1.03	0.29	0.04	0.99
	1.12	0.22	0.25	1.07
	1.43	-0.13	0.27	1.40
	1.28	-0.42	0.17	1.19
	1.61	-0.13	0.24	1.59
	2.08	-0.49	0.08	2.02
	2.33	0.28	0.94	2.11
	2.14	-0.20	0.36	2.10
	2.68	0.25	0.39	2.64
	2.64	0.25	0.38	2.60
c35h180	0.56	0.02	0.13	0.55
	0.63	0.33	0.13	0.52
	0.84	-0.19	0.27	0.78
	0.84	-0.23	0.05	0.80
	1.24	0.29	0.23	1.19
	1.29	0.04	0.19	1.27
	1.39	-0.10	0.26	1.36
	1.80	0.11	0.13	1.79
	2.35	-0.34	0.43	2.29
c35h210	0.56	0.01	0.11	0.55
	0.58	-0.27	0.12	0.50
	0.90	-0.40	0.12	0.80
	0.76	0.25	0.00	0.72
	1.34	0.08	0.18	1.32
	1.26	-0.27	0.02	1.23
	1.52	0.13	0.04	1.51
	1.84	-0.57	0.22	1.74
	2.08	0.47	0.10	2.03
	2.45	-0.01	0.03	2.45
c35h240	0.42	-0.05	0.08	0.41
	0.67	-0.01	0.15	0.66
	0.72	-0.10	0.05	0.71
	1.05	0.18	0.07	1.03
	1.16	0.50	0.00	1.05
	1.39	0.22	0.14	1.36

	1.59	0.57	0.42	1.43
	1.85	-0.06	0.04	1.85
	2.12	-0.22	0.16	2.11
	2.26	-0.04	0.07	2.26
	2.44	-0.24	0.04	2.43
	2.70	-0.20	0.05	2.69
	2.85	0.31	0.00	2.83
	3.17	-0.18	0.36	3.14
	3.25	0.13	0.04	3.25
	3.57	-0.08	0.02	3.56
	3.87	-0.43	0.14	3.84
	4.57	0.21	0.32	4.56
c35h270	0.33	0.05	0.02	0.33
	0.67	0.01	0.14	0.65
	0.82	-0.17	0.03	0.80
	1.05	0.01	0.11	1.04
	1.18	-0.17	0.15	1.16
	1.31	0.37	0.25	1.23
	1.47	-0.04	0.32	1.44
	1.63	-0.52	0.12	1.54
	1.82	0.44	0.71	1.62
	2.01	-0.15	0.02	2.01
c35h300	0.36	0.03	0.03	0.36
	0.30	-0.06	0.08	0.29
	0.73	0.16	0.25	0.67
	0.92	0.24	0.13	0.88
	1.27	0.11	0.20	1.25
	1.25	0.47	0.26	1.13
	1.48	-0.02	0.07	1.48
	1.68	0.65	0.29	1.52
	2.20	0.30	0.00	2.18
	2.12	0.02	0.53	2.06
c35h330	0.38	0.08	0.03	0.36
	0.49	0.03	0.16	0.46
	1.07	0.47	0.12	0.95

	0.84	0.43	0.34	0.64
	1.41	-0.44	0.11	1.33
	1.42	0.62	0.15	1.27
	1.63	-0.46	0.04	1.56
	1.79	-0.48	0.61	1.61
	1.84	0.56	0.39	1.71
	2.58	0.49	0.22	2.53
L60h0	0.57	-0.06	0.14	0.55
	0.67	0.28	0.07	0.60
	0.84	0.25	0.14	0.79
	1.47	0.17	0.34	1.42
	1.41	0.59	0.20	1.26
	1.51	-0.03	0.54	1.41
	1.77	0.34	0.09	1.74
	2.02	-0.56	0.21	1.93
	2.25	0.13	0.21	2.24
L60h30	0.31	0.06	0.17	0.25
	0.63	-0.17	0.18	0.58
	0.93	0.02	0.01	0.93
	1.06	-0.16	0.24	1.02
	1.39	-0.25	0.14	1.36
	1.63	0.34	0.62	1.47
	1.85	0.43	0.52	1.72
	1.87	0.41	0.47	1.77
	2.13	0.54	0.64	1.96
L60h60	0.54	0.14	0.20	0.49
	0.79	0.33	0.17	0.69
	1.03	-0.02	0.02	1.03
	1.23	-0.30	0.12	1.19
	1.40	-0.20	0.01	1.39
	1.58	-0.43	0.08	1.51
	1.81	0.62	0.10	1.70
	2.06	-0.60	0.48	1.92
	2.21	0.47	0.26	2.14
	2.38	0.55	0.48	2.27

L60h90	0.48	-0.21	0.02	0.43
	0.70	-0.20	0.26	0.62
	0.60	-0.14	0.05	0.58
	0.95	-0.12	0.05	0.94
	1.01	0.35	0.26	0.91
	1.26	0.03	0.27	1.23
	1.43	0.49	0.12	1.34
	1.67	0.35	0.36	1.59
	1.76	-0.25	0.75	1.58
	2.33	0.70	0.74	2.09
L60h120	0.45	-0.02	0.02	0.44
	0.74	-0.05	0.23	0.70
	0.88	0.13	0.24	0.84
	0.95	0.10	0.50	0.81
	1.31	-0.35	0.47	1.17
	1.77	-0.21	0.87	1.53
	1.56	-0.22	0.04	1.54
	1.98	-0.47	0.68	1.80
	1.96	0.55	0.47	1.82
	2.24	-0.01	0.59	2.16
L60h150	0.42	-0.05	0.03	0.42
	0.67	-0.01	0.05	0.66
	0.73	-0.09	0.18	0.70
	0.83	0.22	0.13	0.79
	1.18	-0.20	0.14	1.16
	1.44	0.08	0.48	1.35
	1.67	-0.38	0.28	1.60
	1.65	0.61	0.07	1.54
	2.05	-0.54	0.23	1.96
	2.04	0.01	0.40	2.00
	0.24	0.09	0.12	0.19
L60h180	0.42	-0.27	0.00	0.32
	0.53	0.01	0.22	0.48
	1.06	0.20	0.28	1.00
	1.39	0.49	0.28	1.27

	1.32	-0.17	0.26	1.29
	1.57	0.18	0.08	1.56
	1.65	-0.14	0.26	1.62
	2.04	-0.25	0.42	1.98
	2.06	0.53	0.66	1.88
L60h210	0.20	0.02	0.19	0.08
	0.59	-0.14	0.16	0.55
	0.87	0.14	0.14	0.85
	1.01	0.36	0.13	0.93
	1.09	0.18	0.09	1.07
	1.61	-0.39	0.26	1.54
	1.81	-0.61	0.34	1.67
	1.93	-0.51	0.21	1.84
	1.83	-0.01	0.72	1.69
	2.09	0.58	0.03	2.01
L60h240	0.42	0.13	0.05	0.39
	0.65	-0.39	0.28	0.44
	0.89	0.16	0.10	0.87
	1.00	-0.15	0.05	0.98
	1.18	-0.36	0.04	1.12
	1.39	0.11	0.13	1.38
	1.59	0.24	0.21	1.56
	1.63	-0.01	0.16	1.62
	1.94	0.44	0.04	1.89
	2.17	0.17	0.64	2.07
L60h270	0.17	0.10	0.02	0.14
	0.67	0.09	0.26	0.60
	0.66	-0.13	0.03	0.64
	1.15	-0.33	0.09	1.10
	1.14	-0.19	0.01	1.12
	1.46	-0.63	0.18	1.30
	1.78	0.10	0.13	1.77
	2.06	0.77	0.03	1.91
	2.06	0.47	0.25	1.99
	2.30	-0.23	0.62	2.21

L60h300	0.48	0.17	0.11	0.44
	0.81	0.22	0.05	0.78
	0.71	-0.19	0.20	0.66
	0.89	-0.23	0.15	0.84
	0.95	0.26	0.20	0.89
	1.35	0.36	0.32	1.26
	1.40	-0.30	0.29	1.34
	1.74	0.23	0.40	1.67
	1.91	0.35	0.36	1.84
	2.18	-0.37	0.01	2.15
L60h330	0.27	-0.11	0.03	0.24
	0.61	0.24	0.11	0.55
	0.89	0.08	0.38	0.80
	0.81	-0.23	0.20	0.75
	1.29	-0.31	0.30	1.22
	1.43	0.15	0.15	1.41
	2.00	-0.08	1.07	1.68
	1.93	-0.37	0.42	1.85
	1.94	0.65	0.26	1.81
	2.40	-0.09	0.69	2.30
CIE-red	0.56	0.03	0.10	0.55
	0.70	-0.16	0.20	0.65
	1.02	0.35	0.27	0.92
	1.17	-0.28	0.46	1.04
	1.09	0.22	0.44	0.97
	1.29	0.55	0.33	1.12
	1.57	0.26	0.58	1.44
	1.80	-0.23	0.71	1.64
	1.85	-0.34	0.08	1.81
	1.96	0.59	0.31	1.85
CIE-green	0.53	-0.09	0.09	0.52
	0.82	0.04	0.26	0.78
	1.03	-0.11	0.14	1.02
	1.25	-0.05	0.20	1.23
	1.23	0.45	0.34	1.10

	1.45	-0.62	0.09	1.31
	1.82	0.47	0.26	1.74
	2.08	0.62	0.47	1.93
	2.14	-0.44	0.46	2.04
	2.26	0.26	0.80	2.10
CIE-blue	0.57	-0.02	0.06	0.56
	0.76	0.08	0.03	0.75
	0.88	0.00	0.23	0.85
	1.28	-0.31	0.27	1.21
	1.30	0.19	0.34	1.24
	1.56	0.36	0.33	1.48
	1.64	-0.57	0.20	1.53
	0.03	0.00	0.00	0.03
	2.05	0.32	0.29	2.00

APPENDIX C

Programs Used for the Data Analysis

```
/*-----  
This SAS program is the code of the logit analysis with 3-D normit  
function for the main experiments  
-----*/  
  
title1'Logit program with 3-d normit function';  
  
options linesize=72 ;  
  
title2'Testing Logit program with normit function using cyan center';  
  
data main;  
  
    infile "new-ocyana.dat";  
    input obsfail totobs dL dc dh;  
proc print;  
  
proc logistic data=main outest=betas covout;  
    model obsfail/totobs= dL dc dh  
        /link=normit  
        selection=stepwise  
        slentry=0.3  
        slstay=0.3  
        details;  
  
    output out=pred p=phat lower=lcl upper=ucl;  
  
run;  
  
proc print data=betas;  
run;  
proc print data=pred;  
run;  
  
endsas;
```

```

/*-----
The purposes of this program are to calculate observer variance and
inter observer variance
-----*/

```

```

#include<iostream.h>
#include<fstream.h>
#include<stdlib.h>
#include<math.h>

```

```

extern int *vari_tri (double data[432][46]);
extern int *vari_num(double data[432][46]);
extern double *vari_per(int *vari_t, int *vari_n, int n);
extern int *pass_num(double data[432][46]);
extern void print_partI(int *x,int *y,double *z, double *w, int n);
extern double mean_variance (double *vari_p, int n);
extern double stdv_variance (double mean, double *vari_p, int n);
extern double *vari_vec(double data[432][46]);
extern double *mean_var_vec (double *x, int n);
extern double *stdev_var_vec(double *x, int n, double *mean_vec, int l);
extern double *inter_obs(double data[432][46]);
extern double inter_max(double *x, int n);
extern double inter_min(double *x, int n);
extern void print_partII(double *x, double *y, int n);
extern double *pass_rate_diff(double *x, int n);
extern void print_inter(double *x,int n);

```

```

//main function

```

```

int main(void)
{
    int i,j;
    int number_col, number_row;
    cin >>number_col;
    cin>>number_row;
    ifstream inputFile("main-data", ios::in);
    if(!inputFile){
        cerr<<"Cannot open input file"<<endl;
        exit(-1);
    }
}

```

```

double data[number_row][number_col];
double temp;
for(i=0;i<number_row;i++){
    for(j=0;j<number_col;j++){
        inputFile>>temp;
        data[i][j]=temp;
    }
}
inputFile.close();

int l,n,m,k;
l=45;
n=1755;
m=39;
k=990;
int *vari_t=vari_tri(data);
int *vari_n=vari_num(data);
double *vari_p=vari_per(vari_t,vari_n,l);
int *pass_n=pass_num(data);
double *pass_r=vari_per(vari_t,pass_n,l);
double *pass_rd=pass_rate_diff(pass_r,l);
double mean, stdev,vari_max,vari_min;
mean=mean_variance(vari_p, l);
stdev=stdv_variance(mean, vari_p, l);
vari_max=inter_max(vari_p,l);
vari_min=inter_min(vari_p,l);

double *vari_v=vari_vec(data);
double *mean_v=mean_var_vec(vari_v,n);
double *stdev_v=stdev_var_vec(vari_v,n,mean_v,m);
double max_v,min_v;
max_v=inter_max(mean_v,m);
min_v=inter_min(mean_v,m);

double *inter_ob=inter_obs(data);
double min,max,inter_avg,inter_stdev;
min=inter_min(inter_ob,k);
max=inter_max(inter_ob,k);
inter_avg=mean_variance(inter_ob,k);
inter_stdev=stdv_variance(inter_avg,inter_ob,k);

```

```

cout<<"The variance matrix compare with the majority data:";
cout<<endl;
    print_partI(vari_t,vari_n,vari_p,pass_r,l);
cout<<"The mean variance is: "<<mean<<endl;
cout<<"The standard deviation is "<<stdev<<endl;
cout<<"The maximum of variance is "<<vari_max<<endl;
cout<<"The minimum of variance is "<<vari_min<<endl;
cout<<endl;

cout<<"The mean variance and standard deviation for each vector:";
cout<<endl;
    print_partII(mean_v, stdev_v, m);
cout<<"The maximum variance of a vector is : "<<max_v<<endl;
cout<<"The minum variance of a vector is : "<<min_v<<endl;
cout<<endl;

cout<<"Information of inter_observer's variance is: "<<endl;
cout<<"The average inter_observer variance is: "<<inter_avg;
cout<<endl;
cout<<"The standard deviation of inter_observer is: "<<inter_stdev;
cout<<endl;
cout<<"The maximum variance of inter-obsever is: "<<max;
cout<<endl;
cout<<"The minum variance of inter-observer is : "<<min<<endl;

    print_inter(inter_ob,k);
cout<<endl;
cout<<"The relationship between pass-rate diff and inter_var:";
cout<<endl;
for(i=0;i<990;i++)
    cout<<inter_ob[i]<<endl;

return 0;
}

-----Call Functions-----
// This function is for calculating the trial number of each observer

int *vari_tri (double data[432][46])
{

```



```

    int *vari_t=new int [45];
    int n;

    for (int i=0;i<45;i++){
        n=0;
        for (int j=0;j<432;j++){
            if(data[j][i]<2)
                n++;
        }
        vari_t[i]=n;
    }
    return vari_t;
}

//This function is for calculating the disagreement number of each
//observer comparing with majority data

int *vari_num(double data[432][46])
{
    int *vari_n=new int[45];
    int cnt;

    for(int i=0; i<45;i++){
        cnt=0;
        for(int j=0; j<432;j++){
            if(data[j][i]!=data[j][45] && data[j][i]<2)
                cnt++;
        }
        vari_n[i]=cnt;
    }
    return vari_n;
}

//This function is to calcualte the % disagreement of each observer
//comparing with majority data

double *vari_per(int *vari_t, int * vari_n, int n)
{
    double *vari_p=new double[45];

    for (int i=0; i<n; i++)

```

```

        vari_p[i]=1.0*vari_n[i]/vari_t[i];
    return vari_p;
}

//This function is for calculating each observer's variance
//at each vector comparing with majority data

double *vari_vec(double data[432][46])
{
    double *vari_v=new double [2000];
    int cnt,n,k,l;
    cnt=k=0;
    n=l=1;

    for (int i=0;i<45;i++){
        for (int j=0; j<432; j++){
            if(data[j][i]<2 && (data[j][i]!=data[j][45]))
                cnt++;
            if(data[j][i]<2){
                n++;
                l=n-1;
            }
            if(data[j][i]==2){
                vari_v[k]=1.0*cnt/l;
                cnt=0;
                n=l=1;
            }
            k++;
        }
    }
    return vari_v;
}

```

```

//This function is to print out each observer's trial_num, disa_num
//percentage of disagreement comparing with majority data, and
//pass rate

```

```

void print_partI(int *x, int *y,double *z, double *w, int n)
{

```

```

        for(int i=0; i<n; i++){
            cout<<i<<"\t"<<x[i]<<"\t"<<y[i]<<"\t"<<z[i]<<"\t"
            <<w[i]<<endl;
        }
    }
//This function is for calculating the mean of observers' variance

double mean_variance (double *vari_p, int n)
{
    double mean, sum;
    sum = 0;

    for (int i=0; i<n; i++)
        sum+=vari_p[i];
    mean=sum/n;
    return mean;
}

//This function is for calculating the standard deviation of observers'
//variance

double stdv_variance (double mean, double *vari_p, int n)
{
    double stdv, sum_var;
    sum_var=0;

    for (int i=0; i<n; i++)
        sum_var+=(vari_p[i]-mean)*(vari_p[i]-mean);
    stdv=sqrt(sum_var/(n-1));

    return stdv;
}

//This function is for calculating the mean of each observer's variance for
//each vector

double *mean_var_vec (double *x, int n)
{
    double *mean_vec=new double [39];
    double sum;
    int p,k;

```

```

k=0;
sum=0;

for(int i=0; i<n; i++){
    p=i%39;
    if(p==k)
        sum+=x[i];
    if(i==1754){
        mean_vec[k]=sum/45;
        k++;
        i=0;
        sum=0;
        if(k==39)
            i=10000;
    }
}
return mean_vec;
}

```

//This function is for calculating the stdev of each observer's variance
//for each vector

```

double *stdev_var_vec(double *x, int n,
                      double *mean_vec, int l)
{
    double *stdev_vec=new double [39];
    double sum;
    int p,k;
    k=0;
    sum=0;

    for(int i=0; i<n; i++){
        p=i%39;
        if(p==k)
            sum+=(x[i]-mean_vec[k])*(x[i]-mean_vec[k]);
        if(i==n-1){
            stdev_vec[k]=sqrt(sum/44);
            k++;
            i=0;

```

```

        sum=0;
        if(k==l)
            i=10000;
    }
}
delete stdev_vec;
return stdev_vec;
}

//This function is for print mean or stdev for each vector

void print_partII(double *x, double * y, int n)
{
    for(int i=0;i<n; i++)
        cout<<i<<"\t"<<x[i]<<"\t"<<y[i]<<endl;
}

//This program is for calculating inter-observer variance

double *inter_obs(double data[432][46])
{
    double *inter_obsv=new double[990];
    int n,cnt,p,l;
    cnt=p=0;
    l=n=1;
    for(int i=0; i<44; i++){
        for(int k=i+1; k<45; k++){
            cnt=0;
            l=n=1;
            for(int j=0; j<432; j++){
                if(data[j][i]<2 && data[j][k]<2){
                    if(data[j][i]!=data[j][k])
                        cnt++;
                }
                n++;
                l= n -1 ;
            }
        }
        inter_obsv[p]=1.0*cnt/l;
        p++;
    }
}

```

```

        delete inter_obs;
        return inter_obs;
    }

```

//This function is for calculating each observer's pass rate

```

int * pass_num(double data[432][46])
{
    int *pass_n=new int [45];
    int cnt;

    for (int i=0; i<45; i++){
        cnt=0;
        for(int j=0; j<432; j++){
            if(data[j][i]==0)
                cnt++;
        }
        pass_n[i]=cnt;
    }
    delete pass_n;
    return pass_n;
}

```

//This function is to calculate the maximum inter_observer variance

```

double inter_max(double *x, int n)
{
    double max;
    max=x[0];

    for(int i=0; i<n;i++){
        if(x[i]>max)
            max=x[i];
    }
    return max;
}

```

//This function is to calculate the minum_observer's variance

```

double inter_min(double *x, int n)

```

```

{
    double min;
    min=x[0];

    for(int i=0; i<n; i++){
        if(x[i]<min)
            min=x[i];
    }

    return min;
}

//This function is to print out inter observer variance in triangle
void print_inter(double *x,int n)
{
    int k,m;
    k=43;
    m=0;

    for(int i=0;i<n;i++){
        if(i-m<k)
            cout<<x[i]<<" ";
        if(i-m==k){
            cout<<x[i]<<endl;
            m=i+1;
            k--;
        }
    }
}

//This function is to calculate pass-rate difference for each two
//observer

double *pass_rate_diff(double *x, int n)
{
    double * d=new double [2000];
    int k;
    k=0;

    for(int i=0;i<n-1;i++){

```

```
for(int j=i+1;j<n;j++){  
    d[k]=x[i]-x[j];  
    if(d[k]<0)  
        d[k]=-d[k];  
    k++;  
}  
}  
delete d;  
return d;
```


/*-----

The purposes of this program are to calculate T50, fiducial limits, and χ^2 values from the output of the logit program.

-----*/

```
#include<fstream.h>
#include<iostream.h>
#include<math.h>
#include<stdlib.h>
extern double *Y_value(double b1, double b2,double data[][4],
                        int number_row);
extern int * round_x (double *Y, int number_row);
extern int *round_y(double *Y, int *x,int number_row);
extern int *round_z(double *Y, int *x, int *y, int number_row);
extern int *round_a(int *x, int *y,int *z,int number_row);
extern int *round_b(int *a, int *y, int *z,double *Y,int number_row);
extern double *w_value(double matrix[][10], int *a, int *b,
                        int number_row);
extern double nw_value(double data[][4],double *W,int number_row);
extern double nwh_value(double data[][4], double *W,int number_row);
extern double nwhh_value(double data[][4], double *W, int nubmer_row);
extern double mean_dh (double nwh, double nw);
extern double variance (double nwhh, double nwh, double nw);
extern double ld_value(double b1, double b2);
extern double g_value(double b2, double s);
extern double ksq_value(double data[][4],int number_row);
extern int degree_freedom(int number_row);
extern double h_value(int dof, double ksq);
extern double uplimit(double m,double g,double dhm,double nw,double s,
                        double b2, double h);
```

```
extern double lolimit(double m,double g,double dhm,double nw,double s,
                    double b2, double h);
```

```
int main(void)
{
    int i,j;
    int num_col, num_row;
    int number_row,number_col;
    cin >>num_col;
    cin>>num_row;
    ifstream inputFile("w_table", ios::in);
    if(!inputFile){
        cerr<<"Cannot open input file"<<endl;
        exit(-1);
    }
    double matrix[num_row][num_col];
    double temp;
    for(i=0;i<num_row;i++){
        for(j=0;j<num_col;j++){
            inputFile>>temp;
            matrix[i][j]=temp;
        }
    }
    inputFile.close();

    cin >>number_col;
    cin>>number_row;
    ifstream inputFileI("cyana.fnl", ios::in);
    if(!inputFile){
        cerr<<"Cannot open input file"<<endl;
        exit(-1);
    }
    double data[number_row][number_col];
    for(i=0;i<number_row;i++){
        for(j=0;j<number_col;j++){
            inputFileI>>temp;
            data[i][j]=temp;
        }
    }
}
```

```

inputFileI.close();

double b1,b2;
cin>>b1;
cin>>b2;

double *Y=Y_value(b1,b2,data,number_row);
int *x=round_x(Y,number_row);
int *y=round_y(Y,x,number_row);
int *z=round_z(Y,x,y,number_row);
int *a=round_a(x,y,z,number_row);
int *b=round_b(a,y,z,Y,number_row);
double *W=w_value(matrix,a,b,number_row);
double nw, nwh, nwhh,m,dhm,g,s,h,ul,ll,ksq;
int dof;
nw=nw_value(data,W,number_row);
nwh=nwh_value(data,W,number_row);
nwhh=nwhh_value(data,W,number_row);
m=ld_value(b1,b2);
dhm=mean_dh(nwh,nw);
s=variance(nwhh,nwh,nw);
g=g_value(b2,s);
ksq=ksq_value(data,number_row);
dof=degree_freedom(number_row);
h=h_value(dof,ksq);
ul=uplimit(m,g,dhm,nw,s,b2,h);
ll=lolimit(m,g,dhm,nw,s,b2,h);

cout<<"The k-square value of logit fit is: ";
cout<<ksq<<endl;
cout<<"The degree of freedom of the data: ";
cout<<dof<<endl;
cout<<"The heterogeneity factor is: ";
cout<<h<<endl;
cout<<"The LD50 value for this data set is: ";
cout<<m<<endl;
cout<<"The fiducial limit is:"<<endl;
cout<<ul<<"\t"<<ll<<endl;
return 0;

```

```

//This function is to calculate probit Y
double *Y_value(double b1, double b2,double data[][4],int number_row)
{
    double *Y=new double[20];
    for (int i=0; i<number_row; i++){
        Y[i]=b1+b2*data[i][0]+5;
    }
    return Y;
}

//These functions are to round a number
int * round_x (double *Y, int number_row)
{
    int *x=new int[20];
    for(int i=0; i<number_row;i++)
        x[i]=int(Y[i]);
    return x;
}
int *round_y(double *Y, int *x,int number_row)
{
    int *y=new int[20];
    for(int i=0; i<number_row;i++)
        y[i]=int(Y[i]*10-x[i]*10);
    return y;
}
int *round_z(double *Y, int *x, int *y, int number_row)
{
    int *z=new int[20];
    for(int i=0; i<number_row;i++)
        z[i]=int(Y[i]*100-x[i]*100-y[i]*10);
    return z;
}
int *round_a(int *x, int *y,int *z,int number_row)
{
    int *a=new int[20];
    for(int i=0;i<number_row;i++){
        if(z[i]>=5 && y[i]==9)
            a[i]=x[i]+1;
        else
            a[i]=x[i];
    }
}

```

```

    return a;
}
int *round_b(int *a, int *y, int *z, double *Y, int number_row)
{
    int *b=new int[20];
    double *d=new double[20];
    for(int i=0; i<number_row; i++){
        d[i]=a[i]-Y[i];
        if(d[i]>=0.04)
            b[i]=0;
        else if(z[i]>=5)
            b[i]=y[i]+1;
        else
            b[i]=y[i];
    }
    return b;
}

//This function is to calculate the weighting factor of probit
double *w_value(double matrix[][10], int *a, int *b, int number_row)
{
    double *w=new double[20];
    int k,l;
    for(int i=0; i<number_row; i++){
        k=a[i];
        l=b[i];
        if(k<1 || k>8.9)
            w[i]=0.001;
        else
            w[i]=matrix[k-1][l];
    }
    return w;
}

//These functions are to calculate variance and mean value
double nw_value(double data[][4], double *W, int number_row)
{
    double nw;
    nw=0;
    for(int i=0; i<number_row; i++)
        nw+=data[i][1]*W[i];
}

```

```

    return nw;
}
double nwh_value(double data[][4], double *W,int number_row)
{
    double nwh;
    nwh=0;
    for (int i=0; i<number_row; i++)
        nwh+=data[i][0]*data[i][1]*W[i];

    return nwh;
}
double nw hh_value(double data[][4], double *W, int number_row)
{
    double nw hh;
    nw hh=0;
    for(int i=0; i<number_row; i++)
        nw hh+=data[i][0]*data[i][0]*data[i][1]*W[i];

    return nw hh;
}
double mean_dh (double nwh, double nw)
{
    double dhm;
    dhm = nwh/nw;
    return dhm;
}
double variance (double nw hh, double nwh, double nw)
{
    double s;
    s=nw hh-nwh*nwh/nw;
    return s;
}

//This function is to calculate LD50
double ld_value(double b1, double b2)
{
    double ld;
    ld=-b1/b2;
    return ld;
}

```

```

//These functions are to calculate 95% fiducial limits and k-square
//degree of freedom and heterogeneity factor
double g_value(double b2, double s)
{
    double g;
    g=1.96*1.96/(b2*b2*s);
    return g;
}
double ksq_value(double data[][4],int number_row)
{
    double ksq,k;
    ksq=0;

    for(int i=0; i<number_row; i++){
        k=(data[i][2]-data[i][1]*data[i][3])*(data[i][2]-
data[i][1]*data[i][3])/(data[i][1]*data[i][3]*(1-data[i][3]));
        cout<<k<<endl;
        ksq+=(data[i][2]-data[i][1]*data[i][3])*(data[i][2]-
data[i][1]*data[i][3])/(data[i][1]*data[i][3]*(1-data[i][3]));
    }
    return ksq;
}
int degree_freedom(int number_row)
{
    int dof;
    dof=number_row-2;
    return dof;
}
double h_value(int dof, double ksq)
{
    double h,f;
    f=(dof-3)*1.3+6.3;
    if(ksq>f)
        h=ksq/dof;
    else
        h=1;
    return h;
}
double uplimit(double m,double g,double dhm,double nw,double s,
                double b2, double h)
{

```

```

double ul;
ul=m+g*(m-dhm)/(1-g)+h*1.96*sqrt((1-g)/nw+
(m-dhm)*(m-dhm)/s)/(b2*(1-g));
return ul;
}
double lolimit(double m,double g,double dhm,double nw,double s,
double b2, double h)
{
double ll;
ll=m+g*(m-dhm)/(1-g)-h*1.96*sqrt((1-g)/nw+
(m-dhm)*(m-dhm)/s)/(b2*(1-g));
return ll;
}

```